EROBOT

A Second-Generation NDE Inspection Robot

University of Cape Town

Department of Mechanical Engineering

Ian Alan Baldwin 2006

DECLARATION

This thesis is submitted in complete fulfilment of a M.Sc. (Eng) (Mechanical Engineering) at the University of Cape Town.

I know the meaning of plagiarism and declare that all the work in the document, save for that which is properly acknowledged, is my own. Each contribution to, and quotation in, this thesis from the work(s) of other people has been attributed, and has been cited and referenced.

I have not allowed, and will not allow, anyone to copy my work with the intention of passing it off as his or her own work.

Signature:

IAN ALAN BALDWIN

Date:

19TH JANUARY, 2007

SUMMARY

BACKGROUND

Since the early 1950's, **N**on-**D**estructive **E**valuation (NDE) has been revolutionizing all fields of industry but particularly production and maintenance. For the manufacturing sector, the widespread implementation of accurate NDE techniques (such as ultrasonic inspection) as well as the introduction of fracture mechanics, allowed engineers to more accurately predict the lifetime of components before failure [1], leading to an increased rejection in faulty or sub-standard components.

A similar revolution took place in sectors involved with maintenance and inspection. Flaw detection would enable technicians to establish whether failure was imminent, improving safety and preventing scenes as shown in **Figure (A) 1** below:

FIGURE (A) 1: *PRESTIGE* SINKING

This unfortunate photograph is of the Liberian-owned *Prestige* sinking off of the Spanish *Costa de la Muerte* (Death Coast) in late 2002[5]. The Prestige was bound for Singapore and carrying 77 000 tonnes of crude oil, and the resulting slick had enormous environmental, social and economic impacts on the region. Better and more rigorous inspection procedures may have prevented the *Prestige*'s cataclysmic failure.

ROBOTICS & NDE

Inspection of marine vessels in dry-dock can be a hazardous job. Manual NDE techniques require technicians to make use of scaffolding and gantries to be able to gain access to all sections of a ship's hull, which in some cases may be in excess of six stories off of the dry-dock floor. It is also time consuming; in the example of a medium-sized grain carrier, it may take technicians several months to fully inspect the hull and certify the vessel seaworthy.

Shown overleaf in **Figure (A) 2** is a typical setup at the Robertson Dry Dock in Cape Town:

FIGURE (A) 2: MANUAL INSPECTION

Visible in the image is the scaffolding the technicians use to gain access to the extremities of the hulls. Working on a platform which can be in excess of eighteen metres off the dry-dock floor poses a serious accident risk to personnel. Use of a **R**emotely **O**perated **V**ehicle (**ROV**) would eliminate risk to NDE personnel while potentially being able to reduce overall inspection time.

As a result of the growth of robotics as an industry, increasingly more systems are being developed that are capable of conducting NDE inspection. Robotics inspection systems reduce the risk to technicians, and are capable of performing a variety of inspection procedures.

FIGURE (A) 3: REFINERY 'BOTS

Figure (A) 3 shows two robots development for use in petroleum and petrochemical environments. *Neptune*, on the left, is a petroleum-storage inspection vehicle [16], equipped with a payload consisting of video cameras and **U**ltrasonic **T**esting (**UT**) equipment. The adjacent frame show the Explorer II [17], a vehicle designed for pipe inspection in a live-gas environment. While these platforms are well-suited to their designed task, they do not adapt well to marine inspection.

PREVIOUS DEVELOPMENT

Development of a dedicated NDE capable robot was the subject of a 2004 conjoint undergraduate thesis project [26] [27]. Shown in **Figure (A)** 4 overleaf is the end result of the project, dubbed *Pinky*:

FIGURE (A) 4: PREVIOUS NDEBOT

As a first-generation prototype *Pinky* performed adequately; however in order to produce a platform that would be capable of performing in an industrial environment major improvements had to be made to the concept. These included ruggedization of the platform, expansion of the NDE techniques used as well as cost evaluation of the platform, as a whole, to ensure market competitiveness.

This project took the experiences gained from the first NDE prototype and incorporated them into the next generation NDEbot.

EROBOT: 2ND GENERATION NDEBOT

FIGURE (A) 5: EROBOT TRAVELLING ON A VERTICAL WALL

eRobot is a 2nd generation inspection robot fusing the power of modern embedded computing technology with the diversity of low cost robotics. Although primarily designed for the inspection of marine vessels in dry-dock, eRobot makes use of a highly modular design in order to be able to fulfil a variety of inspection tasks. Custom-sintered magnets and custom made drive-units allow eRobot to adhere to ferro-magnetic structures and to travel inverted if required.

Communication is realised over a standard wireless (**WiFi**) network and utilises a standard LAN architecture to provide full internet connectivity, allowing the logging of

position and data to its associated server and website. Control of the robot is made possible by a standard joystick and laptop, giving the operator full and intuitive control of the vehicle. An embedded computer running open-source software and utilising custom communication and control programs ensures a rapid and accurate response to any user-input. Making use of **D**ifferential **G**lobal **P**ositioning **S**ystem (**DGPS**) technology, eRobot is capable of downloading correctional data from its associated DGPS server, allowing for accurate 3-dimensional positioning.

EROBOT: CAPABILITIES

	SPECIFICATION	DESCRIPTION
Physical	Straight line speed	0.2 m/s
	Manoeuvrability	Full manoeuvrability with sufficient adherence to travel inverted.
	Operating Range	Operating range of over 30 metres
	Operating Cycle	Continuous operation for a 2 hour period.
	Multiple Payloads	Capacity to accommodate a variety of NDE techniques
	Modular Design	Allow for incorporation of alternate drive or sensor modules.
	Weight	Weight of 8 kilograms allows one-person operation.
	Profile	Profile allows travel in standard 14" piping.
Control & Interface	Human Interface	Basic user interface with minimal learning or training.
	Expandability	Capacity for future implementation of self - navigation and environmental awareness
	Data Acquisition	GPS enabled to allow co-ordinate mapping
	Media Feed	Capacity for real time video streaming
Other	Commercially competitive	Economically competitive with equivalent market-available platforms.
	Expansion & Upgradeability	Embedded computing allows for future development of more advanced capabilities.

TABLE (A) 1: CAPABILITIES

Conclusions & Recommendations

In conclusion, the base performance of the robot was acceptable. Although the vehicle is not ready for the rigours of an industrial setting, it provided a useful prototype to test the validity of the concept itself as well as other concepts (navigation, networking and so on). The main performance criteria of the system are analysed below and recommendations are made for future development work on the vehicle.

Mechanical Design

Design of the robot in a modular fashion allowed for the simple assembly/disassembly for frequent modifications, and was considered a success. Structurally the robot was sound, and showed no sign of wear at the end of the project. However, reduction in the **weight** of the robot chassis by re-designing the vehicle with an **aluminium chassis** would benefit the overall performance.

Electronics and Computing

The use of the **PC/104** stack meant that development time was minimal, as pre-built programs and code could be implemented and tested quickly on the platform without having to go re-compilation or porting. Nevertheless, **replacement of the PC/104** with a capable modern microprocessor would reduce the space, weight and power requirements of the **C**omputing **M**odule whilst maintaining equivalent capabilities.

Navigation

Use of the networked **GPS system** showed the feasibility of using a Wireless LAN to disseminate positioning information amongst nodes or clients, though use of the system in a restricted or "urban-canyon" environment should be avoided as severe signal degradation occurs. An **alternative Urban-Canyon Navigational Aid** such as the new Antaris 4 SuperSense® Indoor GPS [42] would allow the vehicle to report accurate positioning information, whilst not requiring any modification to the existing LAN architecture.

Data Streaming

Use of an on-board QuickCam web camera showed that the idea of visual inspection was possible (which was expected), but it also showed that a redesign would be required if industry-standard pictures are to be obtained. A **software upgrade** and a switch to the **R**eal **T**ime **S**treaming **P**rotocol would allow the FireWire bus to be fully utilised providing video-streaming capabilities in addition to high quality still images.

Acknowledgements

Firstly, I am deeply indebted to my supervisor Mr. Stephen Marais who endured two long years of equipment abuse and imprudent engineering decisions whilst never losing his composure.

Equal gratitude is due to Professor Andy Sass, I hope in the end I have managed to absorb a minutiae of the volumes you have tried to teach me.

Thanks to Glen Newins and the workshop staff, all of your hard work and accommodating attitudes were greatly appreciated.

Lastly thank you to my long-suffering parents for your unwavering support, I promise I will stop studying soon!

TABLE OF CONTENTS

LIST OF FIGURES

List of Tables

[This page is intentionally left blank]

[This page is intentionally left blank]

1. Introduction

Background

This report details the design and development of an industrial inspection robot capable of carrying **N**on-**D**estructive **E**valuation (**NDE**) equipment and performing NDE tests.

Since the early 1950's, NDE has been revolutionizing all fields of industry but particularly production and maintenance. For the manufacturing sector, the widespread implementation of accurate NDE techniques (such as ultrasonic inspection) as well as the introduction of fracture mechanics, allowed engineers to more accurately predict the lifetime of components before failure [1], leading to an increased rejection in faulty or sub-standard components.

A similar revolution took place in sectors involved with maintenance and inspection. Flaw detection and *characterisation* (the classification of the *type* of defect) would enable technicians to establish whether failure was imminent or if there was still a substantial safety margin, thus striking a balance between safe operation and costly maintenance downtime [2].

NDE has facilitated accurate, rapid inspection ranging from the smallest of components to entire structures. Shown in **Figure 1-1** below are images of various electronic components and **P**rinted **C**ircuit **B**oards (**PCB**). Visible on the left frame is an X-Ray scan of a modern die for an **I**ntegrated **C**ircuit (**IC**) chip. The centre image shows a through-hole in a multi layer PCB that has not been fully plated due to poor solder re-flow and the right frame highlights inconsistencies in drill spacing on another PCB [3].

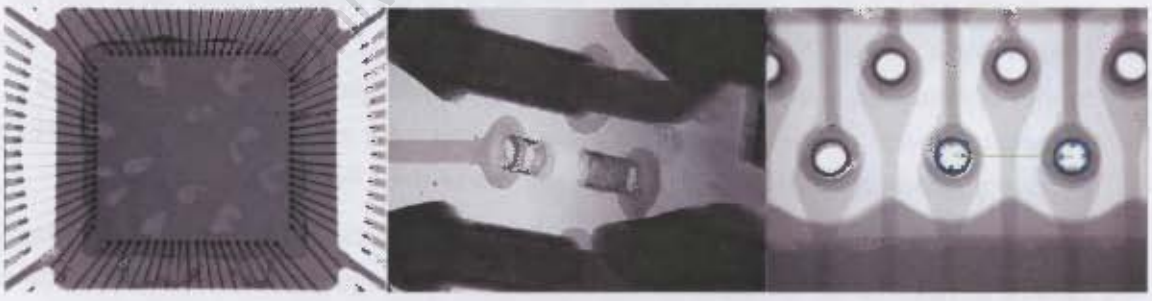

Figure 1-1: X-Ray Inspection of Electronic Components and **PCB**'s

NDE is not confined to the small and **Figure 1-2** overleaf shows one of the largest ships in the world, the *Knock Nevis*. The Knock Nevis is a *supertanker*, or a transport vessel that is capable of transporting more than 500,000 deadweight tonnes of crude oil [4].

FIGURE 1-2: THE MASSIVE *KNOCK NEVIS*

This particular vessel is in excess of 480 metres in length and has a 69 metre girth, and detailed inspection of her internal compartments is a huge, but vital, task.

Even in an enormous freighter such as the *Knock Nevis* small internal flaws in the hull could lead to failure of the structure as a whole, with disastrous consequences. Structural integrity has led to many maritime disasters, one of which is shown in **Figure 1-3** below:

FIGURE 1-3: *PRESTIGE* SINKING

This unfortunate photograph is of the Japanese built, Greek-operated, Bahamas-registered and Liberian-owned *Prestige* sinking off of the Spanish *Costa de la Muerte* (Death Coast) in late 2002[5]. The Prestige was bound for Singapore and carrying 77 000 tonnes of crude oil, and the resulting slick had enormous environmental, social and economic impacts on the region. Fishing restrictions were enforced along the coastline, depriving communities that depended on the sea of their livelihood.

Criticism was heaped upon the shipping community, one claim being that single-walled vessels were no longer suitable for the transport of damaging content such as crude oil [6] (*Exxon Valdez*, which ran aground in Prince William Sound, Alaska, causing massive environmental damage, was also of single-hull construction [7]). Another single-hulled vessel the *Erika* sank off the coast of France in 1999, and the subsequent *Prestige* sinking prompted the **E**uropean **U**nion (**EU**) to call for a phasing out of single-hulls to be completed by 2015 [6].

Severe structural degradation was cited as being one of the primary factors for the ship's hull splitting clean in half [8]. After the accident, the EU called for an increase in the

number of inspections conducted on dangerous freights from once to twice yearly, putting under pressure maintenance workers who were already struggling with the initial inspection quota [6].

Analyzing the entire structure of such a vessel for structural deficiencies is an incredibly manpower-intensive task, requiring the vessel to spend extended periods of time in dry-dock. According to Mr. Jonathan Wamsteker - owner and operator of Sonometrics, a Cape Town based marine inspection company - a medium sized cargo vessel could spend four to five months in dry-dock if it had to undergo detailed inspection.

Traditional methods employed in industry call for rope-access inspection teams to conduct NDE inspection on the sides of the vessel by hand [9]. This is a lengthy process and in addition the working conditions in the dock are hazardous to NDE personnel.

The implementation of a robotic inspection solution would not only eliminate the danger to on site NDE personnel but could also afford other advantages such as reduced inspection time.

Robotics & NDE

Robotics as an industry has experienced rapid growth fuelled by the massive boom in the electronics and computer industries [10]. These advances have allowed the replacement of human technicians with robot stations, as is becoming increasingly commonplace in industry. **Figure 1-4** shows a weld inspector checking mounts on a nuclear reactor vessel [11]. Adjacent to the weld inspector is *BONNIE III*, a non contact ultrasound nuclear boiler inspector. [12]

Figure 1-4: Robot Inspection Stations

Applications of robotics in a fairly standardised, repetitive environment such as an assembly line or inspection station is markedly different to the implementation of an inspection system in a marine dry-dock. Environmental conditions inside a modern factory are tightly controlled, whereas a robot operating in a marine environment will have to deal with all types of real world phenomena, ranging from hostile weather conditions to careless dockside personnel.

However, implementation of such a system would afford NDE personnel safer working conditions as well as potentially reducing inspection time. This combination of factors illustrated the need for the implementation of robotics and automation.

Mr. Wamsteker was first struck with the idea and approached the Department of Mechanical Engineering at UCT to propose the idea as a research project. Consultation with Mr. Wamsteker yielded the basis of the design requirements (a full set of which can be found in the Performance Specifications section beginning on page **12**).

The first criterion was centred on the vehicle's ability to traverse a ship's hull. Mr. Wamsteker indicated that a vehicle that could attain a straight-line speed of 0.5 m/s would provide suitable capabilities for rapid inspection.

Operating in the testing environment of the dry-dock, the platform is required to be reliable with a low maintenance overhead. Effectively, this meant that the robot should only need to be recharged at the end of the day (meaning a 6-8 hour operating cycle) and should not require maintenance more than once a week. The duty cycle was determined to be too demanding for the project initially, and was revised down to two hours.

Mr. Wamsteker also stressed the need for the vehicle to be remotely controlled. He noted that some ships were in excess of 6 stories high from the bottom of the dry-dock, and as such the operator should still be able to control the vehicle. As such, 30 metres was agreed to be the minimum range for the robot.

A simple, user-friendly interface would allow marine technicians with a minimum of training to operate the vehicle. Lastly, the project is required to be commercially competitive with currently available inspections, including manual inspection.

Current Technological Trends

As a result of the growth of robotics as an industry, increasingly more systems are being developed that are capable of conducting NDE inspection. The petroleum sector is an avid proponent of remote NDE technology, due to the huge amount of piping networking and storage vessels that comprise a petroleum refinery, where even a mid-size oil refinery may have in excess of 350 miles of piping [13].

Need for pipeline inspection was highlighted by the February 2006 spill at Prudhoe Bay in Alaska, site of the **B**eyond **P**etroleum (**BP**) Prudhoe Bay Oil Field where 16 "anomalies" (highly corroded regions) were thought to be in one section of pipe. However on detailed inspection after the spill it was found there were over five thousand [14]. Spills such as these have major ramifications in terms of environmental cleanup costs [15].

FIGURE 1-5: REFINERY 'BOTS

Figure 1-5 shows two robots development for use in petroleum and petrochemical environments. *Neptune*, on the left, is a petroleum-storage inspection vehicle [16]. It can navigate on either the internal or external side of the tank, and adheres to the tank by means of magnetic drive tracks. The sensor payload consists of a video camera and **U**ltrasonic **T**esting (**UT**) equipment to conduct detailed inspection. Power is provided to the unit by means of a tether which also provides a data bus to and from the vehicle.

Figure 1-5's right panel is an image of the *Explorer II*, a dedicated gas pipeline inspection robot funded by the United States **D**epartment **o**f **E**nergy (**DoE**) [17]. The *Explorer* is a wireless NDE inspection unit capable of evaluating the structural integrity of pipelines. The system makes use of a modularised design to house its on board electronics and cameras. Design in this fashion not only exploits the advantages of modularity, but it also allows the vehicle to turn through bends in pipes, as well as ascend vertically.

Robots are aptly suited to other hazardous applications, one popular example being pressure vessel inspection in nuclear reactors.

FIGURE 1-6: 'BOTS FOR **HAZ**ARDOUS **OP**ERATION**S** (**HAZOPS**)

Shown in **Figure 1-6** are two inspection robots. On the left is *Pioneer*, a vehicle designed and developed at one of the powerhouses of modern robot development, the Robotics's Institute at Carnegie Mellon University [18]. The primary mission for *Pioneer* was the inspection of Reactor 4 at Chernobyl power station in the Ukraine. Pioneer carries an impressive array of environmental sensors in addition to an onboard core-borer (for retrieving material samples on-site) as well as a mapping unit for creating 3D models of the interior structure of the reactor.

In the adjacent photo is the *ROBUG II*, designed at the Department of Electronics and Computer Science at the University of Southampton in the United Kingdom. *ROBUG II* is a legged robot capable of performing autonomous floor to wall transfers, and is ideally suited for conducting inspection in environments with very limited access (such as nuclear reactor pressure vessels) [19].

Inspection of a ship-hull will require a robot platform that can easily traverse the hull, all the while remaining firmly adhered. A cross-section of some of the alternative Research and Development (R&D) dedicated wall-climbing robots are shown in **Figure 1-7** below:

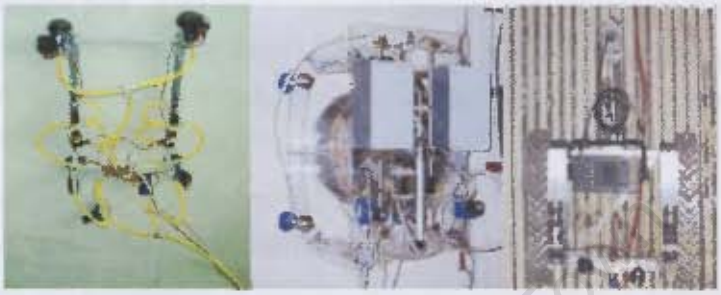

FIGURE 1-7: WALL CLIMBERS

On the left in **Figure 1-7** is *WALLY*, developed by the ***D**ipartimento **E**lettrico **E**lettronico é **S**istemisico* (**DEES**) of Catania University [20]. *WALLY* is a prototype robot designed to conduct surface inspection on industrial chimneys and storage tanks. The centre panel shows an image of *SURFY*, also developed by DEES, which is another articulated pneumatic powered inspection robot [21]. The **T**ennessee **T**echnical **U**niversity **C**entre for **E**nergy **S**ystems **R**esearch (**TTU CESR**) robot on the right was developed to analyse the thickness of water-walls in coal fired power plants [22].

In industry, commercial inspection robots are readily available for a variety of tasks.

FIGURE 1-8: EVEREST VIT: ROVVER® FAMILY

Shown in **Figure 1-8** above are the Rovver® family of visual inspection robots from Everest VIT (now amalgamated into General Electric® Inspection Technologies), mainly for remote pipeline inspection [23]. The smallest member of the family is (the R400, leftmost 'bot in **Figure 1-8**) capable of conducting inspection in pipe diameters as small as 4" (~100mm). Maximum range for the series is 200 metres and the largest version,

the R900 (**Figure 1-8**, right) is capable of carrying additional sensory equipment for other inspection tasks.

FIGURE 1-9: MARAT© INSPECTION ROBOTS

Similar to the Rovver family are the MARAT© series of industrial inspection/cleaning robots. The MARAT robots use a common chassis and different payload modules to fulfil different tasks [24].

One of the major disadvantages of commercially available platforms is cost. For example, the P3-AT, a commercial robot platform targeted at developers (shown in **Figure 1-10**) costs in excess of US$3 000, just for the base unit. Some of the more advanced systems cost upwards of USD$70 000 [25].

FIGURE 1-10: P3-AT

As such one of the design criteria that the project will aim to fulfil will be the development of an equivalent system that would be able to compete commercially in the market-place.

From this brief [and by no means exhaustive] overview, it becomes apparent that there are multitudes of inspection systems available and in development, involving both standard inspection NDE techniques as well as more advanced ones such as ultrasound.

Each system has unique attributes that facilitate its function; however, no system completely fulfils the exact requirements of Mr. Wamsteker and as such a new system would have to be developed.

PREVIOUS DEVELOPMENT

Development of a dedicated NDE capable robot was the subject of a 2004 conjoint undergraduate thesis project [26] [27]. Shown in **Figure 1-11** overleaf is the end result of the project, dubbed *Pinky*.

FIGURE 1-11: 2004 THESIS NDEBOT

Pinky utilised standard Phillips[D] electric screwdriver motors as drive units. Visible in the left frame of **Figure 1-12** is the aluminium frame and the drive units arranged in pairs, located at the front and rear. Adhesion was accomplished with custom-sintered cylindrical rare-earth Neodymium magnets, one of which was located on each of the four drive wheels.

FIGURE 1-12: *PINKY*: A PHYSICAL BREAKDOWN

Inspection was performed with a modified Panametrics[TM] hand-held ultrasonic thickness gauge (encased in a protective housing, visible in the centre panel of **Figure 1-12**) with control being implemented with an embedded PC/104 computer and custom circuitry (**Figure 1-12**, right panel).

As a primitive test-bed, the NDEbot performed adequately. However, while the vehicle was capable of adhering firmly to ferro-magnetic walls, it was not capable of turning or ascending vertically. The modified (some would say jerry-rigged) NDE payload was also subject to regular inconsistencies.

In order to produce a platform that would be capable of performing in an industrial environment, major improvements had to be made to the concept. These included (amongst others): ruggedization of the platform, expansion of the NDE techniques used as well as cost evaluation of the platform, as a whole, to ensure market competitiveness.

This project took the experiences gained from the first NDE prototype and incorporated them into the next generation NDEbot. The report begins with a description of the

platform, followed by an examination of all the major aspects contributing to its performance. Concluding the report is a discussion with respect to recommendations for future work.

2. EROBOT: FINAL SOLUTION

[For video footage of the robot in action, please see the accompanying DVD.]

FIGURE 2-1: EROBOT ATTACHED TO A VERTICAL METALLIC PLATE

eRobot is a 2nd generation inspection robot. It fuses the power of modern embedded computing technology with the diversity of low-cost robotics. Primarily designed for the inspection of marine vessels in dry-dock, eRobot makes use of a highly modular design in order to be able to fulfil a variety of inspection tasks.

Custom-sintered magnets and custom made drive-units allow eRobot to adhere to ferro-magnetic structures and to travel inverted if required.

Communication is realised over a standard wireless (**WiFi**) network and utilises a standard LAN architecture to provide full internet connectivity, allowing the logging of position and data to its associated server and website.

Control of the robot is made possible by a standard joystick and laptop, giving the operator full and intuitive control of the vehicle. An embedded computer running open-

source software and utilising custom communication and control programs ensures a rapid and accurate response to any user-input.

Making use of Differential GPS technology, eRobot is capable of downloading correctional data from its associated DGPS server, allowing for accurate 3-dimensional positioning.

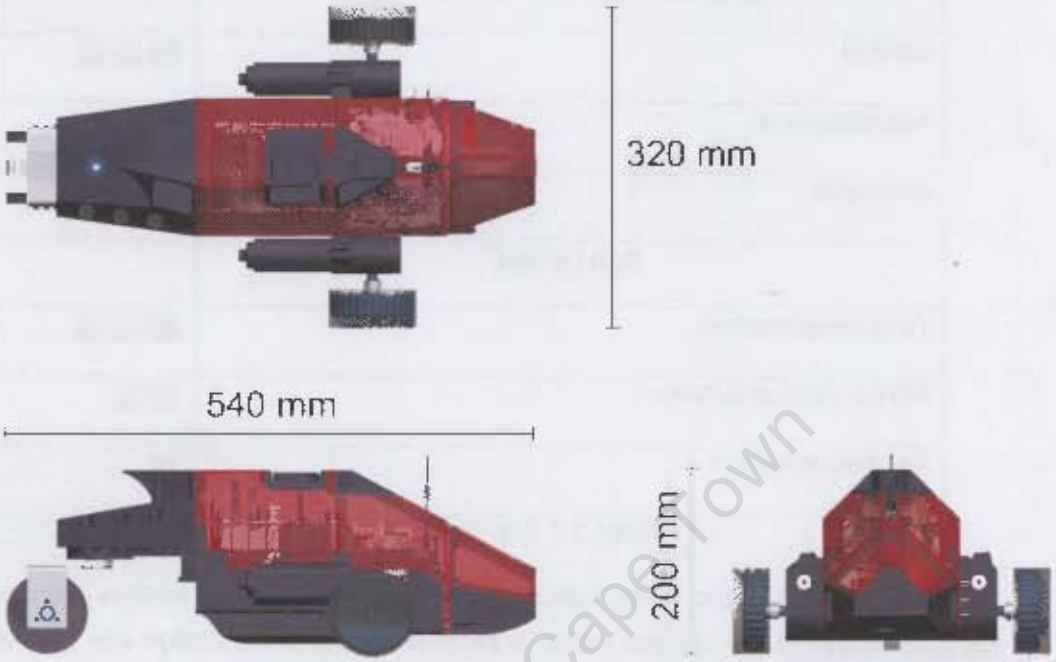

FIGURE 2-2: OVERALL DIMENSIONS

Performance Specifications

2.1 Specifications: KEY

Specification Table Key	
Critical	
Advantageous	
Desirable	
Achieved	
Fully implemented	
Partial implementation	
Not Implemented	

TABLE 1 : SPECIFICATION TABLE KEY

Shown in **Table 1** above is the Specification Table key. The top section describes how each performance criteria was rated. A **critical** aspect of the design was part of the original design specifications as were discussed with Mr. Wamsteker.

An **advantageous** criterion was one which was mentioned by Mr. Wamsteker as being potentially useful, however it was not paramount to the success of the project. Lastly, a **desirable** attribute was one added by the author as an aspect that could be potentially useful to the end-user. The *Achieved* section details the degree of implementation of the design criteria. **Three bars** show a full implementation of the criterion, **two bars** infers a partial or incomplete implementation with more development required. **One bar** means there was no attempt at implementation.

2.2 Specifications: TABLE

SPECIFICATION	DESCRIPTION	RATING	ACHIEVED
Physical Attributes			
Minimum straight line speed	0.5 m/s		
Manoeuvrability	Full manoeuvrability with sufficient adherence to travel inverted.		

Operating Range	Minimum operating Range of 30 metres		
Operating Cycle	Operate continuously for a period of at least 2 hours		
Multiple Payloads	Accommodate a variety of NDE techniques		
Modular Design	Allow for incorporation of alternate NDE payloads or drive techniques		
Weight	To weigh no more than 8kg's, to facilitate easy transport by one operator		
Profile	Have a cross-sectional area small enough to allow travel in standard 14" piping		

Control & Interface			
Human Interface	Easy video-game like intuitive user control, minimal learning or training		
Expandability	Allow for implementation of self navigation and environmental awareness		
Data Acquisition	3D mapping enabled to present data in a simple effective way		
Media Feed	Real time streaming to allow user a robot view perspective		

SPECIFICATION	DESCRIPTION	RATING	ACHIEVED
Miscellaneous			
Commercially competitive	Economically must compete with equivalent market-available platforms & techniques		
Expansion & Upgradeability	Allow for incorporation of more efficient/advanced techniques.		

2.3 Specifications Justification

From the specifications table it can be seen that not all major requirements were fully met. In particular, these were the straight-line operating speed and the duty cycle.

Straight Line Speed

A minimum of 0.5m/s was specified by Mr. Wamsteker in the initial design specifications. When the robot was tested, it was found that the bot could only attain 0.2 m/s. As such, it failed the initial criteria; however suggestions for design modifications have been made in the **Recommendations** section in order to improve the vehicle's speed.

Duty Cycle

A duty cycle of 2 hours was initially outlined for the platform, having been throttled down from the initial 6-8 hour specification. This full extent was unfortunately never tested due to the failure of some equipment in the testing process.

This is fully documented in the **Testing** section, and recommendations for performance improvement have been made in the **Conclusions & Recommendations** section on page **63**.

3. Design

As is the case with any cross-disciplinary project, the design of eRobot spanned a number of engineering fields. Before any detailed or embodiment design work was undertaken, a conceptual design phase was performed, forming the basis of the upcoming detailed design phase.

From the conceptual design, detailed mechanical and electrical design phases were performed, providing the necessary schematics and data for manufacture.

3.1 Conceptual Design

Various conceptual robot configurations were envisioned for the new generation robot, bearing in mind the successes and failures of the preceding prototype. This generation of robot had to address the previous inadequacies that were highlighted by the initial design.

Specifically, this involved the drive configuration, as this was where the initial prototype underperformed substantially.

Trike

Figure 3-1: Trike concept

Conceptually, the trike concept has a number of advantages over a conventional 4-wheeled design. All drive elements are located at the rear, and steering could be accomplished merely by either varying speed of each drive wheel with a front neutral "jockey", or by having an active steering nose wheel and standard rear wheel drives.

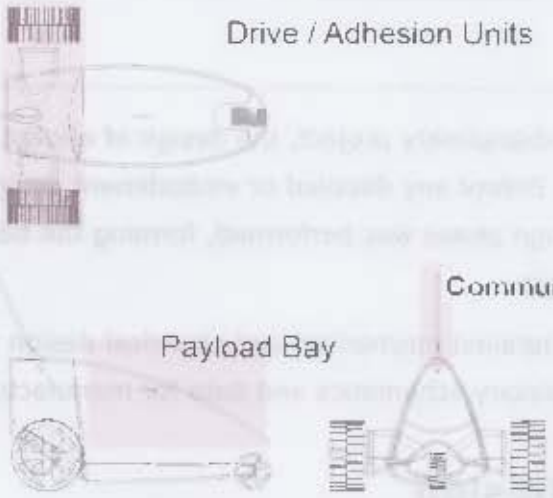

FIGURE 3-2: TRIKE: SCHEMATIC

Although simplistic in nature, this version of the **trike** concept did not lend itself to the envisioned modular design as much as other concepts, and was discarded.

REVERSE TRIKE

FIGURE 3-3: REVERSE-TRIKE

This concept is similar to the **trike** concept outlined above, but differentiated by having the drive wheels near the front of the vehicle, and the trailing neutral "jockey" at the rear. Having the drive/adhesion units in this configuration would allow the substitution of drive units and/or payload without the need for major reconfiguration.

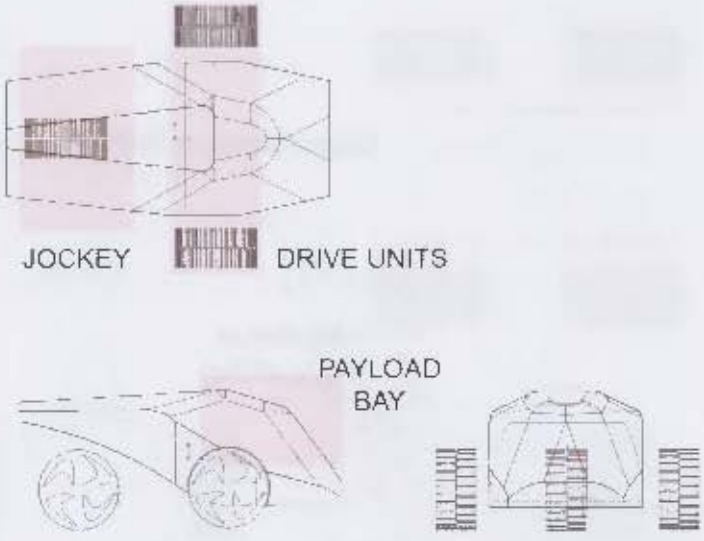

FIGURE 3-4: REVERSE-TRIKE SCHEMATIC

QUAD

FIGURE 3 5: QUAD CONCEPT

This concept, due to its inherent simplicity was the one selected for the first generation of robot. In addition, with four wheels instead of three, the **quad** provides more adhesive power than the previous two concepts.

However, due to the demanding requirements of adherence and low rolling friction, the quad concept requires substantially more driving control than the other two concepts. This was due to the fact that the wheels, due to the intense adhesive force of the magnets, did not allow for any "scuffing". Therefore if this concept was to become viable, a differential drive system would have to be developed, adding substantially to the complexity of the design.

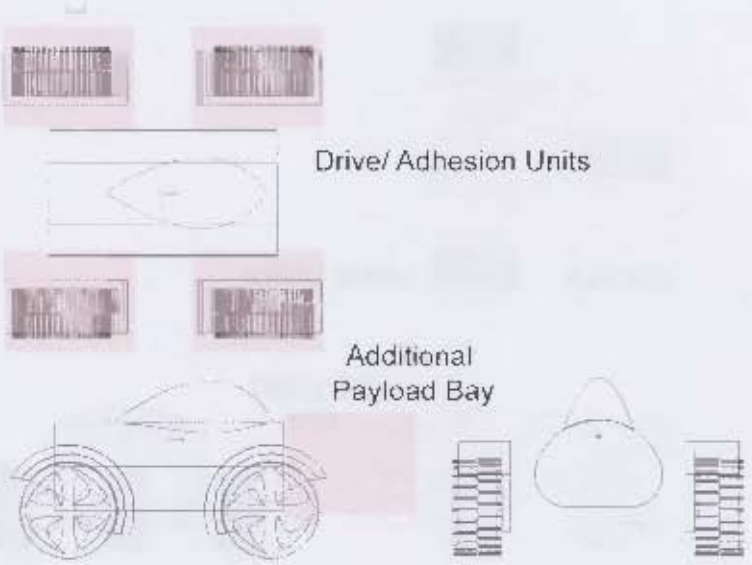

FIGURE 3-6: QUAD SCHEMATIC

Although the **quad** concept was more accommodating for a modular design, the difficulties in implementing a successful driving system eliminated it as a viable concept.

SELECTED CONCEPT

Previous experience with the **quad** concept had shown a number of deficiencies inherent in the design. A lack of perceived expandability eliminated the concept of the **trike**. As such, it was decided that the **reverse-trike** offered the most advantages, and was selected.

3.2 Mechanical Design

FIGURE 3-7: EXPLODED VIEW

Detailed design of the platform had to take into account several factors:

MODULARISATION

Paramount to the success of the robot was its ability to adapt to different environments. Developing a drive system that was capable of adhering to (and providing grip on) ferro-magnetic surfaces **and** being capable of traversing other environments (such as the interior of a piping network) successfully would have been an exceedingly complex task.

Instead the entire design was conceived as a system of modules, which could be configured appropriately depending on the environment. For the case of marine inspection, three magnetic wheels were required, however if the 'bot was used in a standard "rover" role, they could be substituted for a set of large non-magnetic high-profile wheels.

Therefore each module had to be self-contained with only the minimal amount of connections required to other modules, as extensive need for assembly/disassembly would negate the entire purpose.

MATERIAL SELECTION

From the outset, **H**igh **D**ensity **P**oly-**E**thylene (**HDPE**) was chosen as the material of choice. HDPE is a low cost urethane plastic with a number of characteristics that make it useful for robotic construction. Primarily, HDPE is cost effective with most standard thicknesses below 40mm being readily available in a variety of colours. It

is also easy to machine, with high cutting speeds being used (up to and including 1000mm/min 5mm deep cuts) leaving an excellent surface finish.

Orange Perspex® was used primarily in the canopy construction, and gave the platform an aesthetic appeal. However, Perspex also is very tough and provided good structural reinforcement, particularly for the front section of the frame.

Fabrication

To reduce manufacturing errors to a minimum, all parts were designed to be machined on the Department's CNC Centre, consisting of a 3-Axis Milling machine and a 2-Axis Lathe.

However, the work envelope of the CNC mill was only 300mmx250mmx250mm (Length, Width and Height). Therefore each module (or the components that it consisted of, if it was not one-piece) had to fit comfortably inside the mill's work volume.

Design Criteria

As with any remote self-powered application, the lighter the platform the less demanding it is in terms of power requirements. Therefore, use of **F**inite **E**lement **A**nalysis (**FEA**) techniques to determine the optimal design in terms of structural integrity and weight were considered.

Previously regarded as a post-design add-on, the infusion of aesthetic appeal to the platform should proceed conjointly with the Mechanical and Electrical design, ensuring the 'bot was not only functional, but also pleasing to the eye.

Taking into account these design criteria, the following sections analyse the design of each module.

Drive Units

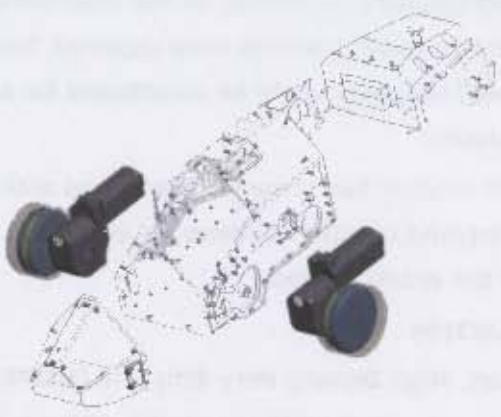

Figure 3-8: Drive Units

As eRobot was designed destined initially for marine inspection, its capacity to adhere to vertical surfaces was critical. As such, design and fabrication of the drive

units was one of the most critical aspects of the design. A number of design iterations had to be performed before a solution was reached.

In the initial (1st Generation) prototype, electric-screwdriver motors were used. These provided insufficient power to effectively move the platform vertically, and therefore other motors had to be sourced.

A relatively inexpensive alternative was to use standard windscreen-wiper motors, which are readily available from scrap yards and motor spares shops. They run off of 12V, and are specified to provide up to 1Nm of Torque [28]. However, they are notorious for power consumption (running under full load, it was seen that a single motor could consume up to 3 Amps at 12V!).

Preliminary housings were developed and tested to evaluate the motor's performance.

FIGURE 3-9: GEARBOX COMPONENTS (LEFT) AND GEARBOX (RIGHT)

Shown in **Figure 3-9** are the components of the first gearbox and the gearbox itself. This initial 'box was a 3-piece assembly, and there were issues in locating the rotor completely accurately within the housing. Any amount of play led to either the rotor locking completely, or failing to mesh with the helical drive gear. However, with careful assembly (and the use of shims) two functional gearboxes were assembled and used in an initial test vehicle (see the **Frame** section), showing the concept to be feasible.

Once the validity of the design was proven, an improved version of the gearbox was designed. The new design reduced the number of structural components from three to two (allowing for more precise location of the rotor) in addition to incorporating weight saving features.

FIGURE 3-10: GEARBOX EXPLODED

Figure 3-10 shows an exploded view of the final design. This design also incorporates a notched aluminium shaft encoder, as well as recesses for the accompanying opto-isolator. In addition, a temperature sensor was mounted on the interior of the motor casing to allow for monitoring of the thermal performance of the motor.

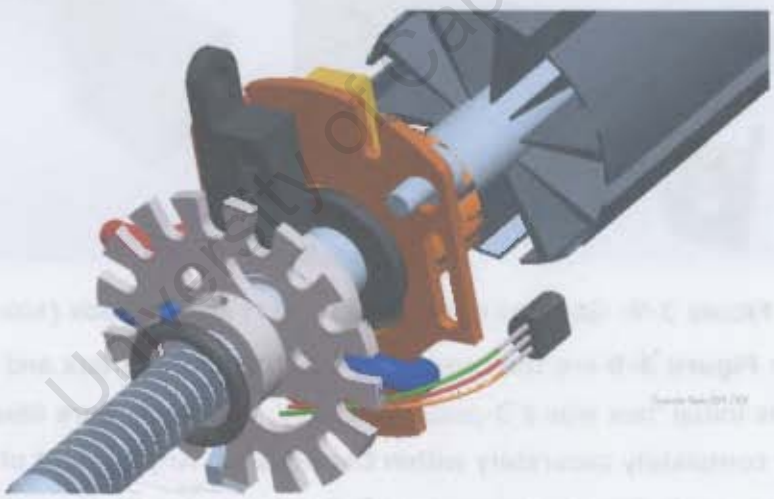

FIGURE 3-11: GEARBOX SHOWING SHAFT ENCODER AND TEMPERATURE SENSOR

In order to adhere to a vertical ferro-magnetic surface (such as a ship-hull) eRobot made use of permanent rare-earth Neodymium magnets. However, neodymium rare earth magnets are very brittle as a result of the sintering process and require some sort of protection. The magnets are also very smooth, and afford almost no traction. As such, a wheel assembly had to be designed that would accommodate the magnet and allow it to adhere to an underlying ferro-magnetic surface, while simultaneously protecting it from the harsh working conditions and providing grip on the surface.

Material selection for the wheels was not trivial, and a variety of compounds and techniques were evaluated before a solution was reached.

FIGURE 3-12: TRIAL WHEELS

Initially, plain electrical shrink-tubing was used around the wheel; however this exhibited very poor traction and wear characteristics. On consultation with **A**dvanced **M**aterial **T**echnologies (**AMT**) (a Cape Town based composite speciality company), it was decided that a casting-silicon "shoe" would be preferable to plain shrink-wrap.

In **Figure 3-12** (left), the (destroyed) silicon shoe can be seen in the lower-right corner. Although displaying better traction and wear characteristics than the shrink-tubing, it lasted a mere 10 minutes of testing.

An alternative composite, a casting poly-urethane was evaluated next (**Figure 3-12**, right), and this showed exceptional traction capabilities. However, resilience was again an issue and the shoe did not last substantially longer than the previous attempts.

It was noted that the casting procedure used left a substantial number of air bubbles in the mix, degrading the structural integrity of the compound. In addition, the ridged galvanised steel discs whose purpose was to provide a greater area for adhesion of the matrix only served to initiate tears on the inner surfaces of the shoe, rapidly leading to failures.

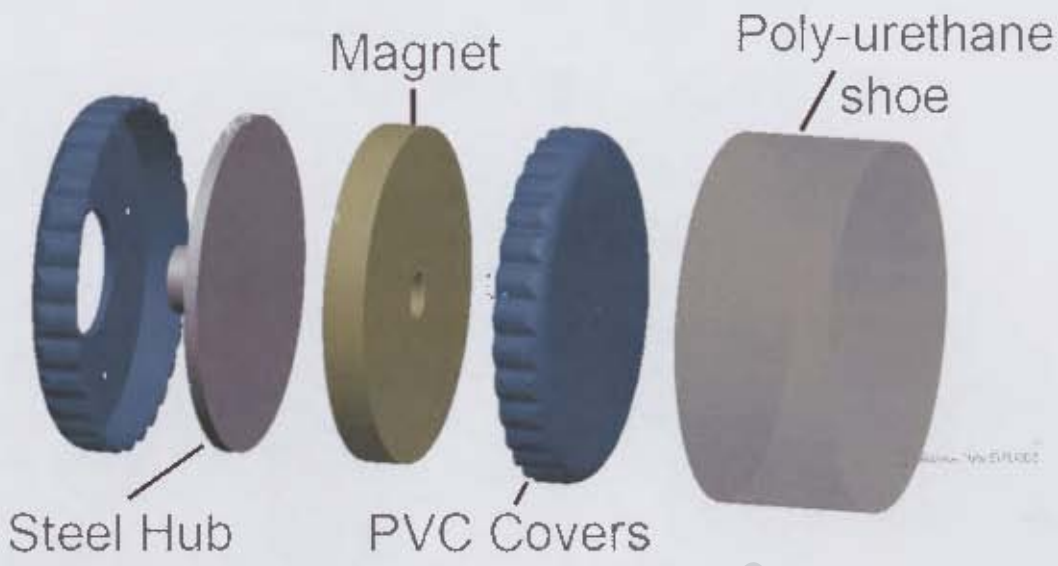

FIGURE 3-13: RE-DESIGNED WHEEL ASSEMBLY

The solution (as seen in **Figure 3-13**) was to redesign the wheel assembly with PVC covers eliminating the sharp inner edges. In addition casting of the entire wheel was performed in a vacuum chamber to reduce the number of air bubbles present.

FIGURE 3-14: MACHINING THE MOLDS (LEFT), THE MOLD ASSEMBLY (CENTRE) AND THE VACUUM SETUP (RIGHT)

Shown in **Figure 3-14** are the steps for casting the wheel. First the mold negative was machined on a CNC milling machine (left), the wheel assembly to be cast was assembled (centre) and placed in a home-made vacuum chamber (right) which consisted of a vacuum pump and a reinforced Tupperware© container. Setting time was specified on the packaging to be 16 hours, however due to the cold weather at the time (temperatures were in the 15-19°C range), each wheel took approximately 24 hours to set completely.

FIGURE 3-15: FINAL WHEEL ASSEMBLY

This final revision, with smoothed internal surfaces and reduced air-bubble content exhibited markedly better performance in terms of both traction and resistance to wear, and in fact lasted the entire length of the project without needing replacement.

FRAME

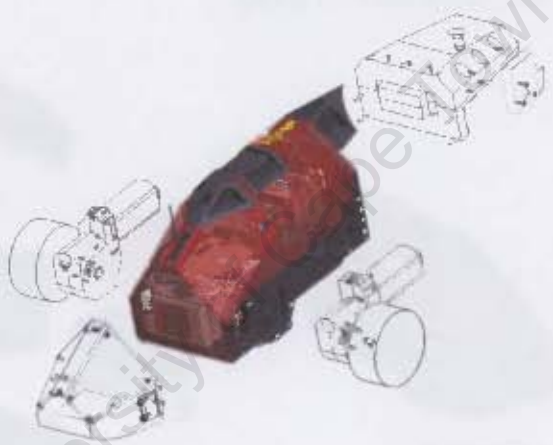

FIGURE 3-16: FRAME

Core to the entire robot is the main chassis or **frame**. The premise behind the frame was that it would remain central to the system, capable of interfacing with a variety of drive units and sensor arrays.

In order to evaluate the viability of the frame, and its capacity to carry load, a trial unit was constructed. Shown in **Figure 3-17** overleaf is the preliminary chassis used to evaluate the performance not only of the chassis as a structural member, but also of the load carrying capabilities of the robot and the viability of using the rear wheel as a free-slipping jockey.

FIGURE 3-17: TESTING CHASSIS

In this test the robot chassis was powered from a standard bench power-supply, and its ability to manoeuvre in the vertical plane was evaluated. (For the videos, please see the accompanying DVD).

FIGURE 3-18: EXPLODED VIEW OF FRAME

As the central module of the entire vehicle, the frame was required to house all the necessary electronics and power supplies for the add on modules. Specifically, this comprised the **P**ower **S**upply **U**nit (**PSU**), the **E**lectronics **M**odule (**EM**) and the **C**omputing **M**odule (**CM**). Also visible in the above image are the canopy sections, which served both to protect the internals of the vehicle and accommodate the GPS Active Antenna (in the rear canopy unit) to ensure the uBlox had an unobstructed sky-view.

Assembly and disassembly operations are crucial in a constantly-evolving development project. As such, the **CM** and **EM** were designed to be easily extractable. The CM slides into grooves machined into the frame, while the EM is fastened and unfastened by means of 4 easily accessible hex-bolts.

FIGURE 3-17: TESTING CHASSIS

In this test the robot chassis was powered from a standard bench power-supply, and its ability to manoeuvre in the vertical plane was evaluated. (For the videos, please see the accompanying DVD).

FIGURE 3-18: EXPLODED VIEW OF FRAME

As the central module of the entire vehicle, the frame was required to house all the necessary electronics and power supplies for the add-on modules. Specifically, this comprised the **P**ower **S**upply **U**nit (**PSU**), the **E**lectronics **M**odule (**EM**) and the **C**omputing **M**odule (**CM**). Also visible in the above image are the canopy sections, which served both to protect the internals of the vehicle and accommodate the GPS Active Antenna (in the rear canopy unit) to ensure the uBlox had an unobstructed sky-view.

Assembly and disassembly operations are crucial in a constantly evolving development project. As such, the **CM** and **EM** were designed to be easily extractable. The CM slides into grooves machined into the frame, while the EM is fastened and unfastened by means of 4 easily accessible hex-bolts.

HDPE is relatively dense, and therefore various weight-saving features were incorporated into the design; however care had to be taken to ensure that the frame still had the required rigidity to hold the entire vehicle together.

FIGURE 3-19: FRAME WEIGHT REDUCTION (LEFT) AND BATTERY INSERTS (RIGHT)

Shown in the left panel of **Figure 3-19** are some of the weight saving insets that were machined in to reduce the overall weight of the frame. The right panel shows the PSU with its associated switches. These **S**ingle-**P**ole **D**ouble-**T**hrow (**SPDT**) centre-off switches allowed for each battery to have three modes: On, Off and Recharge, allowing for the batteries to be replenished from an external charger without having to remove the module.

FIGURE 3-20: FRAME: PARTIALLY ASSEMBLED (LEFT) AND FULLY ASSEMBLED (RIGHT)

Figure 3-20 shows the frame in various stages of assembly. Visible in the left image is the partially assembled frame with the rear brace and the bottom cover yet to be assembled. The right image shows the assembled unit, with the protective plastic layer still covering the Perspex bulkhead.

Also visible in the images are the circular openings for the cooling fans. These fans were required to regulate the temperature of the on-board electronics and were designed in such a way that air was drawn over the motor casings providing simultaneous cooling for the drive units.

Tail Unit

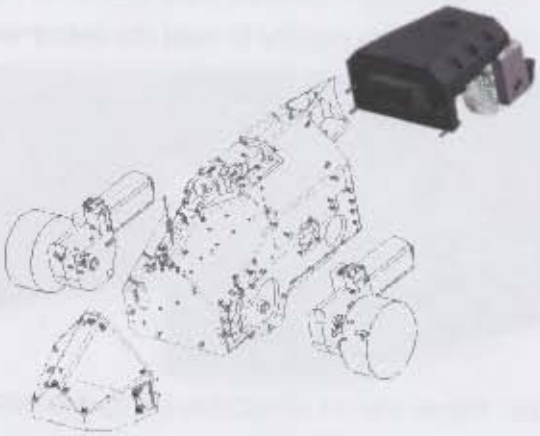

Figure 3-21: Tail Unit

In order to overcome the difficulties of the previous prototype, the drive configuration was modified from 4 to 3, with the rear wheel being a "jockey" wheel. The function of the **T**ail **U**nit (**TU**) was to allow the jockey wheel to rotate completely around its axis, allowing the robot to be driven forwards and backwards with equal ease.

As with all of the modules, design of the TU had to allow for the fact that other modules could be attached, and therefore should not dictate design requirements specific to its needs. Therefore, a slot and four 3mm bolts provide a standardised interface for securing whatever further modules may be attached.

Figure 3-22: Rear (left) and exploded (right)

As can be seen in **Figure 3-22**, the unit is mainly an assembly of two members, a top and bottom section which bear the structural load. The jockey wheel itself runs on a double bearing set. The top bearing is a conventional deep-groove bearing, while the bottom one is a thrust bearing.

The top and bottom members are fastened together by means of an array of nine 3mm hex-bolts, ensuring structural rigidity.

As the rear's capacity to handle load was of primary concern, a basic **F**inite **E**lement **A**nalysis (**FEA**) was conducted on the assembly, to ensure it would not deform substantially under load.

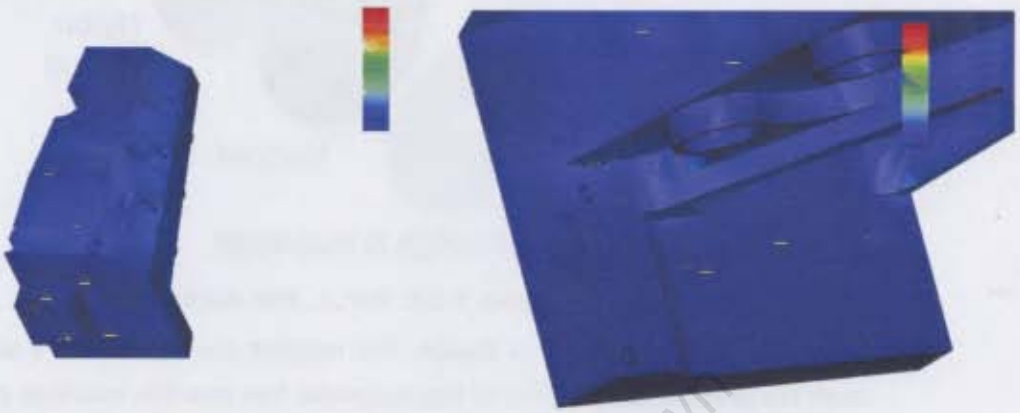

FIGURE 3-23: FINITE ELEMENT ANALYSIS

Figure 3-23 gives a graphical representation of the analysis, and the maximum deflection of the shaft under load was only 2 millimetres, which was deemed acceptable.

A uniformly distributed load of 10 kilograms was placed on the internal bearing recess of the lower section. This was 125% of the design weight of the entire robot, leaving a large safety factor. The resultant maximum von-Mises stress was 1.9MPa, and with the yield strength of HDPE being approx 25MPa, there was a substantial safety factor for the assembly. In the above figure, the red gradient corresponds to 2.0 MPa, whilst blue is unstressed.

This led to the development of the machining models and the production of the required G-code for the CNC. Both sections were fabricated from solid blocks of HDPE. In both cases multiple machining operations were required, more for the top section (5 as opposed to 3 for the bottom section).

One major difficulty in the fabrication of the tail unit was the hitch sub-assembly. In the initial trial design, the jockey wheel ran on two silver-steel half-shafts and mating hubs, and was covered in electrical shrink-tubing to allow for slippage. However this arrangement did not provide the wheel with continuous smooth rotation, due to constant misalignment of the half shafts. This meant that the magnetic disc itself would have to be modified to allow a shaft to pass through. Machining of the shaft hole was a delicate procedure as the magnets themselves were very brittle; however Mr. Glen Newins of the Mech. Eng. workshop did an excellent job.

FIGURE 3-24: HITCH: EXPLODED

Figure 3-24 shows the final design. The magnet accommodates a solid aluminium shaft (to prevent channelling of the magnetic flux into the bearings causing a reduction in operating life) and is encompassed by a nylon shroud. The entire sub-assembly, including the bearings and housing, is attached to the aluminium hitch by means of six 3mm hex bolts.

Shown in **Figure 3-25** are the two main elements of the tail unit during manufacture:

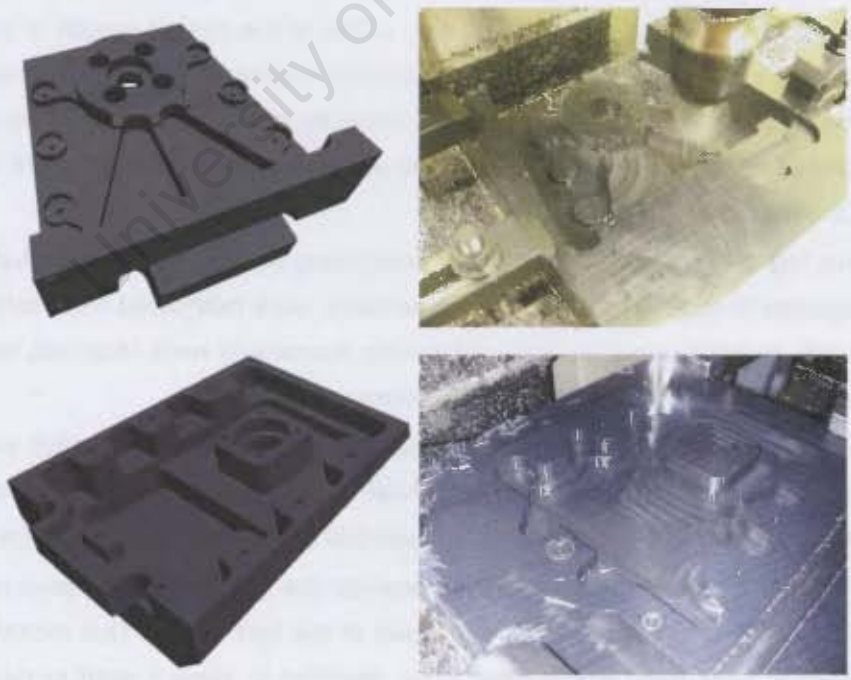

FIGURE 3-25: MACHINING OF TAIL UNIT COMPONENTS

In total, the fabrication of the final drive units took over 10 hours, with 12 individual machining operations and one combined operation. The structural

stiffness of the assembly was excellent, and the unit itself was aesthetically pleasing.

FIGURE 3-26: TAIL UNIT ASSEMBLY

Figure 3-26 above shows various shots of the tail unit in assembly. The ribs visible in both the centre and left frames of **Figure 3-26** were inserted into the design after the FEA analysis during the design process showed excessive deflection of the assembly under load.

PAYLOAD BAY

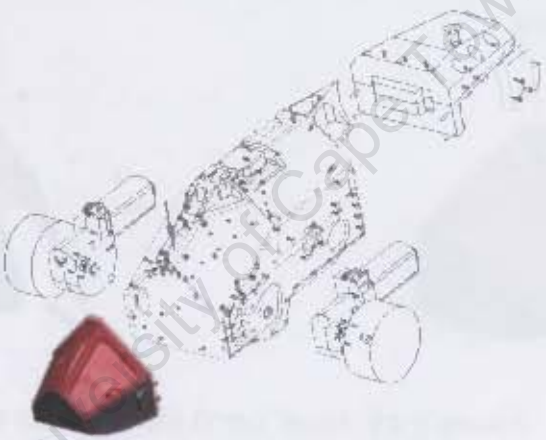

FIGURE 3-27: PAYLOAD BAY

As the name suggests, the payload bay is responsible for accommodating the NDE/inspection equipment for the vehicle. The modular design of all the sections allows for the replacement of one inspection module for another with minimal effort.

For this test vehicle, a FireWire® camera was used to capture images of the underlying surface, to allow for post-examination. This particular camera, a Fire-i® camera was capable of capturing a 640 pixel x 480 pixel stream at 30 fps in video mode. Although more suited to streaming media, the camera was designed to be used in still capture mode.

FIGURE 3-28: FRONT SHOWING FIREWIRE CAMERA

Figure 3-28 shows the Fire-i and its associated connector. Also visible in the image are the weight-reducing volumes that were milled out to keep the weight of the bay to a minimum.

FIGURE 3-29: FRONT (LEFT) AND EXPLODED VIEW (RIGHT)

The bay is of single-piece construction, and required 18 operations and a total machining time of approximately 6 hours to complete (not including set-up and programming). Initially, the bay was going to be constructed of several inter-locking sections (as the Hercus CNC lacked the work envelope to fabricate it out of one solid section) however the Department of Mechanical Engineering took delivery of a bigger CNC in late October 2006.

This allowed the author to re-design the bay to take advantage of the greater work-volume of the bigger CNC. As such, the bay is more rigid and required fewer fasteners than the comparative multi-piece design.

FIGURE 3-30: FRONT: MACHINING

Shown in **Figure 3-30** is the single-piece bay as designed (left) and being machined on the CNC (right). The operation in progress is the smoothing of the faceted edges using a ball-nose cutter. In order to obtain a quality surface finish, the cutter is stepping along at 0.3mm intervals, and as such constituted one of the most time-intensive operations.

MANUFACTURE & ASSEMBLY

Manufacture of the platform was accomplished almost exclusively on the CNC machinery of the Department of Mechanical Engineering. Design for CNC manufacture allowed for more complex geometry than would otherwise be possible. In addition, once the author had shown proficiency in the CNC process, he was free to use the machines at any time. This allowed for a much greater scope of independence than would otherwise be possible.

An overview of the design process from concept to construction for one of the parts that was machined (there were over 30 in total) is given below.

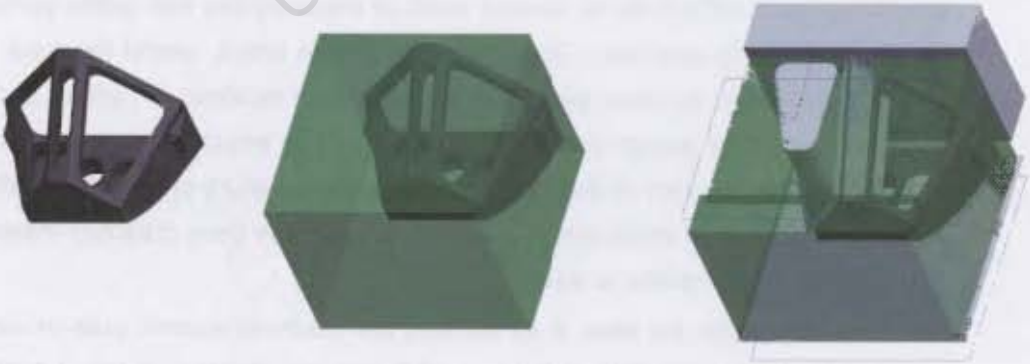

FIGURE 3-31: PART, WORK-PIECE, MANUFACTURING MODEL

On the left of **Figure 3-31** is part to be manufactured once design has been completed in Pro/ENGINEER. Pro/ENGINEER is a parametric 3-dimensional **CAD** (**C**omputer **A**ided **D**esign) software package widely used in industry. Boeing, Airbus and John Deere are some of the biggest users of Pro/ENGINEER software.

It is, of course, very important to design with manufacture in mind, specifically with how the component is to be located and held in the CNC machine. This particular component (the nose section of the **P**ayload **M**odule (**PM**)) required no less than 12 machining operations for a sum total of 24 NC sequences.

Assembly of the **workpiece** and component in the Pro/MANUFACTURE environment is the next step in the process. Pro/MANUFACTURE is an add-on multi-axis prismatic machining module that allows Pro/ENGINEER designs to be fabricated on a CNC machine.

The workpiece represents the stock that is going to be machined to leave the final part. This step is optional, however omitting the workpiece can lead to visualisation difficulties of how the component actually looks when the process gets complicated (for the operator, not the software).

FIGURE 3-32: TOOL-PATH GENERATION & CHECK

Pro/MANUFACTURE allows for several ways of checking the tool-paths generated for the manufacturing geometry. There is an on screen check, useful for quick debugging, as well as more advanced modules such as Vericut©, which gives other capabilities such as gouge-checking (checking to see whether the tool rapids incorrectly into any part of the job). The parametric nature of Pro/ENGINEER (the ability to modify any attributes of a feature after it has been created) means that modification of tool paths is relatively easy.

Once the tool paths are seen to be correct, the machine-specific post-processor is invoked. With the help of Gary Phipson of Automated Reasoning (local distributors of Pro/ENGINEER software), the initial post-processor was developed for the Hercus® CNC Milling Centre (which previously had relied on 2D CAD software of limited capacity).

At this point it should be noted that mechanical design of the robot had to take into account the limited work-envelope of the Hercus. The introduction of the new Syntech CNC in late November had a minimal effect on the project.

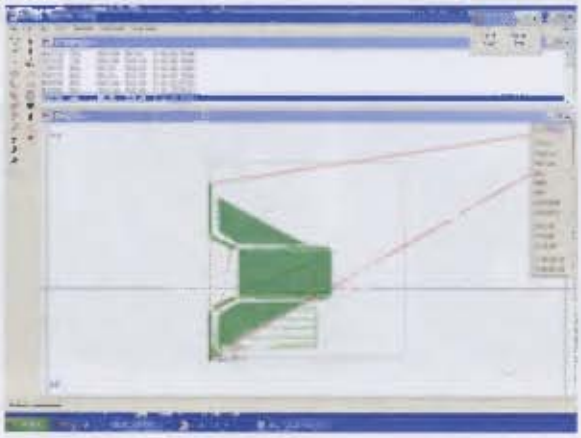

FIGURE 3-33: G-CODE SIMULATION

The machine G-code generated by the post processor was checked on a simulator before it was taken to the machine. This allowed for last-minute error-checking to prevent errant code from causing an expensive mishap later on. Shown below is a chronological cross-section of the CNC machining process as it matured:

FIGURE 3-34: BASIC MANUFACTURE

Shown above in **Figure 3-34** are some of the earlier machining attempts. The leftmost image was a failed attempt at the Tail Unit top section. Centre and right are images of the final unit.

FIGURE 3-35: DIFFERENT MATERIALS & TECHNIQUES

Various materials were used in the project, all providing different challenges. The aluminium tail hinge is shown on the left, with one of the Perspex© **C**omputing **M**odule (**CM**) supports shown in the centre. Manufacture of the side panels of the

frame was testing, in that accurate locating of the part (to perform the reverse-side machining operations) was tricky as the component had complex and non-perpendicular geometry. This particular problem was solved by machining the **negative** shape of the part into a block of wood, and pressing the component in.

FIGURE 3-36: MULTI-PROCESS MACHINING

Some components had to undergo multiple machining operations. The drive units were composed of two individual components (one of which is shown on the left in **Figure 3-36**) which required machining on both the top and bottom surfaces. These were then assembled together and the bearing recesses and locating holes were machined in (**Figure 3-36**, centre). Finally an aesthetically appealing round was machined in with a ball-nose cutter (**Figure 3-36**, right).

FIGURE 3-37: EXTENDED ONE-PIECE MACHINING

With the introduction of the larger CNC machine, it became possible to perform more complex machining tasks. The Payload Bay frame has been discussed previously, machining sequences from which are shown in **Figure 3-37** above. On the left is the roughing sequence (identifiable by the contour-like ridges left behind), with the surfacing sequence on the right hand side.

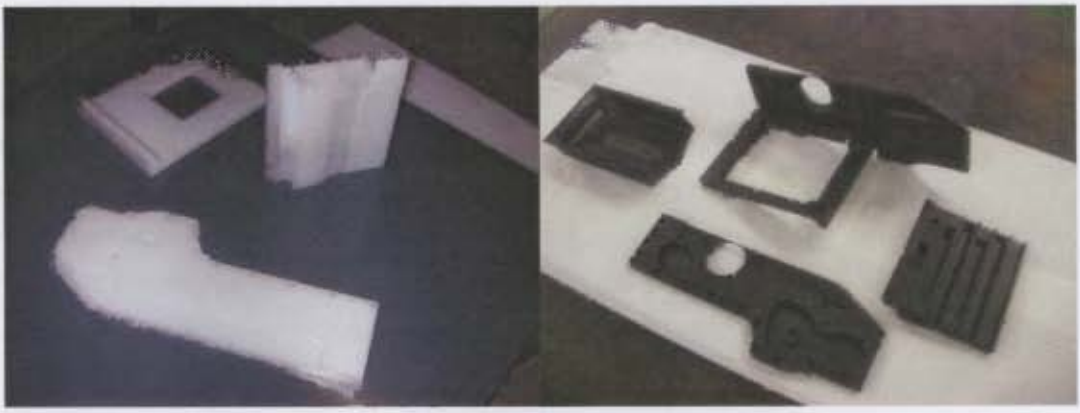

FIGURE 3-38: INITIAL PROTOTYPES (LEFT) AND FINAL COMPONENTS (RIGHT)

Finally, **Figure 3-38** shows the differences in the frame sections of the initial prototype (left) and the final sections (right).

3.3 Electrical Design

Design Envelope

As design for all individual modules was performed concurrently, a design volume or **envelope** had to be allocated for the required low-level electronics. It was uncertain at the time of allocation how much space would be required for the electronics module. However, it was known that the module would be required to:

1. Dissipate the heat generated by the motor driver circuitry
2. Interface with the uBlox **G**lobal **P**ositioning **S**ystem unit
3. Electrically and physically separate the computing and electronic circuitry

Use of Pro/ENGINEER and Eagle CAD (a freely available **E**lectrical **C**omputer **A**ided **D**esign (**ECAD**) package) allowed for the design of boards that were electronically correct, in addition to being of the right form to integrate seamlessly with the mechanical design.

Design Outline

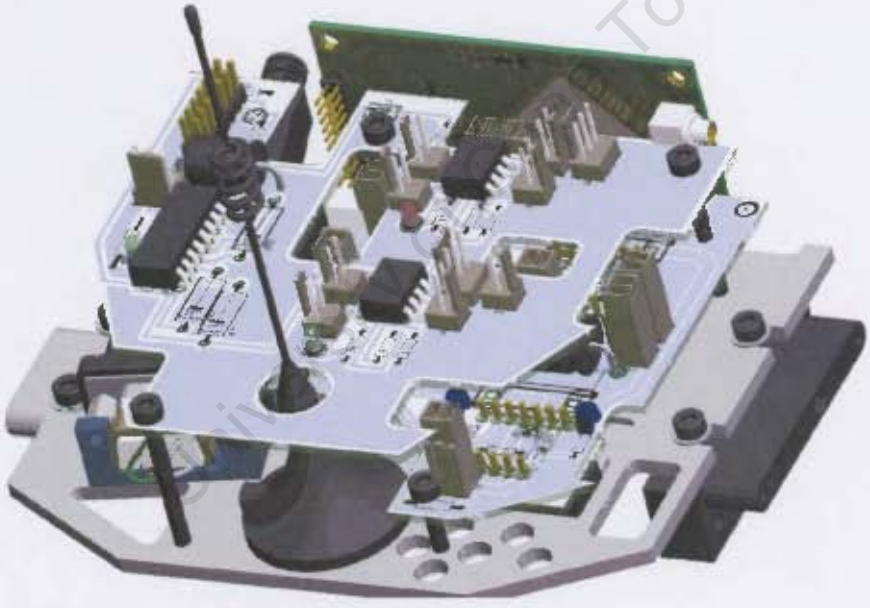

FIGURE 3-39: **E**LECTRONICS **M**ODULE (**EM**)

From the allocated design volume it was possible to segment the electrical components into layers, a short description of which is given below (moving from the bottom layer upwards):

First Layer – Power Circuitry

This layer was responsible for isolating a motor-control signal from the PC104 **C**omputing **M**odule (**CM**), and accommodating necessary electronics for the drive motors.

SECOND LAYER – GPS INTERFACING CIRCUITRY AND SPEED CONTROL

Use of the GPS board required providing it with supply voltages, as well as a reduced voltage for antenna gain-switching, and connectors to the on-board serial ports. In addition the layer would accommodate the interface circuitry for the motor thermal and speed sensors.

THIRD LAYER –ADDITIONAL CONTROL MODULES

The third layer was designated for any other control modules that would be needed during the course of the project.

LOWER BOARD

As mentioned previously, the purpose of the lower board was to isolate a **P**ulse-**W**idth **M**odulated signal from the **CM** and deliver an amplified PWM signal (i.e. from 0V to 5V) to the input of the LMD18200 H Bridge driver chips.

For this board the H-bridge chips are mounted on the solder side. This was because the tabs of the H-bridge had to be in thermal contact with the underlying aluminium base. In this case, insets were machined into the base during manufacture, to allow for a greater heat transfer from the H-bridge to the base.

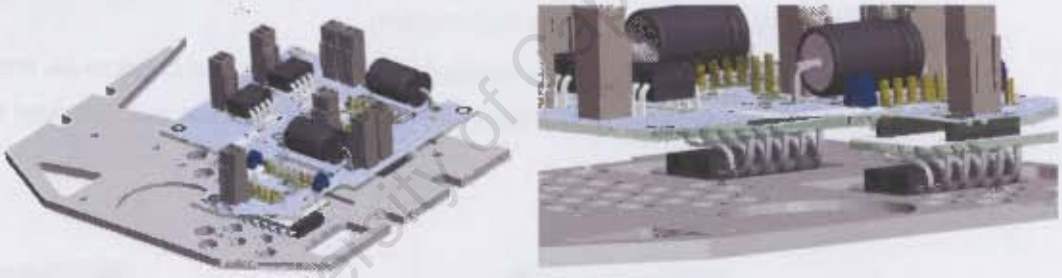

FIGURE 3-40: BOTTOM BOARD (LEFT) AND H-BRIDGE RECESSES (RIGHT)

LAYOUT

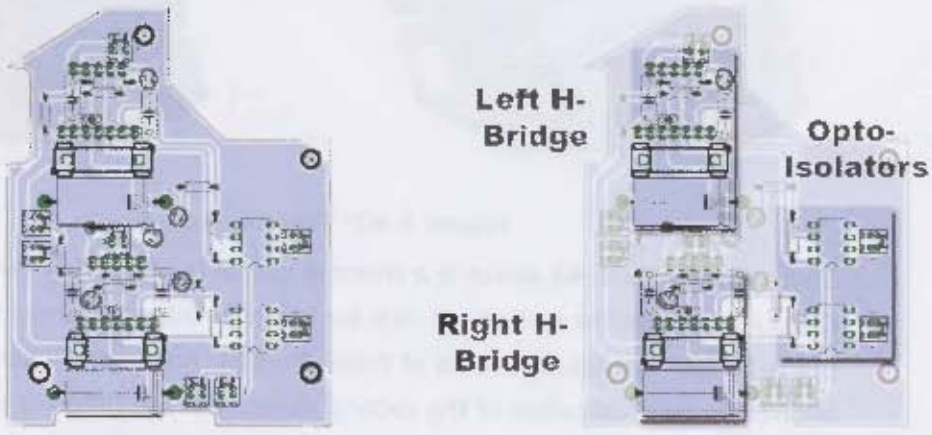

FIGURE 3-41: ELECTRONICS: H-BRIDGE INSETS (LEFT) AND UBLOX GPS (RIGHT)

Several revisions were made during the course of the project. The LMD18200 Motor Driver Chips have an integrated thermal protection circuit, which meant that once the chip's temperature exceeds 158°C, the outputs are no longer driven.

Cooling was therefore vital, and as such mounting on the underlying aluminium base was critical. This led to the initial (overly optimistic) design as shown below:

FIGURE 3-42: INITIAL BOARD

The initial design allowed for each motor driver chip to be sunk into the aluminium base, affording excellent thermal contact to the aluminium. Ultimately it proved to be unworkable, as it required each lead of the 11 pin H bridge to be routed by means of a wire onto the board itself. This led to an overwhelming number of connections as can be seen from the extreme right panel of **Figure 3-42** (dubbed unkindly "the Porcupine" by some bystanders).

As a result of this, the design was revised to incorporate the chips in an inverted position on the solder-side of the board, which is not unusual but can lead to some soldering difficulties.

FIGURE 3-43: THERMAL PLOT

Shown in **Figure 3-43** above is a thermal plot of the heat flow through the board. Clearly visible on the right-hand plot are the high-intensity areas corresponding to the H-bridge heat tabs. The use of Finite Element Analysis software in this way allowed for a visualisation of the cooling capacity of the different aluminium base designs. In this analysis, the blue region corresponds to the ambient temperature (assumed to be 25°C) with the yellow sections corresponding to the thermal maximums of the H-Bridges (i.e. 158°C).

Centre Board

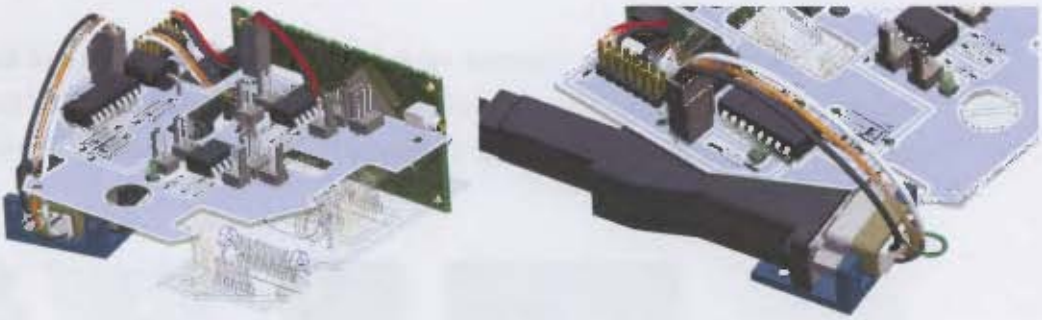

Figure 3-44: Centre board (left) and GPS interface (right)

Interfacing with the uBlox© GPS module was the primary requirement for the second (centre) board.

Due to the stacking procedure on the PC/104, both serial ports had to be sacrificed (i.e. their dedicated **I**nterrupt **Req**uests or IRQ's were required by the other boards), and so therefore a USB-to-serial converter was integrated in to the system (visible in **Figure 3-44**). A USB-to-TTL converter would have been more appropriate, as the logic levels undergoes a shift from USB to RS232 to serial; however a USB-to-serial converter was easier to obtain.

This required the use of a level shifter, as RS232 voltages operate from -3V to -15V (logic "high") and 3V to 15V (logic "low"). TTL and CMOS logic requires 0V to 5V, and so a MAX232 transceiver chip was used. The MAX232 is a **full-duplex** chip, allowing concurrent transmission and reception.

Layout

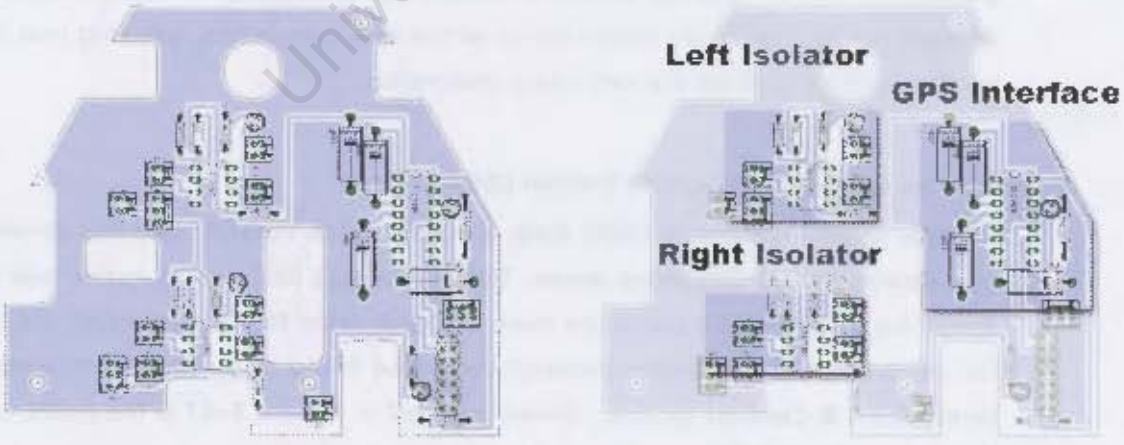

Figure 3-45: Centre board

The unusual geometry of the board is due to the design methodology used. As the base board was of primary concern to the motion capabilities of the robot, the

centre board was designed to allow access to all the Molex® connectors of the lower board.

Design of the boards was an iterative cycle between Pro/ENGINEER and Eagle CAD. A board outline was generated in Pro/ENGINEER and exported as a *.dxf* file. This was converted (by means of a script generator) into a sketch on the dimension layer of Eagle's Board editor.

FIGURE 3-46: PART->.DXF->.BRD->.TIF ->ASSEMBLY

All of the required tracks and pin placements were performed, taking care not to violate the perimeter of the board. From the board editor, a *.tif* file was exported showing all the component placements. The *.tif* file was imported back into Pro/ENGINEER, and converted into a texture. This texture was then mapped onto the initially generated board design, and then populated with 3D models of the components.

Design in this method was sometimes laborious, however it ensured that there were a minimum of interferences when the module was assembled. Provision could also be made for the minimum bend-radii of all the wire connectors, ensuring that thick wires would not prevent the unit being assembled.

DIFFERENTIAL GLOBAL POSITIONING SYSTEM (DGPS) CARD

In order to obtain accurate DGPS data, a transportable PC/104 node was developed as a dedicated GPS-streaming server. This lightweight unit's sole function was the streaming of GPS data back to the main server in order to calculate DGPS data. A full explanation of the system architecture can be found in the **Communication, Navigation & Control** section. Shown overleaf in **Figure 3-47** is the board as designed in Eagle CAD:

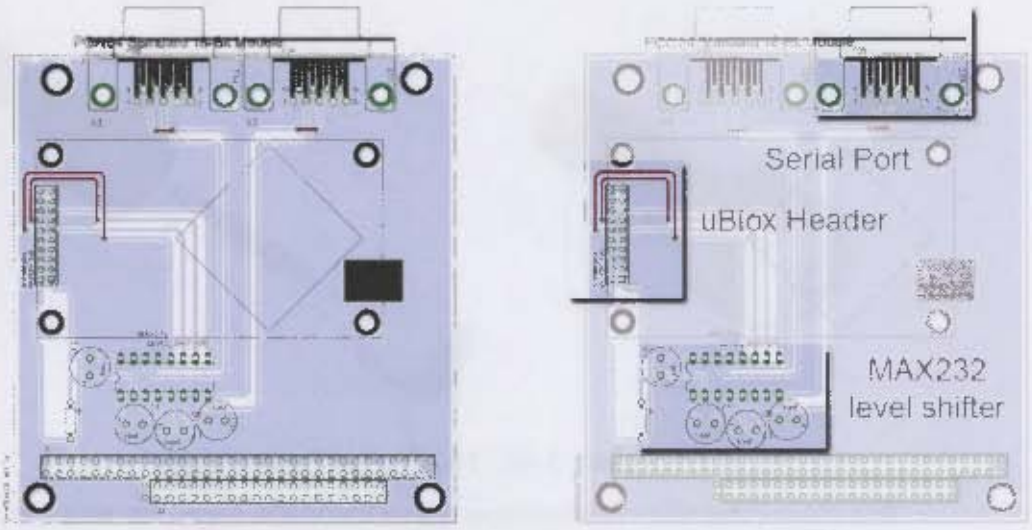

FIGURE 3-47: DGPS BOARD

The board was designed to be stackable on a standard PC/104 bus. The uBlox GPS unit used in the project has two serial outputs, and these are accommodated on the board by means of two DB9 serial headers, visible in **Figure 3-47**.

BOARD MANUFACTURE & ASSEMBLY

Fabricating boards used to be an intensive process, both financially and with respect to time. As the **EM** required exacting shapes and layouts in order to be able to integrate with the rest of the robot, it was decided to attempt to fabricate the boards on the Departments Hercus CNC 3-Axis Mill.

Documentation on the mill states the accuracy of the slides to be 0.01mm. This corresponds to a board accuracy of approximately 3mils (not to be confused, as the author initially was, with the metric slang for millimetres. 1 mil in board fabrication parlance is $1/1000^{th}$ of an inch.)

On consultation with Cadshop, a Pretoria based CNC board milling specialist, a variety of milling tools were purchased. The width of the tools ranged from 0.4mm (15 mils) to 0.7mm (27 mils). The tools shipped were long series, and it was obvious that some sort of tool adaptor would have to be constructed to prevent tools failing repeatedly at the neck.

FIGURE 3-48: TOOL SUPPORT AND ADAPTOR

This meant that the minimum spacing (track/track, track/via, etc) was 27 mils. A set of design rules was constructed in Eagle CAD to ensure that this was not violated. However, 27mil spacing meant that tracks could not be routed between IC leads. This, in conjunction with the fact that only a single-sided board could be fabricated with any accuracy, gave rise to a crowded first board.

FIGURE 3-49: BOARD MANUFACTURE: TESTING

Shown in **Figure 3-49** are the initial testing steps that were performed to see if in-house board fabrication was possible. An end-mill sharpened to a cone was the initial test-tool and as can be seen from the centre photograph the tracks (although very burred) can be easily discerned.

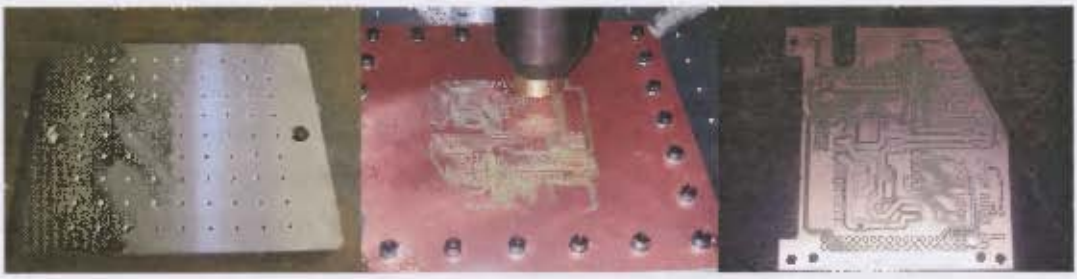

FIGURE 3-50: BOARD MANUFACTURE: PRODUCTION

In order to ensure that the board was completely flat when machined (as the blank PCB had a tendency to curl) a base plate was ground, then drilled on the CNC and tapped. This allowed for the board to be fastened by no less than twenty-six 3mm bolts, ensuring the board was uniformly flat.

ASSEMBLY

FIGURE 3-51: ASSEMBLED BOTTOM BOARD

Figure 3-51 shows the end result of the manufacture, with the components soldered in and the H-Bridges on the solder side ready for incorporation into the electronics module.

Nearing the end of the project, it became possible to use the Department of Electrical Engineering's LPKF PCB Milling Machine. All boards after the initial drive board were then manufactured on the LPKF, allowing for tighter tolerances, in the order of 10mils.

In **Figure 3-52** the base and bottom board of the **EM** assembly can be seen, as compared to the initial board. On the right of **Figure 3-52** the board is being installed into the dedicated electronics bay of the robot.

FIGURE 3-52: BOARD ASSEMBLED (LEFT) AND INSTALLED IN ROBOT (RIGHT)

4. Communication, Navigation & Control

4.1 Embedded Computing

Central control and communication for the robot platform was achieved with use of an embedded PC/104 stack. The PC/104 format is a particular computing standard that promotes stacking – that is, various modules can be stacked progressively onto each other adding capabilities to the base motherboard, and is very common in **A**utomated **T**eller **M**achine's (**ATM**'s) and other high intensive embedded applications.

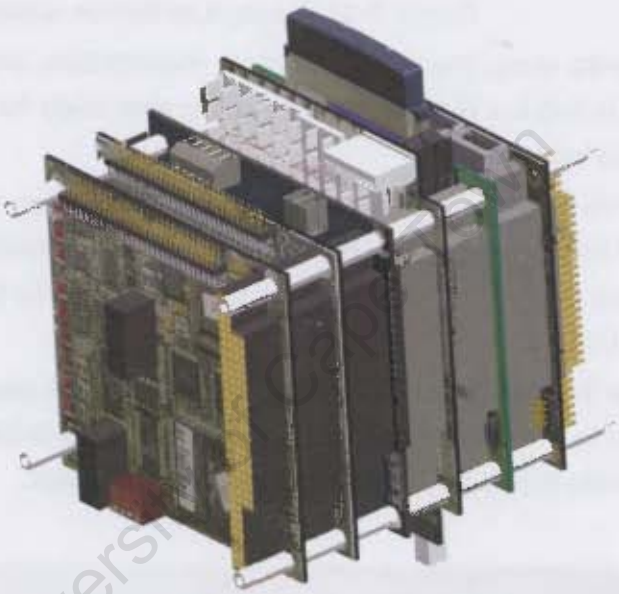

Figure 4-1: The PC/104 "stack" (rendered)

Shown above is a Pro/ENGINEER rendering of the PC/104 stack. The stack itself is a mixture of **RTD Embedded Technologies** Digital I/O boards, and **Advantech** conventional PC/104 and PC/104-*Plus* components.

Hardware Description

As mentioned previously, the PC/104 architecture is very modular and used for a variety of embedded tasks where robustness and size is important. Amongst other things, PC/104's can be found in vending machines, medical instruments and industrial control systems. The system used in this case is also PC/104-*Plus* compatible, meaning both ISA and PCI buses are available.

More information on the architecture can be found at the PC/104 Embedded Consortium's website. [29]

PCM-3370 & Power Supply

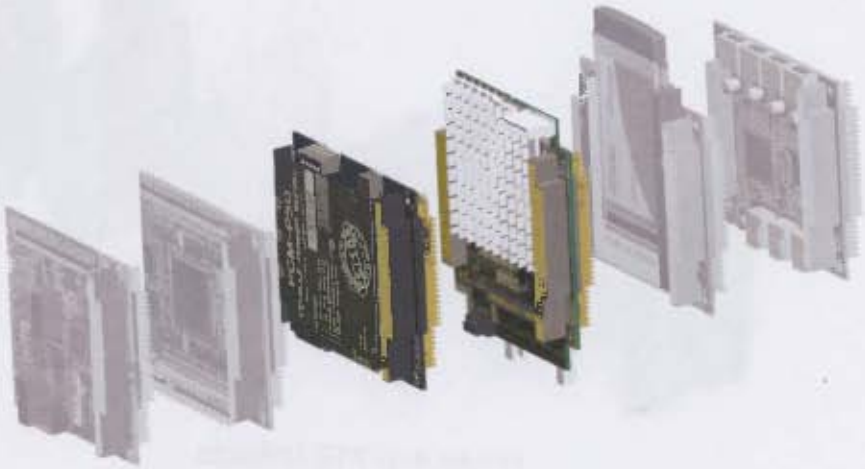

Figure 4-2: Advantech PCM3370

Each PC/104 unit is commonly referred to as a "stack". Each stack must have a motherboard and **C**entral **P**rocessing **U**nit (**CPU**), which together is commonly referred to as a **S**ingle-**B**oard **C**omputer (**SBC**). This SBC was an Advantech PCM-3370, running an **U**ltra **L**ow **V**oltage (**ULV**) Celeron® 650 processor, with 512Megabytes of RAM. The board accommodated both PC/104 and PC/104-*Plus* connectors, allowing the addition of the **R**eal **T**ime **D**evices (**RTD**) data acquisition boards and the USB and **PCMCIA** expansion boards. In its factory configuration, the PCM-3370 had 3 free interrupts available for peripheral devices, however the **B**asic **I**nput-**O**utput **S**ystem (**BIOS**) allowed for peripherals (such as the on board USB, serial ports, Ethernet port and so on) to be disabled, freeing up resources.

The PCM-3370 was a power-hungry unit, requiring two 11.1**V**olt Lithium-Ion batteries configured in parallel in order to provide sufficient power to the unit. In the cases where the battery voltage started to drop (and were not capable of providing 3 Amps peak current) the unit would exhibit erratic boot behaviour.

A 50W PCM-P50 power supply regulated the power from the batteries and provided +12V, +5V, ground, -5V and -12V supplies. Unfortunately, the power supply did not have a through-header for the PC/104-*Plus* bus, which required the stack to be assembled in a certain order.

DM6420

FIGURE 4-3: RTD DM6420

Real **T**ime **D**ev ces (**RTD**) are manufacturers of a large variety of "computer modules and systems for Industrial and Aerospace Applications" [30]. In particular they develop a large number of **I**nput/**O**utput (**IO**) devices in the PC/104 form factor. One of these boards that the Department possessed was a DM6420 Data Acquisition board, with 8 differential (16 single-ended) analogue input channels, a 12 bit **A**nalogue-to-**D**igital **C**onverter (**ADC**) and a host of timers and counters, all useful for sensor monitoring and sampling.

DM6816

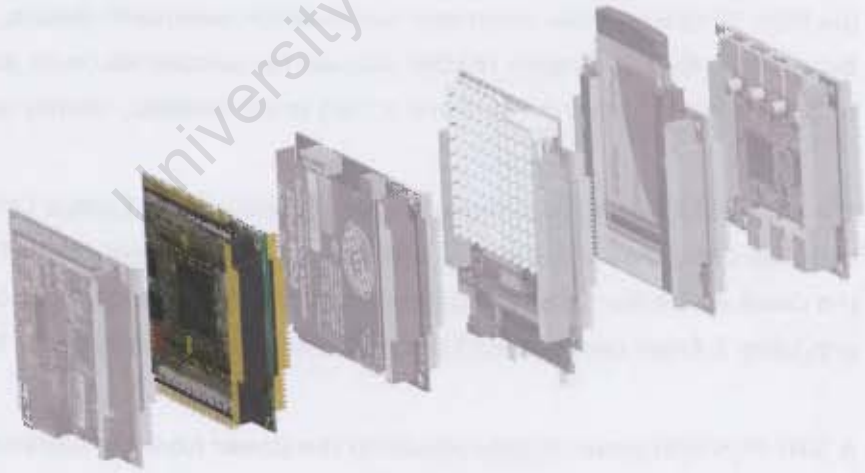

FIGURE 4-4: RTD DM6816

Also developed by RTD is the DM6816, which is a **P**ulse **W**idth **M**odulator (**PWM**) and Digital I/O board. The DM6816 has 8 dedicated 8-bit PWM channels and 8 digital I/O ports, making it very useful for controlling motors.

PCMCIA Expansion Board

Figure 4-5: Advantech PCMCIA Expansion Card

Wireless networking capacity was provided by the PCMCIA expansion board, which had two slots for Type I/II/III or CardBus cards. In the case of eRobot, an 802.11g WiFi card was used. In conjunction with the booster aerial, the card had a rated working range of 1km. This was very optimistic, however as the network became unstable (excessive numbers of dropped packets) over 250 metres.

IEE1394 FireWire©/USB 2.0 Expansion Board

Figure 4-6: FireWire©/USB 2.0 Expansion Board

As the PCM-3370 motherboard only had two USB 1.1 connections, an add-on expander board was used to provide 3 FireWire© ports and two USB 2.0 ports. However, the **usb-uhci** and **usb-ohci** Linux drivers would not allow peripheral access to **both** the on-board and the expansion board ports. Therefore the low-speed native USB 1.1 ports were sacrificed for the add-on USB-2.0 ports.

Operating Systems

eRobot:

RedHat Linux was chosen as the operating system for the robot. This choice was made fairly early on in the development cycle, for a number of reasons.

Firstly, it was observed that the loading and unloading of drivers in Windows® 2000 was sometimes erratic. This may have been due to the way the device drivers were loaded (i.e. only when calls were made to the device driver). Also, nodes on the wireless network had a nasty habit of displacing other nodes at random times (although in retrospect this may have been due to the **ad-hoc** architecture of the network).

Secondly, from the documentation on the two Digital I/O boards, RedHat Linux 9.0 (Shrike) was the most recent open-source platform for which development had been done. As most of the chipsets that were being used were common to standard PC's, compatibility for the rest of the PC/104 components was not an issue.

Although open-source RedHat has been discontinued (and has been re-named Fedora) RedHat 9.0 was still supported as a legacy build at UCT's **L**inux **E**nthusiast's **G**roup (**LEG**) website [31].

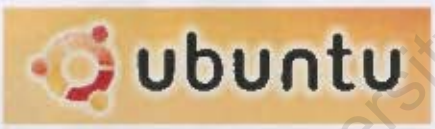

Server Cluster:

Ubuntu is a Debian-based Linux distribution that is rapidly becoming one of the most popular flavours of Linux. Ubuntu was chosen for the servers as it is relatively easy to install and configure (compared to other more powerful but complex versions such as Slackware). Ubuntu has a very user-friendly package manager known as **apt**, and this in conjunction with an Ubuntu mirror hosted at the UCT LEG website greatly simplified the installation and configuration of software packages.

DGPS Node:

The DGPS node was a minimalist PC/104 stack with Windows® 2000 as the **O**perating **S**ystem (**OS**). Use of the Windows® OS allowed access to a greater number of binaries (executable files) developed for GPS applications than

would otherwise have been possible with a Linux-only architecture. In addition the incorporation of a Windows machine shows the compatibility of the system for a variety of operating systems.

Software

Use of existing programs and code allows for a quicker development-test cycle than would be possible if code was to be developed independently for every element of functionality.

Figure 4-7: SOFTWARE: GPSD, GPSDRIVE AND APACHE

As such, open-source software was utilised as much as was feasible to develop the system. An overview of some of the most pertinent software used is outlined below.

GPSD

gpsd is an open source daemon that is capable of monitoring several GPS devices on a system and making the data available on TCP port 2947 [32]. This enabled the GPS data from the robot to be made available on the LAN.

GpsDrive

GpsDrive is a "car (bike, ship, and plane) navigation system)" [33]. GpsDrive is a Linux application that allows the plotting of a NMEA-compatible receiver on a scaleable map; however most importantly for the project it stores this data in an e**X**tensible **M**ark up **L**anguage database (**XML**) file, making the data available for post-processing. GpsDrive makes use of Gpsd to access GPS devices.

Apache

Apache is an established open-source web-server developed at the Apache Software Foundation. Apache is an easy-to-use, highly configurable web server that supports Perl, Python, Tcl and PHP scripting [34].

Shown in **Figure 4-8** overleaf is a screenshot of the website developed for the robot (a full mirror of the website is available on the accompanying DVD).

Development of the website provided the author with experience in various aspects of Web design, including **C**ascading **S**tyle **S**heets (**CSS**) for a more aesthetically pleasing site and Perl **C**ommon **G**ateway **I**nterface (**CGI**) scripting for dynamic website content.

As one of the initial hopes for the system was that users would be able to view the robot data over the web in real-time, the implementation of a web server and a **MySQL** database on the vehicle meant that the lead time to develop a fully-fledged system that would make this possible is significantly reduced.

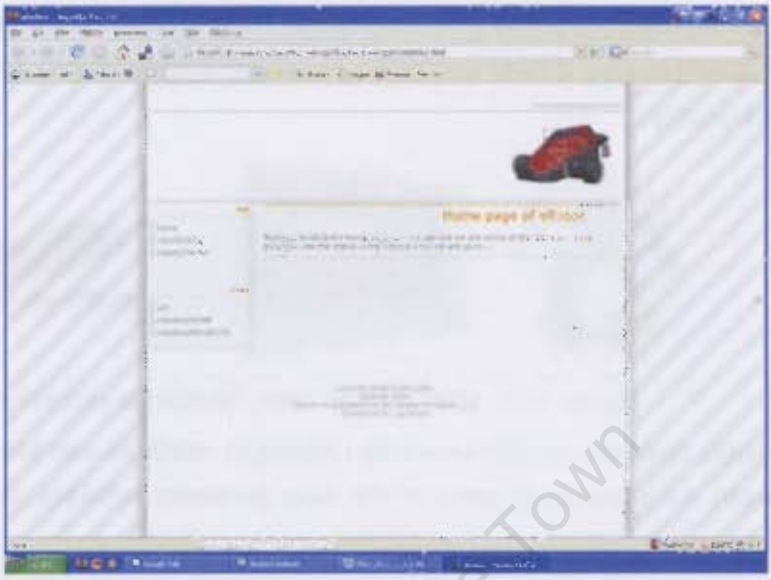

FIGURE 4-8: WEBSITE RUNNING ON EROBOT

IMAGE ACQUISITION

FIGURE 4-9: SCREENSHOT: XAWTV

Storing images from the FireWire camera would be essential in order to correlate the co-ordinate data from the positioning system with the data obtained from the camera in order to build a complete picture of the ship hull. **Xawtv** is an open-source program that allows image capture from webcam devices.

4.2 Wireless Communications

Most of the common Linux variants have a package manager utility that enables the installation and upgrading of packages and binaries. Without the package manager, installation of modules becomes a nightmare of manual dependency searches.

In order to allow the robot to download and install required packages, a LAN was set up as shown below:

FIGURE 4-10: LAN

In this LAN architecture, the server is free to access the internet. Running on the server is the **Firestarter** daemon, which is an open-source firewall package for Linux. The server then shares its network connection over the wireless network with the LAN clients, which include the robot and a laptop.

One of the major advantages of this setup is that the server acts as a gateway between the LAN clients and the internet, ensuring that malicious network traffic is filtered out. In addition, any number of clients maybe added to the LAN without excessive IT administration issues. Of course with the addition of a client that wishes to access the internet, internet bandwidth for the remaining clients is reduced.

This network type, known as a **Managed** network (as opposed to the point-to-point or **Ad-hoc** network, used in the 1st generation prototype) exhibited substantially better client performance in terms of link uptime. Previously, it was not uncommon for the robot to lose the network connection with the laptop several times an hour. In an industry setting this loss would be unacceptable, and would have potentially

far-reaching consequences if the vehicle was operating in a space that was difficult to manually access.

This basic setup, once tested and seen to be viable, was modified to implement a redundant data storage node, as well as the DGPS node.

FIGURE 4-11: FULL LAN ARCHITECTURE

The main server mounted the backup-server's disks across a **N**etwork **F**ile **S**ystem (**NFS**). Data stored on the main server was then written to the network disks every 6 hours (there were four file systems) by **cron**, a Linux scheduling daemon.

METHODS & IMPLEMENTATION

One of the major issues with the initial design was the **latency** or dead-time between when the user moves the joystick, and when the control command is implemented on the platform. At times (in the Windows™ environment), this was in excess of 15 seconds.

As such, one of the challenges of this revision was to reduce (or if possible, eliminate) the latency. One advantage of human-generated control commands (i.e. from a joystick) is that the control implementation only has to be faster than the reaction times of the user. As such a reaction time for the robot (i.e. from when the user inputs a "stop", to when the robot actually stops) must be under half a second.

PROTOCOL SELECTION

In the first generation robot, Matlab© in conjunction with a community-developed tool called **P-net**, was used to control the robot. **P-net** worked by establishing a **T**ransmission **C**ontrol **P**rotocol (**TCP**) session between a host and client node. As

mentioned previously, this delay (running under Windows© 2000) was sometimes in the order of 15 seconds, and never exhibited better performance than 4 seconds.

In order to reduce this delay, the decision was made to migrate from higher-level interpreted languages (such as Matlab) to a lower level language such as C++. In addition, a protocol switch was made from TCP to the **U**ser **D**atagram **P**rotocol (**UDP**). UDP is a connectionless protocol, meaning there is no error checking or handshaking between the host and clients.

TCP

+	Bits 0–3	4–9	10–15	16–31
0	Source Port			Destination Port
32	Sequence Number			
64	Acknowledgment Number			
96	Data Offset	Reserved	Flags	Window
128	Checksum			Urgent Pointer
160	Options (optional)			
160/192+	Data			

UDP

+	Bits 0 - 15	16 - 31
0	Source Port	Destination Port
32	Length	Checksum
64	Data	

FIGURE 4-12: TCP vs UDP

In **Figure 4-12** above, a comparison of the packet headers is made between the UDP and TCP [35] [36] protocols, with the TCP header at the top. As can be seen from the headers, the TCP protocol requires a lot more *data overhead* per packet, requiring acknowledgement from the recipient to make sure the connection is intact and data integrity will not be compromised.

Conversely, in the UDP packet, all that is required is a destination address and port. This greatly speeds up the packet transmission speed; however it comes at the (potential) sacrifice of data integrity.

However it should be noted that the potential for data loss (or "dropped packets" as they are referred to) is reduced in this network, merely because of the small number of nodes constituting the clients and the corresponding minimal amount of network traffic. As clients nodes are increased, data integrity checks will have to be implemented on all client-side applications.

CODE DIAGRAM

Shown in **Figure 4-13** overleaf is a graphical interpretation of the control flowchart for the system. On the **user side**, an operator makes use of a joystick to send commands across the wireless network to the **client** (in this case eRobot).

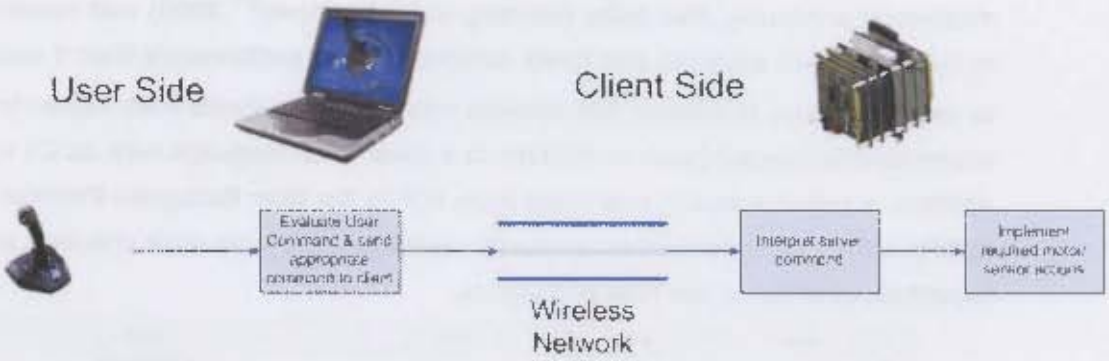

FIGURE 4-13: OVERALL CONTROL

The client is responsible for interpreting the user command and implementing the appropriate commands to the drive units or sensors. This methodology was chosen as it required an absolute minimum of network traffic – a simple command of "forward" could be transmitted from the user side, with all the required implementation (accessing the motor driver and turning both drive motors on) would be implemented by software on the client.

Open-source projects such as the Joystick Wrapper Library [37] and Practical C++ Sockets [38] enabled the author to construct a system that was very responsive to user input and had reaction times in the order of milliseconds.

For a full code listing, please see the documentation in the Appendices and the accompanying DVD.

4.3 Global Positioning System (GPS) Locating

The **G**lobal **P**ositioning **S**ystem (**GPS**) has been in widespread civilian use since the mid-nineties, allowing for relatively accurate positioning for outdoor enthusiasts. However, it was only until the removal of **S**elective **A**vailability (**SA**) in 2000 that GPS became an accurate (within the order of metres) navigational aid.

Officially known as **Nav**igational **S**ignal **T**iming **a**nd **R**anging GPS (**NAVSTAR GPS**), it is operated by the United States Air Force 50th Space Wing and consists of 24 space vehicles in medium-earth orbit in six orbital planes [39].

Price and availability of GPS capable units in South Africa have decreased and increased respectively, with several resellers in the Western Cape area having off-the-shelf development boards ready for purchase. For this project the local branch of RF Design was used for all GPS hardware requirements.

FIGURE 4-14: ANTARIS RCB-LJ RECEIVER

Shown in **Figure 4-14** above is the Antaris RCB receiver used in the project. This model is specifically designed for embedded applications, requiring a standard 5V power supply and providing a host of features such as:

Feature	Description
Active Antenna Supervision	Allows for antenna shut-down/start-up for power conservation
DGPS Support	Support for incoming Differential GPS data to facilitate more accurate positioning
Hot/Warm/Cold start	Different switch-on methods: **HOT:** Receiver has valid ephemeris, almanac and time, 3.5s Time-to-First Fix (**TTFF**) **Warm:** Valid ephemeris, valid almanac, not time, 5s TTFF **Cold:** Valid almanac, 34s TTFF
NMEA/uBlox message output	Multiple message output formats allow for compatibility with other software/systems

TABLE 2: UBLOX ANTARIS FEATURES

DATA OUTPUT

NATIONAL MARINE ELECTRONICS ASSOCIATION (NMEA) DATA STRUCTURE

$	<Address>	{,<value>}	*<checksum>	<CR><LF>

TABLE 3: NMEA DATA STRUCTURE

The NMEA GPS specification is one of the most widely used throughout the world and is supported by most makes and models of GPS units. As such it is useful for interfacing with commercially/publicly available software.

The data consists of a starting **$** sign, the address entry (which describes whether the packet is a positional fix, satellite data, et cetera) and the corresponding value. The penultimate value is a checksum for the packet, with <CR><LF> always terminating the packet. A full description of the protocol can be found on the NMEA website [40].

uBlox Data Structure

Synch Char1	Synch Char2	Class	ID	Length	Payload	CK_A	CK_B

TABLE 4: UBLOX DATA STRUCTURE

uBlox have developed an in-house proprietary system for data display [41]. The uBlox data structure is more descriptive than NMEA 0183 structure; however it is not widely recognised in the open-source community. The first two characters are the synch characters **µ** and **B** (signifying uBlox), followed by the message class which defines the basic message subset and the ID Field which describes the message payload. The length defines the size of the payload, and the 2-byte checksum provides error-checking capability.

GPS: Accuracy

Depending on the receiver (not all makes and models are equal) a conventional GPS signal can be accurate to within several metres. Although this is significantly better than original GPS accuracies before SA was turned off (typically >20m!) it still provides too much of a margin of error for reliable robot positioning. Several techniques are available for the reduction of GPS error, some of which are described below:

Real time Kinematics (RTK) correction

By far the most advanced (and hence most difficult to implement) strategy, **R**eal **T**ime **K**inematics correction is based on the use of carrier phase measurements of GPS satellite signals. RTK finds application in a variety of systems, but when used in conjunction with GPS it is commonly referred to as **C**arrier **P**hase Enhancement **GPS** (**CPGPS**). A full explanation of the mechanics of CPGPS is beyond the scope of this thesis, however it is suffice to say it requires sophisticated statistical and analysis techniques with **full access to the raw satellite signal**. However, access to satellite feeds is not provided, so some other method of error correction had to be implemented.

as **C**arrier-**P**hase Enhancement **GPS** (**CPGPS**). A full explanation of the mechanics of CPGPS is beyond the scope of this thesis, however it is suffice to say it requires sophisticated statistical and analysis techniques with **full access to the raw satellite signal**. However, access to satellite feeds is **not** provided, so some other method of error correction had to be implemented.

Differential Global Positioning System (DGPS)

Differential **GPS** (**DGPS**) is a widely used technique that uses a corrected feed from a well-surveyed base station to provide correctional vectors to GPS clients in the area. The principle factor behind DGPS is that the majority of GPS error is generated by the **ionosphere** (the portion of earth's atmosphere reaching upwards from 85 kilometres), and as these errors are usually constant for receivers within the same ionospheric conditions, a large portion of the error can be eliminated.

Of course errors generated from multi-path receptions (where the GPS signal reflects off of local structures i.e. trees, buildings, etc) can not be accounted for, and the correction data will not be applicable to those receivers experiencing differing ionospheric conditions.

DGPS Correction Data

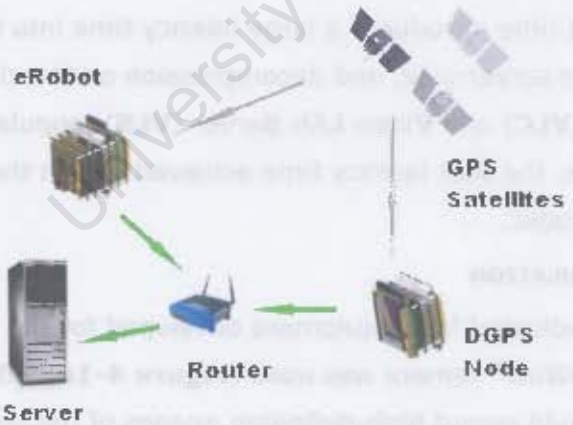

Figure 4-15: DGPS setup

GPS correction data requires an accurately mapped base-station. In the case of the robot, the base station will be changing all the time, as the mobile portions of the system (i.e. the DGPS node and the robot) are transported from location to location. As such, the method used for the positioning is known as ***statistical* DGPS**.

In this case, the readings from the robot GPS system are subtracted from the readings given by the stationary base station, giving the difference in position between the base station and the vehicle.

Data from the robot and the station are streamed across the network, meaning any node can have access to the data from every other node. As the data can be streamed on any port, each node can be given an individual port setting to identify itself.

4.4 Data Streaming

An important aspect of the robot's performance was its ability to stream data back to the user. Making use of the 802.11g standard allows a maximum transfer rate of 54.0 Mbps. Note that in this case, the standard is defined in mega**bits** per second and this translates roughly into 6.75 Mega**bytes** per second. A problem was thus encountered in real-time video streaming. A raw **RGB** (**R**ed, **G**reen and **B**lue) or YUV (PAL system of analogue video) frame can easily be in excess of 9 Megabytes. This is calculated by frame size (640x480) and multiplied by image "depth" (in the most intensive case, 32-bit colour).

At a standard 30 **f**rames-**p**er-**s**econd (**fps**), this would be 270 Megabytes/second, or 2.2 Gigabits/second. This would overwhelm the network, and therefore to reduce the size of the stream, encoding is used.

However, encoding time introduces a large latency time into the stream due to the compression on the server-side, and decompression on the client side. Using **V**ideo-**L**AN **C**lient (**VLC**) and **V**ideo-**L**AN **S**erver (**VLS**), popular open-source streaming software, the best latency time achieved was in the order of 3-4 seconds using an MPEG-2 codec.

NDE Payload Simulation

As there was no dedicated NDE equipment developed for the robot, a standard UniBrain Fire-i FireWire© camera was used (**Figure 4-16**, left), the principle being that the camera could record high-definition images of the surface for post-analysis in conjunction with the recorded GPS data.

5. TESTING

5.1 Mobility

[For videos of the vehicle in action, please see the accompanying DVD.]

FIGURE 5-1: TESTING OF VEHICLE ON A VERTICAL FERRO-MAGNETIC BOARD

Shown in **Figure 5-1** above is the "testing area" used for the robot. It consisted of a conventional chalkboard bolted onto a wall. While this was probably not completely representative of a real life environment, such as a section of ship hull, it did provide taxing conditions for the robot.

Firstly, the thickness of the board was in the order of 1-2 millimetres. This means that the magnetic flux channelled into the board from the magnets was reduced, providing less adherence capability for the robot. Ship hulls (in good condition) are orders of magnitude thicker, and thus will afford more adherence capability.

Secondly, surface of the chalkboard was coated with an aggregate of chalk and oil/grease. This provided a low-friction surface which sorely tested the traction characteristics of the drive wheels.

VERTICAL ASCENT

Although the chassis of the robot is relatively light (6 kg's inclusive of the CM), the weight of the drive units (including wheels) increased the weight to over 8 kg's. This weight of course had a detrimental effect on the robot's vertical speed. Despite this, it managed to successfully navigate the entire periphery of the board.

HORIZONTAL TRAVEL

When not requiring a direct vertical ascent, the robot performed adequately, travelling horizontally (both backwards and forwards) with a minimum of difficulty. This bodes well for its operation in the field, as most scanning would be done in the horizontal plane, with vertical ascents only being performed at the terminal point of the inspection run.

5.2 Control

With the implementation of the control code in C++, reaction times of the robot were negligible. Use of UDP streaming across a sparsely-populated network meant that control messages were delivered almost instantaneously, with a typical delivery time being in the order of tens of milliseconds.

This was well with in the specified target for the system, and was one aspect of the system that performed well.

5.3 Navigation

GPS Positioning

Testing of the platform in the test area practically negated the use of the GPS, as no signal could be obtained. Although the GPS is optimised for use in what is known as "urban canyons" (i.e. the restricted sky-space between tall buildings), it was not capable of attaining a signal in the bottom of a building, which was expected.

DGPS Feed

Once the server was initialised, it was possible to stream data over the internal network. Initialisation involved positioning the DGPS server so it had access to a substantial portion of the sky, allowing multiple satellite-vehicle signals. Over a period of time, the positional error for the stationary DGPS box tended towards zero. However, this data was of limited use as the robot GPS unit was not capable of receiving a signal.

5.4 Data Acquisition

Because of the proximity of the camera to the surface of the chalkboard and the lack of sufficient lighting, images obtained from the device were of poor quality.

5.5 Duty Cycle

Model-aircraft Lithium Polymer batteries were used for the **P**ower **S**upply **U**nit. These units are prolific energy suppliers, capable of supplying 7 Amps (peak current) at 11.1 Volts. Unfortunately, due to their age (the batteries were over 3 years old) 2 battery failures were experienced. Replacement batteries could not be sourced quickly, and therefore full testing of the platform's operational capabilities was not possible.

6. CONCLUSIONS & RECOMMENDATIONS

"..[we] decided it was better to come up with a few recommendations, less than ten. No-one takes more than ten recommendations seriously"

Neil Armstrong, remark made during the *Challenger* Space Shuttle Investigation

Hansen, J.R., 2003, *"First Man: The Life of Neil A Armstrong"*

In conclusion, the base performance of the robot was acceptable. Although the vehicle is not ready for the rigours of an industrial setting, it provided a useful prototype to test the validity of the concept itself as well as other concepts (navigation, networking and so on). The main performance criteria of the system are analysed below and recommendations are made for future development work on the vehicle.

MECHANICAL DESIGN

Design of the robot in a modular fashion allowed for the simple assembly/disassembly for frequent modifications, and was considered a success. Structurally the robot was sound, and showed no sign of wear at the end of the project.

However, the **weight** of the robot chassis overall meant that the drive units were required to work harder and draw more power from the **PSU** leading to a reduction in the operating time of the robot. In addition, the vehicle failed to ascend at the required speed.

Recommendation:

Aluminium Chassis

Use of an aluminium skeleton would reduce the weight of the robot considerably. HDPE could still be used for panels; however the aluminium frame would be responsible for the rigidity and structural integrity of the vehicle.

Redesigned Tail Unit

To compensate for its lack of structural strength, the tail unit was over-designed. In this way it was detrimental to the operation of the vehicle, as the increased weight induced serious performance penalties. A re-design of the unit with aluminium bracing would allow for a lighter assembly.

ELECTRONICS AND COMPUTING

The use of the **PC/104** stack meant that development time was minimal, as pre-built programs and code could be implemented and tested quickly on the platform, without having to go re-compilation or porting. In this regard the capacity of the PC/104 was not utilised to its full extent, meaning that further behavioural work could be carried out on the platform without the need for any modifications.

If the robot is to be implemented in an industrial setting as is, the excessive computing power of the CM would not be required.

Recommendation

Replacement of PC/104

Modern microprocessors such as the ARM9 (used in handhelds and GPS units by PALM© and Garmin© respectively) can support a multitude of peripherals including networking, Bluetooth and high-speed data-transmission protocols such as USB 2.0. Replacement of the PC/104 with a dedicated microcontroller such as the ARM9 would reduce the space, weight and power requirements of the CM.

NAVIGATION

Use of the networked **GPS system** showed the feasibility of using a Wireless LAN to disseminate positioning information amongst nodes or clients. GPS is an excellent outdoor navigational tool, and with further refinement in its implementation as a navigational aid would be a useful system for accurate positioning of the robot(s), though use of the system in a restricted or "urban-canyon" environment should be avoided as severe signal degradation occurs.

Recommendation

Alternative Urban-Canyon Navigational Aid

FIGURE 6-1: ANTARIS SUPERSENSE© DATA IN A SHOPPING MALL

Use of the standard uBlox Antaris GPS was not feasible for accurate navigation in a sky-restricted environment such as a ship dry-dock. Nearing the end of the project, uBlox released a new version of the Antaris line, the Antaris 4 SuperSense© Indoor GPS. The website describes the unit as providing:

> *"...ultra low power consumption, providing reliable indoor coverage for any GPS-endowed application, be it a handheld device or other."* [42]

Replacing the Antaris with the Antaris 4 SuperSense® would allow the vehicle to repo accurate positioning information, whilst not requiring any modification to the existing LAN architecture.

As GPS is not well suited for precision altitude measurement, a redundant altitude recording system (such as an ultrasonic pulse-echo system that uses Time-of-Flight calculations to determine height above the ground) should be implemented.

Data Streaming

Use of the QuickCam showed that the idea of visual inspection was possible (which was expected), but it also showed that a redesign would be required if industry-standard pictures are to be obtained.

Recommendation

Software Upgrade

Upgrading the entire system to a currently supported Linux version would allow the FireWire bus to be fully utilised. To improve the image quality, super-bright LED's should be embedded around the periphery of the camera to ensure adequate lighting

Dedicated Streaming System

Switching to a dedicated streaming protocol such as the **R**eal **T**ime **S**treaming **P**roto would facilitate the streaming of real-time video over the network. This would allow a operator to view the inspection surface as the robot is in motion.

This would mean the vehicle would only have to stop to inspect surfaces that the operator considered to be suspect, speeding up the inspection process.

REFERENCES

[1] Stultz, G.R., Bono R.W., Schiefer, M.I., *"Fundamentals of Resonant Acoustic Method NDT"*, Advances in Powder Metallurgy and Particulate Materials, 2005 Vol. 3, pp 11-1, 11-11.

[2] Anderson, T.L., *"Fracture Mechanics: Fundamentals and Applications"*, pages 3-5, 1195 CRC Press, Technology & Industrial Arts, 1995.

[3] *"Phoenix X-Ray: Manufacturers of high-resolution 2D X-ray inspection Systems"*, 2006. Accessed on January 9, 2007. Available at: http://www.phoenixxray.com/en/applications/semiconductors_electronic_components/index.html

[4] *"DNV Exchange: Registry > Knock Nevis"*, *Det Norske Veritas*, Norwegian ship Classification Society. Accessed on January 9, 2007. Available at: https://exchange.dnv.com/exchange/main.aspx?extool=vessel&subview=owner&vesselid=16864

[5] Daniel. P, Josse. P, Lefevre. P et al., 2004, *"Forecasting the* Prestige *Oil Spills"*, Proceedings of the 2004 InterSpill Conference and Exhibition.

[6] Frank, V., March 2005, *"Consequences of the Prestige Sinking for European and International Law"*, The International Journal of Marine and Coastal Law Volume 20, no. 1.

[7] Cohen. M.J, Feb 1995, *"Technological Disasters and Natural Resource Damage Assessment: An Evaluation of the* Exxon Valdez *Oil Spill"*, The Journal of Land Economics, Vol 71 no. 1, University of Wisconsin Press

[8] Tscheliesnig. P, Nov 2006 *"Detection of corrosion attack on oil tankers by means of Acoustic Emission (AE)"*, Proceedings of the 12th Asia-Pacific Conference on NDT, Auckland NZ.

[9] Constantinis D.A, Richardson A.J, 1994 " *Enhanced Surveys – A cost effective method"*, Journal of The Institute of Marine Engineering, Science and Technology, Trans ImarE, Vol. 107, no. 1, pp47-56

[10] *"History of Robotics"*, 2007, Robotics Research Group, University of Texas at Austin. Accessed on January 9, 2007. Available at http://www.robotics.utexas.edu/rrg/learn_more/history/

[11] Olsen H.O, Vesth L, Jeppesen L, 1998 *"Automated Ultrasonic Examination of Inclined Nozzle Welds Using Robot and 3D Reconstruction"* Proceedings of the 7th European Conference on Non-Destructive Testing, Vol. 3, no. 10.

[12] Slinn, M., 2007, "BONNIE III – *Non-Contact Nuclear Boiler Inspection"*. Accessed on January 9, 2007. Available at: http://www.mslinn.com/sites/mike/OntHydro/

[13] Lettich, M.J, 2003, "*Insulation Management and its Value to Industry"* Steam Digest Volume IV, Energy Efficiency and Renewable Energy, U.S Department of Energy. Available at: http://www1.eere.energy.gov/industry/bestpractices/pdfs/steamdigest2003_insulation_mgmt.pdf

[14] Schmidt, C.W, Jan 2002, "*Petroleum: Possibilities in the Pipeline"* , Journal of Environmental Health Perspectives, Vol. 110 no. 1, The National Institute of Environmental Health Sciences.

[15] Etkin, D.S, 1999 "*Estimating Cleanup Costs for Oil Spills"*, Proceedings of the 1999 International Oil Spill conference no. 168.

[16] Schempf , H. Chemel, B. Everett, N., June 1995 "Neptune: *above-ground storage tank inspection robot system",* IEEE Robotics & Automation Magazine, Robotics Institute, Carnegie Mellon University.

[17] Schempf, H., January 31 2006 "Explorer-II: *Wireless Self-Powered Visual and NDE Robotic Inspection System for Live Gas Distribution Mains"*, Topical Report for the Department of Energy, National Energy Technology Laboratory, Carnegie Mellon University, The Robotics Institute .

[18] Abouaf, J., July/August 1998 "*Trial by Fire: teleoperated robot targets Chernobyl"* Journal of Computer Graphics and Applications, Volume 18 Issue 4, pp10-14.

[19] B.L. Luk, D.S. Cooke, A.A. Collie, N.D. Hewer, S. Chen. 2001 "*Intelligent Legged Climbing Service Robot for Remote Inspection and Maintenance in Hazardous Environments"* Proceedings of the 8th IEEE Conference on Mechatronics and Machine Vision in Practice, Hong Kong.

[20] Arean, P., Muscato, G., Lavorgna, M., Caponetta, R., September 1998 *"New trends in the control of walking robots"*, Proceedings of the 1998 IEEE International Conference on Control Applications, Volume 1 pp418-422.

[21] La Rosa, G., Messina, M., Muscato, G. Sinatra, R., February 2002 *"A low-cost lightweight climbing robot for the inspection of vertical surfaces"*, Dipartimento Elettrico Elettronico e Sistemisico, University of Catania, *Mechatronics*, Volume 12 Issue 1.

[22] "Inspection Robots" 2006, Centre for Energy Systems Research, Tennessee Tech University. Accessed on January 9, 2007. Available at: http://www.cesr.tntech.edu/research/robot/robot.html

[23] *"Robotic Crawlers"* 2006, General Electric Inspection Technologies. Accessed on January 9, 2007. Available at: http://www.geinspectiontechnologies.com/en/products/rvi/rovver/

[24] *"Robot Systems"* 2006, MARAT Company, San Buenaventura, California, U.S.A. Accessed on January 9, 2007. Available at: http://www.maratcompany.com/

[25] *"The High Performance All-Terrain Robot: P3-AT"* 2006, MobileRobots Inc. Accessed on January 9, 2007. Available at: http://www.activrobots.com/ROBOTS/p2at.html

[26] Monadjem V., *"Small Explorer Robot for Non-Destructive Testing"*, Undergraduate Thesis, Department of Mechanical Engineering, University of Cape Town, 2004

[27] Baldwin I., *"Sensor Array for Robotic NDT"* Undergraduate Thesis, Department of Mechanical Engineering, University of Cape Town, 2004

[28] *"Windscreen Wiper Motors and Systems"*2005, LAP Electrical Limited. Accessed on January 9, 2007. Available at: http://www.lapelec.co.uk/windscreen14w.htm

[29] *"PC/104 Embedded Consortium"* 2008. Accessed on January 9, 2007. Available at: http://www.pc104.org/

[30] *"RTD Embedded Technologies, Inc"* 2006. Accessed on January 9, 2007. Available at: http://www.rtd.com/

[31] *"UCT Linux Enthusiasts Group"* 2007. Accessed on January 9, 2007. Available at: http://www.leg.uct.ac.za/

[32] *"gpsd – a GPS service daemon"* 2007. Accessed on January 9, 2007. Available at: http://gpsd.berlios.de/index.html

[33] *"GpsDrive – GPS Navigation Software for Linux"* 2007. Accessed on January 9, 2007. Available at: http://www.gpsdrive.cc/

[34] *"The Apache Software Foundation"* 2007. Accessed on January 9, 2007. Available at: http://www.apache.org/

[35] *"User Datagram Protocol"* 2007, Wikipedia – The Free Encyclopaedia. Accessed on January 9, 2007. Available at: http://en.wikipedia.org/wiki/User_Datagram_Protocol

[36] *"Transmission Control Protocol"* 2007, Wikipedia – The Free Encyclopaedia. Accessed on January 9, 2007. Available at: http://en.wikipedia.org/wiki/Transmission_Control_Protocol

[37] *"libjsw – Joystick Wrapper Library"* 2006. Accessed on January 9, 2007. Available at: http://wolfpack.twu.net/libjsw/

[38] Donahoo, J. 2007 *"Practical C++ Sockets"*. Accessed on January 9, 2007. Available at: http://cs.baylor.edu/~donahoo/practical/CSockets/practical/

[39] *"NAVSTAR Global Positioning System Joint Program Office"* 2006. Accessed on January 9, 2007. Available at: http://gps.losangeles.af.mil/

[40] *"The National Marine Electronics Agency"* 2007. Accessed on January 9, 2007. Available at: http://www.nmea.org/

[41] "u-center Mobile" 2007. Accessed on January 9, 2007. Available at: http://www.u-blox.com/products/u_center_mobile.html

[42] *"SuperSense© Indoor GPS"* 2007. Accessed on January 9, 2007. Available at: http://www.u-blox.com/technology/supersense.html

[43] *"Glossary of Terms"*, The Corrosion Source Handbook, 2002. Accessed on January 9 2007. Available at:http://www.corrosionsource.com/handbook/glossary/f_glos.htm

[44] *"Neodymium Magnet"* 2007, Wikipedia – The Free Encyclopaedia. Accessed on January 9, 2007. Available at: http://en.wikipedia.org/wiki/Neodymium_magnet

[45] 2007, *"Motor Control Bridges > LMD18200"*, National Semiconductor. Accessed on January 15, 2007. Available at: http://www.national.com/pf/LM/LMD18200.html

I/O – Input/Output

LAN – Local Area Network

NDE – Non Destructive Evaluation

NMEA – National Marine Electronics Association

PCB – Printed Circuit Board

PCI – Peripheral Component Interconnect

PCMCIA – Personal Computer Memory Card International Association

PSU – Power Supply Unit

PWM – Pulse Width Modulation

TU – Tail Unit

XML – eXtensible Mark-up Language

BIBLIOGRAPHY

Negus, C., 2005 *"Linux Bible, 2005 Edition"*, Wiley Publishing, Inc.

Sobell, M., 2006 *"A Practical Guide to Red Hat Linux"*, Third Edition, Prentice Hall

Scherz, P., 2000 *"Practical Electronics for Inventors"* McGraw-Hill

Horowitz, P., Hill, W., 2002 *"The Art of Electronics"* Second Edition, Cambridge University Press

APPENDIX A: LITERATURE REVIEW

APPENDIX B: DESIGN AND MANUFACTURE

APPENDIX C: COMPUTER SYSTEM SETUP & CODE

Appendix A

Literature Review

SUMMARY

This Appendix forms part of the eRobot project at the University of Cape Town.

FIGURE (A) 1: EROBOT TRAVELLING ON A VERTICAL WALL

This literature review serves to present the reader with a cross-section of the state of the art of robotic inspection. A basic overview of the various methods of robot locomotion is presented, in addition to a review of current **N**on **D**estructive **E**valuation (**NDE**) techniques currently used in remote inspection.

A variety of commercially available robots and research projects are then presented, with a brief overview of pertinent or interesting features of each design. The penultimate section presents some of the current and pending patents relating to the field of robotic inspection, with the final section consisting of conclusions drawn from the review.

List of Figures

List of Tables

1. INTRODUCTION

This Appendix provides insight into the current trends involving robotics and automation in the field of **N**on-**D**estructive **E**valuation (**NDE**). NDE has been steadily evolving since the nineteen-forties [1], and combined with the rapid growth in robotics has provided the means for accurate, fast inspection systems.

A summary and description of some of the more widespread systems are presented here. Robots involved in inspection employ a variety of methods for both locomotion and adhesion, a brief outline of which is also discussed. Some robot platforms were included that were not involved in NDE or any type of inspection, but possessed desirable design attributes.

1.1 Plan of Development

In order to provide the reader with some basic robotic background, an overview of the common methods of robot locomotion is discussed, including the drive systems of basic legged and wheeled robots. Following this is an overview of the most popular methods of adhering robots to structures, and a brief background on the NDE methods that current robots employ.

In the subsequent section is a detailed breakdown of a large cross-section of the currently available NDE and inspection robots. The penultimate section gives details on currently available patents concerning robots, inspection and NDE. This appendix closes with concluding remarks about the pertinent aspects gained from the review.

1.2 Limitations and Scope

The scope of this Literature Review is limited to those robotic platforms that are involved with NDE and general purpose inspection. This Appendix must not be considered a definitive review of all of the currently available inspection robots. It merely presents a cross-section of what is currently available. In addition, only a few of the more common NDE methods pertaining to robots and automation have been briefly presented; an exhaustive review on NDE methods was not conducted.

Some literature pertaining to robotic platforms that are not involved with inspection has been included with the intention of broadening the design horizon.

2. COMMONLY USED METHODS OF ROBOTIC LOCOMOTION

2.1 Tracked or Wheeled Robots

Wheels and tracks are the easiest method of locomotion to implement on a robot whether it must travel horizontally, or is required to traverse an inclined (or vertical) surface.

FIGURE 2-1: WHEELED ROBOTS

Figure 2-1 above shows a variety of robots, from the famous Mars Sojourner (left) [2] to the military explorer robot Mini-Andros II [3], and the Department of Energy's "mini-robot" (right) [4]. As can be seen, wheeled robots are found in diverse applications from exploring Mars, to transporting hazardous materials and miniature exploration. When considering the design of the drive train for wheeled or tracked robots, the most commonly used methods are discussed below:

ELECTRIC DRIVE MOTORS

As was expected, by far the most commonly used method of wheeled propulsion was the electric motor. Electric motors are available in a variety of sizes and they are by far the easiest to interface and therefore are the most used.

ULTRASONIC DRIVE MOTORS

Recently, the advent of ultrasonic motors has begun to revolutionise traditional thinking about drive systems. **NASA**'s **J**et **P**ropulsion **L**aboratory (**JPL**) has been instrumental in developing **U**ltra**s**onic **M**otors (**USM**), as they have potential for use in space missions [5].

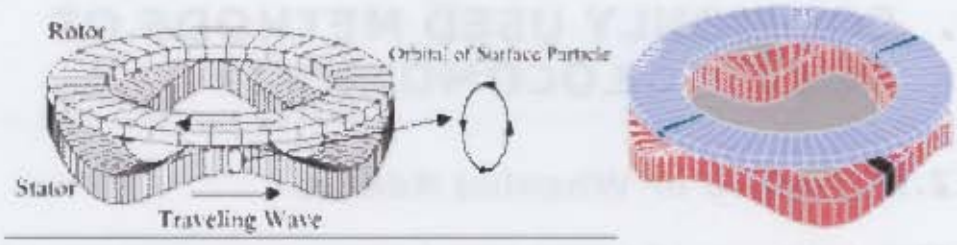

FIGURE 2-2: ULTRASONIC MOTORS

Ultrasonic motors produce excellent low speed torque and have a built-in breaking system. In addition they require less power than equivalent sized electric motors.

As can be see in **Figure 2-2** above, the Ultrasonic Motor consists of a stator and a rotor, which is where the similarities to a conventional motor end.

The stator is constructed of piezoelectric elements which, when excited by a high-frequency voltage signal (typically in the range of 30 kHz) begins to oscillate in a manner that generates a travelling wave. Friction between piezoelectric elements on the stator and the rotor cause the rotor to rotate in a direction opposite to that of the wave [5].

2.2 Walking Robots

Walking robots can provide capabilities not afforded by conventional wheeled techniques, such as better all-terrain capability. In the field of inspection where the robot's environment is uncertain, legged motion offers promising advantages, however the difficulty in reliable implementation of such a system may negate some of these.

FIGURE 2-3: LEGGED ROBOTS

Legged robots are becoming more prolific in both industry and the home. The novelty sensation Aibo© [6] (**Figure 2-3**, left) has become a household toy, with some astounding capabilities. No less popular is the LEGO MindStorms© Kit [7], which is rapidly becoming the rapid prototyping platform of choice. On the right in **Figure 2-3** is the Sprawlita© [8] robot which uses pneumatic drives and was built in the novel **S**urface **D**eposition **M**anufacturing (**SDM**) method, in which electrical components are embedded into the design while it is "grown".

One of the complexities of legged robot design is dynamic stability. With wheeled robots, the **c**entre-**o**f-**m**ass (**COM**) of the robot is (usually) supported in the centre of three (or more) points of contact and therefore COM requirements are less of a design issue than with legged robots, whose points of contact are in constant motion.

Bipedal robots have to deal with a constantly shifting centre of mass which makes the issue of dynamic stability more complex. Robots with more legs, such as *Sprawlita* use an *alternating gait* common in nature [8], where three legs are grounded at any one time. This leads to a stable platform, but can restrict speed. Legged robots utilise a variety of methods to achieve locomotion, some of which are described below:

Electric Motors (Servo and Stepper)

Figure 2-4: Walking robots: Electric motors

The most popular drive configuration for walking robots is the use of stepper or servo motors to provide the desired leg motion. **Figure 2-4** illustrates a number of different walking robots; on the left is the bipedal walking robot *Asimo* [9] designed by Honda; the centre image shows a six-legged walking robot designed by IT Innovation for hazardous-environment inspection [10] and the final image on the right is a Mobile Robotics Research Group prototype walker [11].

Servos and steppers are easy to interface and run off the same power as the controlling electronics, which makes them a logical first choice for most robotic platforms. Disadvantages of servo or stepper motors are their relatively low power to weight ratio in comparison to that of hydraulics or pneumatics.

Pneumatic Drive

Figure 2-5: *Sprawlita* and *Boadicea*

Pneumatic cylinders are widely used in robotic applications. The most popular use for pneumatics is in pick-and-place robotics; these are typically stationed robots that perform tasks in a limited work envelope. However, *Sprawlita* (pictured in **Figure 2-5**, left) uses pneumatic rams for perambulation, while *Boadicea* [12] (**Figure 2-5**, right) uses pneumatic cylinders as "air muscles" to obtain its walking gait.

Pneumatic systems rely on high pressure air to facilitate the extension and contraction of pneumatic rams. Various types of cylinders are available such as single-acting, double-acting and a host of others. The disadvantage for remote robotic systems is the need to have a restrictive tether, or an on-board compressor and storage unit.

Pneumatic drive systems can typically be found on robotic platforms in the manufacturing sector, particularly those robots performing pick-and-place operations (such as chip placers in an industrial **P**rinted **C**ircuit **B**oard manufacturer).

Hydraulic Drive

Figure 2-6: WL-12 robot

Hydraulic systems are similar to pneumatic systems in that a fluid is forced into a cylinder to extend a ram, however while pneumatics makes use of air, hydraulics makes use of liquid (typically oil). While pneumatics is typically restricted to lighter work, hydraulic systems are capable of heavier application forces, making them vital in heavy-duty industry.

Unfortunately, hydraulic systems suffer from the same disadvantages as pneumatic systems; they require a hydraulic pump and storage facilities as well as the usual complement of valves and piping. One robot that successfully used hydraulics to achieve human-like motion was the WL-12 [13] (**Figure 2-6**, previous page). This robot was the designed and built in 1986 at the Takanishi Laboratory in Japan and makes use of electronically controlled hydraulic cylinders to develop a human-like walking gait.

ELECTRO-ACTIVE POLYMERS (EAP)

FIGURE 2-7: SWIMMING ROBOT

EAP technology is a rapidly developing branch of robotics. This technology is usually described as "artificial muscle" in that electrically stimulating the polymer will produce a contraction, just as in a human muscle.

Robot development, particularly in the field of biomimetics has benefited from this technical advance and soon robots may be developed that can mimic the behaviour of insects and animals exactly.

EAP's have applications outside of robotics (for instance in the replacement or repair of human muscle tissue) and therefore vast amounts of **R**esearch and **D**evelopment (**R&D**) work is being conducted on their development.

Figure 2-7 is a computer-rendered image showing a swimming robot developed using a type of EAP [14] as dorsal fins, emulating a sting-ray's swimming motion.

2.3 Motor Comparisons

Actuator Technology	*Power Density (W/kg)*	*Stall Torque Density (Nm/kg)*
McGill/MIT electromagnetic motor	15	200
Namiki 7CL-1701	13	0.06
Sarcos hydraulic rotary actuator	120	600
Utah electropneumatic servovalve	20	200
NiTi shape memory alloy	1	6
PVA-PAA polymeric actuator	17	6
Burleigh piezo inchworm motor	3	0.1
Magnetostrictive wave motor	500	5
Human biceps muscle	20	50
MIT 8 mm USM (Fucia,Green)	**108**	**2.9**

TABLE 1: MOTOR COMPARISONS

Shown in **Table 1** is a comparison between various types of motor [15]. The first four entries in the table are for electromagnetic DC motors. The smallest commercially available motor is the Namiki 7CL 1701 which is only 7 mm in diameter. Highlighted in bold at the foot of the table is MIT's 8mm ultrasonic motor. Comparing these two motors shows that the ultrasonic motor has approximately 35 times the stall torque density and power density of more than 5 times the power density that of the /CL-1701.

3. COMMONLY USED METHODS OF ADHESION

3.1 Magnets

Magnets provide an easy solution to the problem of adherence (to ferro-magnetic structures) as they are relatively cheap to obtain and are available in an array of sizes and strengths.

PERMANENT MAGNETS

FIGURE 3-1: NEODYMIUM RARE-EARTH MAGNETS

Permanent magnets are used in a wide variety of applications from latches to cathode-ray tubes [16]. Neodymium rare earth magnets are some of the most popular, and can be sintered to a specific strength and ordered in a range of sizes and geometries, as can be seen in **Figure 3-1**[17].

Neodymium magnets are available locally, however problems could arise if custom-specification magnets are required as the majority of rare-earth magnets seem to be manufactured in the Far East and as they are classified as hazardous materials, transportation to South Africa is difficult.

ELECTROMAGNETS

Electromagnets are safe to store, do not require advanced manufacturing processes, and can also be designed in a variety of strengths and geometries. However, electromagnets cannot achieve the same flux density as strong permanent magnets can (for the same physical size).

For example, a grade N42 Neodymium-Iron-Boron magnet has a magneto-motive force of 11, 000 ampere turns per centimetre [18]. An equivalent (physical) sized 'C' shaped electro-magnet, 15 cm in length, would have a maximum of about 10,000 turns (using 28 gauge wire). Taking into account the resistance of this length of wire (approximately 1 kilometre), it would require over 300 volts to

generate 1.5 amps in the coil, giving a total of about 15,000 ampere turns or 1000 turns/centimetre. This is approximately 10% of what the permanent magnet is capable of. As such, electro-magnets impose design penalties in terms of power consumption and physical constraints.

3.2 Vacuum Adhesion

Vacuum methods are typically used when the structure/object that the robot adheres to is not ferromagnetic. Use of vacuum techniques allows adherence to a wide variety of structures; however the implementation of such a technique is generally complex.

Pneumatic Vacuum

Figure 3-2: Vertibug

Pneumatic adhesion is becoming more popular as designers are looking to traverse structures/environments that are not ferromagnetic. Shown in **Figure 3-2** above is the Vertibug© toy, which successfully uses suction cups to traverse smooth surfaces [19]. This toy is capable of walking up and down windows, and uses a vacuum system to ensure sufficient adhesion with its "suction cups" to the underlying glass. However, vacuum adhesion to coarse surfaces is very difficult to implement, and poses an interesting design challenge.

Vortex

Figure 3-3: Vortex Holding LLC VMRP

The basic concept of vortex adhesion is the "reverse hovercraft" principle [20]. Large amounts of air are drawn up through the vehicle by high speed fans. This generates a low pressure zone between the robot and the underlying surface, providing an adhesive force.

Figure 3-3 (previous page) shows an industrial inspection robot that employs vortex adhesion. Issues with the design may arise when the vehicle is required to perform a wall-wall or wall-floor transition or if there is an on-board power failure.

4. NDE METHODS: A BRIEF OVERVIEW

With continuing advances in computer technology, robots are becoming able to carry more functional payloads than before. In order to better understand the methods employed by the inspection robots in the next section, a brief overview of the most common forms of NDE is presented here.

4.1 Ultrasonic Testing

Ultrasonic **T**esting (**UT**) can be described as the workhorse of the NDE industry. **UT** is reliable, accurate, and rugged and is responsible for a large percentage of the inspection done in industry [1]. The primary weakness of UT is its reliance on coupling fluid.

UT BASICS

UT is based on the theory of wave reflection. An acoustical wave is imparted into a specimen, with the time taken for the wave to return to the source from either an inclusion (flaw) or from the back wall of the object being known as the time of flight. This, combined with the known speed of sound in the material, enables the distance travelled by the wave to be calculated, which provides both thickness data for the specimen as well as flaw depth and size [21].

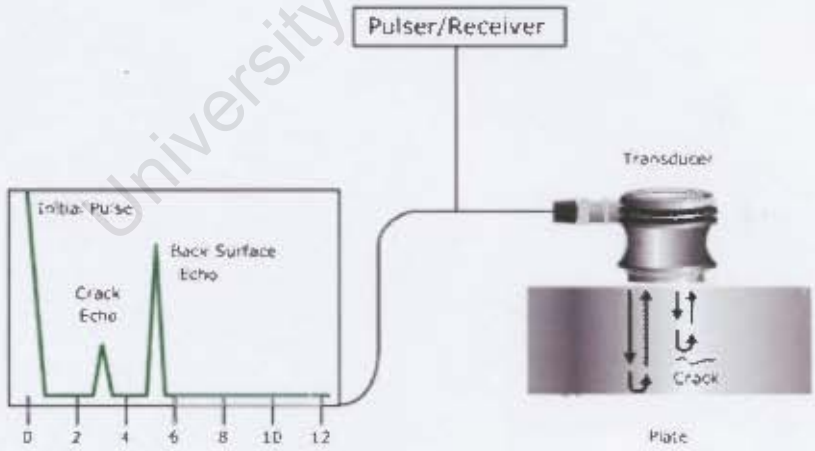

FIGURE 4-1: UT: BASIC THEORY

In **Figure 4-1** above [21], the graph on the left shows the waveform that is received by the receiving transducer. Some of the ultrasonic wave is reflected by the small crack present in the material, with the majority being reflected by the rear of the specimen (giving the largest "spike").

The basic components of an UT system include a pulser/receiver unit (which is contained in the transducer), coupling gel and waveform analysis components.

Shown in **Figure 4-2** below [22] is the sensor side of the system. The transducer is in contact with the test material by means of couplant.

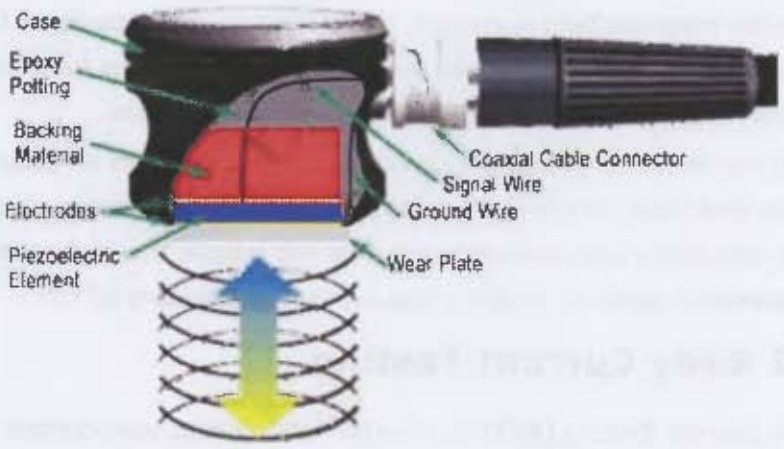

FIGURE 4-2: TRANSDUCER CROSS-SECTION

Couplant is present to facilitate the transmission of the pulse from the transducer into the test material. Couplant is a vital part of UT; however it is a hindrance to any remote system wishing to make use of UT as a testing procedure.

ELECTRO MAGNETIC ACOUSTIC TRANSDUCER (EMAT)

EMAT's are an alternative to the conventional ultrasonic transducer; however they can only be used in electrically conductive materials.

They are similar in that they also impart an acoustical wave into the specimen, but they differ in the respect that they do not need couplant. An EMAT generates waves in the test specimen by means of electro-magnetic induction, the process is completely non-contact.

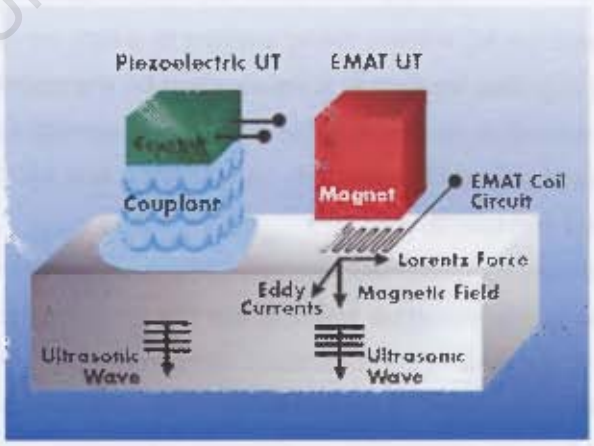

FIGURE 4-3: COMPARISON OF UT AND EMAT MODES OF OPERATION

Shown in **Figure 4-3** [23] is the basic operation of an EMAT, compared to that of a standard piezo-electric transducer. A strong magnetic field is produced at the

surface of the test specimen by either a permanent or an electro-magnet. A **R**adio **F**requency (**RF**) current is introduced into the wire, which will cause the wire to induce eddy currents in any electrically conducting material in its proximity. If a static magnetic field is present, these currents will experience Lorentz forces which will induce a shear wave into the material. This wave is functionally similar to the one induced by standard Ultrasonic Testing techniques.

In the receiving phase, the reverse process occurs and an eddy current is induced in the EMAT coil circuitry, which is then measured by sensing electronics. This system is completely non-contact and it does not require the surface to be in good condition, which is usually a requirement in standard UT [24].

4.2 Eddy Current Testing

Eddy **C**urrent **T**esting (**ECT**) is an extremely reliable, non-contact measuring technique that has found widespread use in the NDE environment. ECT eliminates the need for a probe to be in direct contact with the surface object or structure being evaluated, and this allows for rapid scanning.

ECT Basics

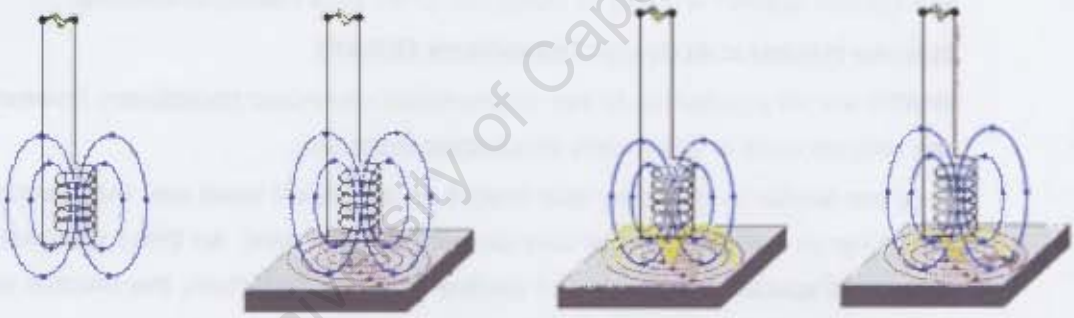

FIGURE 4-4: EDDY CURRENT BASICS

ECT begins with an AC voltage being applied to a coil, as can be seen on the left in **Figure 4-4** [25]. The frequency is determined by the technician, and depends on the type of test being conducted. The alternating current set up in the coil produces dynamic magnetic field (**Figure 4-4**, centre-left), one which is constantly expanding and collapsing.

When a specimen is placed near the coil eddy currents are generated in the specimen due to the inductive effect of the dynamic magnetic field. Once the eddy currents are generated in the specimen, they will begin forming their own secondary magnetic field (**Figure 4-4**, centre-right), which will oppose the primary magnetic field.

When a flaw is present in the specimen, (**Figure 4-4**, right) the eddy currents will be disrupted and the secondary magnetic field produced will be weaker. Comparing

the non-flawed readings to the flawed readings will give an indication of the severity of the inclusions or flaws.

4.3 Visual Inspection

Visual **I**nspection (**VI**) is probably the widest used method of inspection, and by far the simplest. A number of industries, from construction to maintenance employ large numbers of skilled NDE technicians to visually examine structures or components. For example, visual inspection is the standard for bridge inspection in the US, and over 80 percent of aircraft inspection is visual [26].

The major disadvantage of VI is the inability to detect any flaws or inclusions that may have developed beneath the surface. In this regard, VI may serve to provide an initial analysis, but further (more thorough) inspection techniques must be conducted in order to fully analyse the integrity of the structure or component.

Visual Inspection Basics

Skilled NDE technicians examine the structure or component in question for any signs of flaw or defects. Technicians may use mirrors, boroscopes and magnifying glasses in order to better inspect the surface of the object. As can be expected, the results a technician obtains purely through visual inspection can be affected by a number of variables, such as ambient light, environmental conditions and even how fatigued the technician is. A number of tools are available to the technician, as discussed in the following sections.

Visual Inspection Aids: Liquid Penetrant

Possibly the first form of any Non-Destructive Evaluation, is the process of **L**iquid **P**enetrant **I**nspection (**LPI**). In the late Nineteenth Century railway-yards used the "oil-and-whiting" method to reveal cracks in tracks. The track was dipped in oil and then pasted in whiting (chalk and alcohol). Any cracks would seep oil back onto the white surface, and thus become visible [27].

FIGURE 4-5: LIQUID PENETRANT TESTING

Techniques have advanced somewhat from the oil-and-whiting, and the left image of **Figure 4-5** (previous page) shows the penetrant inspection of two wheels from a time-of-flight spectrometer from the *Institut Laue-Langevin* in France [28]. The use of **U**ltra-**V**iolet penetrants makes cracks all the more visible under fluorescent light, as can be seen in the failed component in **Figure 4-5** on the right [29].

Visual Inspection Aids: Magnetic Particle

In order to assist technicians while conducting Visual Inspection, **M**agnetic **P**article **I**nspection (**MPI**) was developed. Although only effective with structures and components that have ferromagnetic properties, this method greatly enhances the accuracy with which technicians can detect surface cracks.

In this technique, either wet or dry particles are used to conduct inspection. As the name suggests, one technique uses particles in a solution, while the other uses them in a solid form. These particles are ferromagnetic and are highly visible (either through natural appearance or the ability to fluoresce).

FIGURE 4-6: MAGNETIC PARTICLE INSPECTION

The basic idea behind MPI is the flow of a magnetic field through a material. When a magnetic field passes through a ferro-magnetic specimen, it will take the path of least (magnetic) resistance. Air has a lower magnetic permittivity than the metallic specimen, and therefore the flux lines tend to pass through the specimen.

If a surface crack is present in the specimen, magnetic poles will form at the tip. If magnetic inspection particles are now placed on the specimen, they will adhere to where the flux lines break out of the specimen i.e. at the surface of the crack. This provides an excellent quick way to observe where surface-breaking cracks have formed.

5. DEDICATED NDE INSPECTION ROBOTS

This section covers robots that are specifically designed for NDE inspection and use dedicated NDE inspection methods (such as Ultrasonic Testing, Eddy Current Testing et cetera) with unique or pertinent design features highlighted.

5.1 NASA MACS

FIGURE 5-1: NASA MACS

NASA's **M**ultifunction **A**utomated **C**rawling **S**ystem (**MACS**) is one of the forefront robots in terms of NDE, and was developed at NASA's Jet Propulsion Laboratory (JPL) [30]. The vehicle uses suction cups to adhere to surfaces and is used in a variety of industries. MACS uses ultrasonic motors instead of normal electric motors and this lowers power consumption as well as increasing torque. Development of MACS was greatly aided by the concurrent development of NASA's exploratory Mars Rovers.

5.2 Pioneer

FIGURE 5-2: *PIONEER* INSPECTION ROBOT

Pioneer was specifically developed to be deployed in the Unit 4 reactor building at Chernobyl power station in the north central Ukraine [31]. The explorer vehicle is

capable of deploying a variety of sensors and taking physical samples of its environment. In addition to this, *Pioneer* is capable of mapping the environment to create photorealistic 3D models of the building interior.

5.3 Neptune Tank Inspector

FIGURE 5-3: *NEPTUNE* INSPECTION ROBOT

Neptune is designed specifically for the inspection of **A**bove-ground **S**torage **T**anks (**AST**'s) while immersed in petroleum products. *Neptune* is capable of performing both ultrasound and visual inspection on the inner surfaces of AST's [32]. The entire system consists of the robot, a deployment system and a position-tracker in order to ascertain its exact location inside the tank.

5.4 TTU CESR Inspection Robot

FIGURE 5-4: CESR INSPECTION ROBOT

The Centre for Energy Systems Research (CESR) at Tennessee Technical University (TTU) developed this inspection robot for the analysis of water walls in coal-fired power plants. Holes in such walls can cause a severe drop in efficiency which calls for the entire plant to be shut down, which can cost in the order of $20,000 to $100,000 per hour [33].

This robot has the ability to travel where temperatures are too extreme for technicians and can be deployed rapidly as no scaffolding is required.

5.5 NETL: EXPLORER II

FIGURE 5 5: EXPLORER II

This robot designed by the **N**ational **E**nergy **T**echnology **L**aboratory (**NETL**) in the United States is intended for use specifically in live gas pipelines to analyse corrosion. It was designed because of the concern over the ageing pipeline infrastructure throughout major metropolitan centres in the US. Features of the robot include a tether-less design and the ability to operate in extremely hazardous environments. Explorer II boasts an advanced sensory payload, including both visual and UT testing equipment. [34].

6. GENERAL INSPECTION ROBOTS

6.1 Toshiba Micro-Inspection Robot

FIGURE 6-1: TOSHIBA INSPECTION ROBOT

This micro-inspection robot is capable of inspection in pipes as small as 1 inch (~25mm). Novel features of the robot are a manipulator (visible at the front of the vehicle in **Figure 6-1**) and planetary drive wheels to ensure the robot does not become trapped easily [35].

6.2 VERSATRAX Family

FIGURE 6-2: VERSATRAX ROBOTS

The VersaTrax family of robots are developed by American Standard Robotics and are billed as robots for operation in hazardous environments [36].

VERSATRAX 150

The VersaTrax 150 pipe inspection system (**Figure 6-2**, left) is a long range pipe inspection system. ASR uses a very modular design for all of its systems, allowing for great flexibility and adaptation to changing environments. According to the literature on the 150, it is suitable for sewers, storage tanks, pressure vessels and steam headers.

VERSATRAX VLR 300

This pipe inspection system (**Figure 6-2**, centre-left) is the largest in the VersaTrax range, and is designed specifically for use in hydro-electric schemes. As such, the VLR 300 is suitable for piping in excess of 300mm. The large piping networks in hydro-electric power schemes require a unit with an extended range, which is accommodated by the VLR 300 up to a maximum of 1830m. This unit is also depth-rated to 100m and carries 4 cameras for inspection.

MICRO CGTV

Designed for long distance inspection, this inspection robot is capable of changing profile to accommodate varied terrain types (**Figure 6-2**, centre right). The **V**ariable **G**eometry **T**racked **V**ehicle (**VGTV**) is capable of transforming from a standard crawler profile to a triangular one whilst remaining fully operational. Standard with the platform are a pair of CCD cameras (one black and white, the other colour) with a 300° rotational tilt.

VERSATRAX DEEP BLUE

An underwater submersible, the Deep Blue (**Figure 6-2**, right) is designed for deep missions. According to the literature, the unit has a 305 metre tether, and is also depth-rated to 305 metres. The unit is capable of being controlled by wireless game controllers or by user-developed software, giving it great marketplace appeal. Standard with the unit are two video cameras and high-intensity halogen lights.

6.3 DanDuct CLEAN Family

DanDuct are a specialist duct cleaning company, offering a variety of duct-cleaning solutions [3/].

FIGURE 6-3: DANDUCT ROBOTS

DANDUCT: INSPECTOR

The Inspector (**Figure 6-3**, left) is a small, remote-controlled inspection robot. The Micro Inspector has remarkably small dimensions: 65mm x 150mm x 80mm (W x L x H), and a weight of only 1.5 kg, making it ideal for duct inspection. Micro Inspector provides video feedback with the aid of 2 wide-angle digital cameras with ultra-bright LED's providing illumination. The range of the 'bot is limited to 30 metres due to tether restrictions.

DanDuct: Multi Purpose Robot

This **M**ulti **P**urpose **R**obot (**MPR**) (**Figure 6-3**, centre) is a combination of inspection and cleaning robot. The platform itself is user-controlled via a joystick. Like the previous mentioned Inspector, the MPR has dual wide-angle cameras as well as variable-intensity halogen lamps. Locomotion is accomplished by 4 independent drive wheels, and in addition to this two separate drive motors are responsible for driving the cleaning head (which can be adapted for either round or square ducting). Range, like the previous robot, is limited to 30m due to the umbilical tether.

DanDuct: IceTech System

A complete system called IceTech (**Figure 6-3**, right) completes DanDuct's robotic range. IceTech is a dry-ice (solid carbon-dioxide) cleaning system, with the robot acting as the end effector providing pressurised dry-ice to the cleaning surface. A 360° rotating nozzle at the front of the vehicle allows the IceTech robot to apply dry-ice to every section of a pipe interior completely removing grease and dirt.

6.4 MPRS Project: URBOT

Figure 6-4: URBOT

The Man Portable Robotic System is an American military project for the deployment of highly mobile robots into hazardous environments [38]. As can be seen in **Figure 6-4**, the **UR**ban ro**BOT** (URBOT) has an invertible chassis, meaning a self-righting mechanism (in the event of the vehicle being overturned) is not required. Control is implemented on board by a PowerPC ipEngine, which provides a **F**ield **P**rogrammable **G**ate **A**rray (**FPGA**) allowing for highly configurable behaviour.

6.5 DEES - University of Catania

DEES, or the ***D**ipartimento **E**lettrico **E**lettronico é **S**istemistico* at the University of Catania in Italy has a well founded robotics program, and have developed a number of wheeled and legged robotic systems designed to operate in the harshest of conditions.

SURFY

FIGURE 6-5: *SURFY* ROBOT

SURFY is as a robot capable of traversing vertical and inclined surfaces. Pneumatic actuators are used to achieve suction, while an electric motor is responsible for directional control. At the time of publication a dedicated inspection system had not been developed for the platform, however inspection is hoped to be achieved by an independent NDE capable robotic manipulator [39].

WALLY

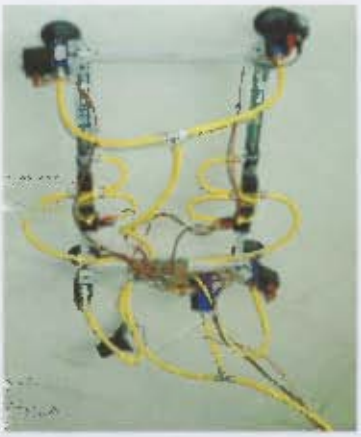

FIGURE 6-6: *WALLY* ROBOT

WALLY is another dedicated wall-climbing robot, and is intended for use in industrial plants, storage facilities, and coal-fired power stations. *WALLY* is capable of manoeuvring in small spaces, as well as having the ability to carry a multitude of

NDE sensors. Pneumatic suction cups are responsible for adhesion, while pneumatic pistons control positioning of the arms [40].

6.6 MARAT Robots

MARAT is a California-based company that specialises in "Technology and Innovation" [41]. Of particular interest is their ranging of cleaning and inspection robots.

FIGURE 6-7: MARAT INSPECTION ROBOTS

MARAT INSPECTION ROBOT

This robot (**Figure 6-7**, left), made by MARAT is a general-purpose visual inspection robot. The system runs off of standard mains power and is compatible with 220V/110V at either 50 or 60 Hz. Another robot that is developed specifically for pipe inspection, it has modest dimensions of (L x W x H) 203mm x 159mm x 140mm with a total weight of 3.5 kg. The range is limited by a 30m tether.

MARAT WORKER ROBOT

Very little literature is available about the Worker Robot from MARAT (**Figure 6-7** centre, right), but as these pictures suggest it is capable of incorporating a variety of sensor modules onto one basic chassis in a very modular method.

6.7 SCRAPPY

FIGURE 6-8: *SCRAPPY* INSPECTION SYSTEM

Scrappy, otherwise known as the EPFL-ASL Air duct Inspection Robot [42], was designed specifically for air-duct inspection. According to the designers, most

existing air-duct inspection platforms were not capable of inspecting all the existing types of ducting, and as such Scrappy was designed. *Scrappy* can operate up to 30 metres away from the operating station (its range is limited by a tether) and has a camera capable of pan and tilt motions with a zoom capability of 10X. Shown in **Figure 6-8** (previous page) is *Scrappy* (left) and its associated control laptop (right).

6.8 ROVVER Family

FIGURE 6-9: ROVVER INSPECTION ROBOTS

The Rovver© family is developed by Everest VIT, now amalgamated into General Electric Inspection Technologies [43]. The smallest of the Rovvers© is the R400 (**Figure 6-9**, left), which is capable of conducting visual inspection on pipes as small as 4" in diameter. Visual feed is provided by an on-board colour camera with halogen lighting, with full pan and tilt functionality. The range of the unit is restricted to 200m due to a tether. Next up in size and functionality is the R600 (**Figure 6-9**, centre) which is capable of inspecting pipe diameters from 6" upwards. Largest of the series is the R900 (**Figure 6-9**, right), which is designed for large bore pipe inspection. The R-series robots have automatic camera levelling features that allow constant, clear views throughout their travel throughout piping networks. In addition, the R900 is capable of carrying additional inspection payloads to further enhance its versatility.

6.9 RoboProbe Technologies

RoboProbe is a commercial company that specialises in "professional remotely operated television and robotic systems" [44].

MICROMAG MAGNETIC CRAWLER

MICROMAG (**Figure 6-10**, overleaf) in the literature from the RoboProbe website is described as a waterproof inspection robot that can traverse steel plating at any inclination to the horizontal as well as a multitude of other surfaces.

FIGURE 6-10: MICROMAG

Adhesion is provided by two Neodymium rare-earth magnets, and the range is governed by a 30 metre tether. Video capabilities are provided by a pan and tilt colour camera.

NANOMAG MAGNETIC CRAWLER

The *NANOMAG* [45], unlike its larger counterpart the *MICROMAG*, is not a waterproof platform. However, designers RoboProbe claim the robot is suitable for ship hull inspection, pipe inspection and reactor vessel inspection to name a few. The recommended price for the robot is USD$35 000.

FIGURE 6-11: NANOMAG

7. Other Robots

Robots here are presented merely for design perspective. Some design aspects from the platforms below may be pertinent or useful for the upcoming design.

7.1 Octopus Robot

Figure 7-1: Octopus robot

An ingenious design developed at the Swiss Federal Institute of Technology (EPFL) the Octopus robot has 15 degrees of freedom and, as shown in **Figure 7-1** above, is capable of traversing complex environments whilst maintaining 8 driven points of contact on the ground. In addition, Octopus is capable of climbing stairs and righting itself when it senses tilting [46].

7.2 Sojourner

No robot review would be complete without mentioning one of the pinnacles of robot technology, the Mars *Sojourner* [2]. Weighing in at only 11 kilograms, the *Sojourner* carried a stereoscopic vision system, an Atmospheric Structure Instrument/Meteorology Package, an Alpha Proton X-ray spectrometer and three other cameras. Although only designed to last a month, *Sojourner* went on to last for three, with final contact being lost in September 1997.

Figure 7-2: *Sojourner*

8. ROBOTIC NDE PATENTS

There are currently a number of patents relating to the field of NDE robotics. Some patents focus specifically on the method of adhesion or locomotion, while others encapsulate the system as a whole. Brief overviews of all of the most pertinent patents are described below. All patents sourced below were located using:

freepatentsonline

DELPHION

United States Patent and Trademark Office

esp@cenet

epo line

8.1 Gas pipe explorer robot

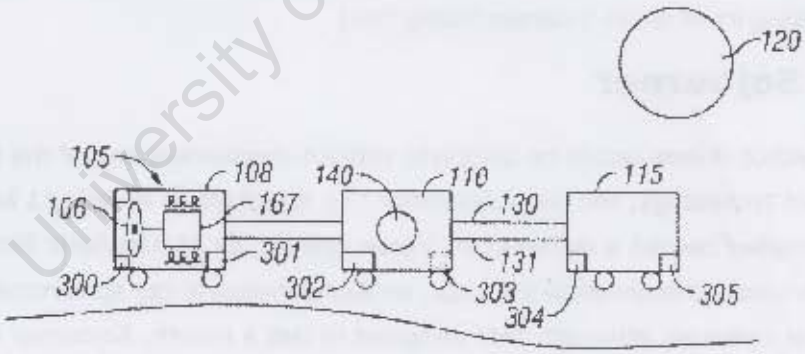

FIGURE 8-1: GAS PIPE EXPLORER ROBOT

Patent Location: UNITED STATES PATENT

Patent Number: US 6,697,710 B2

Date Patented: Feb 4, 2004

Patent Owners: Wilcox, Brian

Patent TYPE: PATENT

As can be seen from the preceding section, gas-pipe inspection is one of the most lucrative and important function of autonomous robot inspection. Correspondingly,

the number of patents concerned with pipeline inspection outnumbered all the other patents quite substantially. This patent for an articulated robot is designed specifically for gas-pipe exploration. Each connected segment provides drive capability, allowing the robot to traverse a multitude of different piping sizes and geometry. The leftmost section in **Figure 8-1** is designated the "sensor" section, with the right-most section being the communications section.

8.2 Autonomous robotic crawler for in-pipe inspection

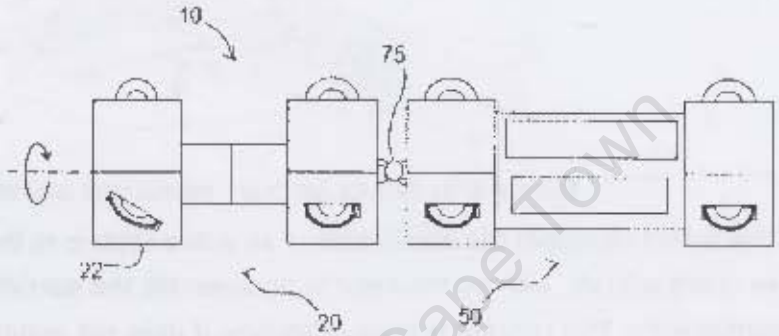

FIGURE 8-2: PIPE INSPECTION ROBOT

This patent describes the design of an autonomous pipe exploring robot that, according to its designers, is capable of traversing unlimited distances through small-diameter enclosed spaces. As can be seen, the rearmost wheels are offset from the longitudinal axis of the robot. The designers recommend some form of fluid-driven screw-drive with the concept being that the rearmost section, when rotated, will form a drive section and essentially corkscrew the robot through the conduit.

Patent Location: UNITED STATES PATENT APPLICTION PUBLICATION

Patent Number: US 2004/0173116 A1

Date Patented: Sep 9, 2004 (published)

Patent Owners: Ghorbel, Faithi Hassan; Dabney, James Bruster

Patent TYPE: PATENT APPLICATION PUBLICATION

8.3 Non-destructive inspection, testing and evaluation systems for intact aircraft and components and methods therefore

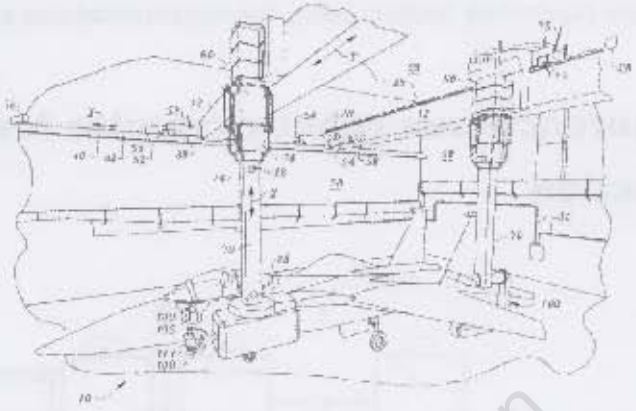

FIGURE 8-3: INTACT AIRCRAFT INSPECTION SYSTEM

This patent describes the application of an entire system to the NDE evaluation of an entire aircraft, without the need to disassemble the aircraft into its individual components. This concept is unique because it does not require the aircraft to be field stripped, which greatly reduces the maintenance period.

Patent Location: UNITED STATES PATENT

Patent Number: US 6,637,266 B1

Date Patented: Oct 28, 2003

Patent Owners: Froom, Douglas Allen

Patent TYPE: PATENT

8.4 Inspection robot

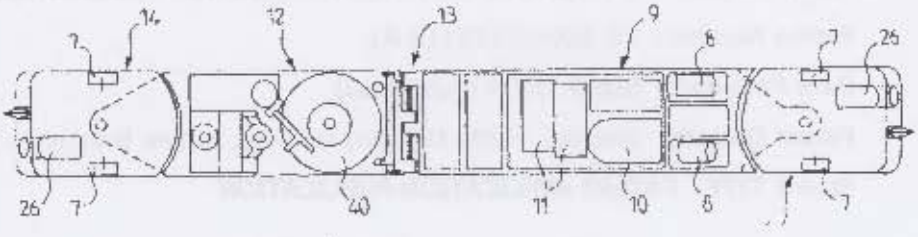

FIGURE 8-4: INSPECTION ROBOT

This patent describes the design of a robot designed for a number of inspection environments. In the extreme left of **Figure 8-4** the two drive wheels marked 7 are noticeable, both of which are part of an articulated head. The sections 8,9,10 and 11 describe the inspection cameras, drive circuitry and power supply. The rear unit

(at the right of **Figure 8-4**) is responsible for letting out and retracting the cable, depending on the direction of travel of the robot.

Patent Location: OMPI

Patent Number: WO 2004/016981 A1

Date Patented: Feb 26, 2004

Patent Owners: Cylergie, Elyo

Patent TYPE: PATENT

8.5 Multifunction Automated Crawler System

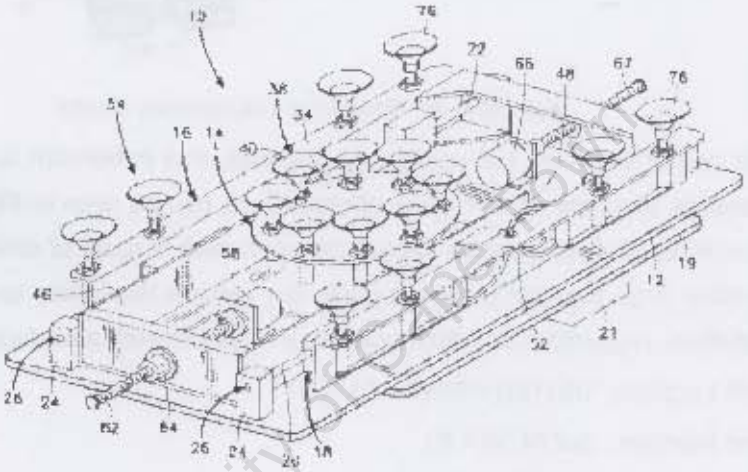

FIGURE 8-5: MULTIFUNCTION AUTOMATED CRAWLER SYSTEM

This crawler, developed at the California Institute of Technology, was designed to address the perceived need for a manoeuvrable platform capable of effectively adhering to a wide variety of surfaces. In addition to two rails (visible on either side of the robot in **Figure 8-5** above) responsible for straight line movement, the robot also possesses a central adherence section that is capable of rotating the robot to orientate it in any direction.

Patent Location: UNITED STATES PATENT

Patent Number: 5,890,553

Date Patented: Apr 6, 1999

Patent Owners: Bar-Cohen, Yoseph; Joffe, Benjamin; Backes, Gregory

Patent TYPE: PATENT

8.6 Apparatus for obstacle traversing

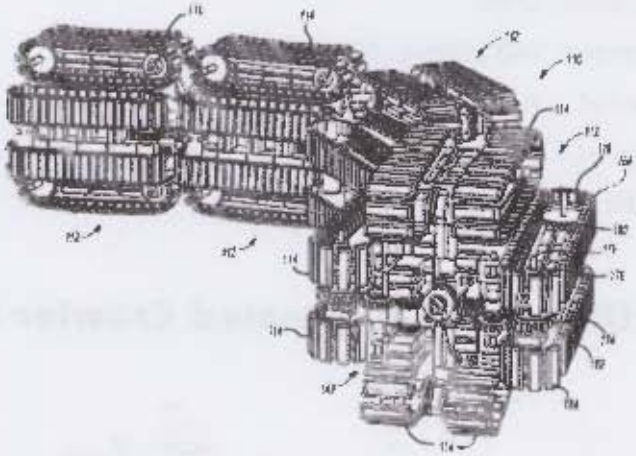

FIGURE 8-6: OBSTACLE TRAVERSING ROBOT

By far one of the most unusual looking robots, this behemoth is designed to be able to traverse any type of terrain or obstacle. As can be seen in **Figure 8-6**, the robot is comprised of 4 articulated segments, each with 4 pairs of drive tracks. This incredibly large number of tracks gives the vehicle the ability to move in any orientation, regardless of which track is in contact with a surface.

Patent Location: UNITED STATES PATENT

Patent Number: 6,774,597 B1

Date Patented: Aug 10, 2004

Patent Owners: Borenstein, Johann

Patent TYPE: PATENT

8.7 Method and apparatus for inspecting a submerged structure

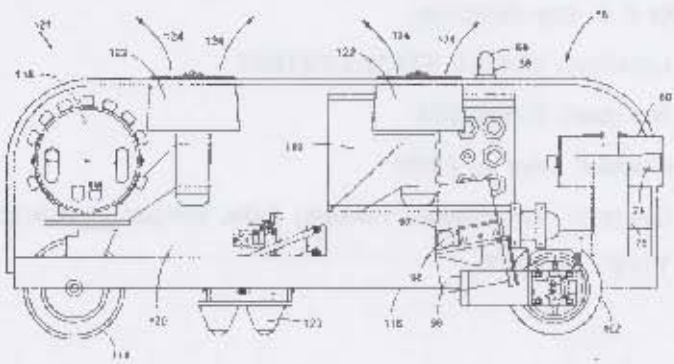

FIGURE 8-7: UNDERWATER INSPECTION ROBOT

This design is one of the most pertinent when considering the future direction of an autonomous NDE inspection robot. This platform is capable of inspecting the structure of the ship hull by means of NDT inspection cameras as well as ultrasonic probes.

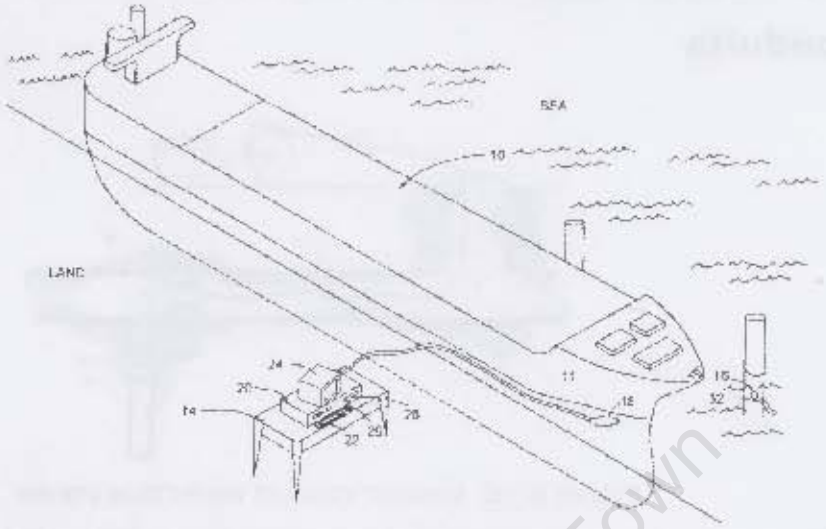

FIGURE 8-8: SYSTEM OVERVIEW

In **Figure 8-8** above, an overview of the system is presented. Control of the system is shore based, with a tether providing power and receiving feed from both cameras and ultrasonic probes.

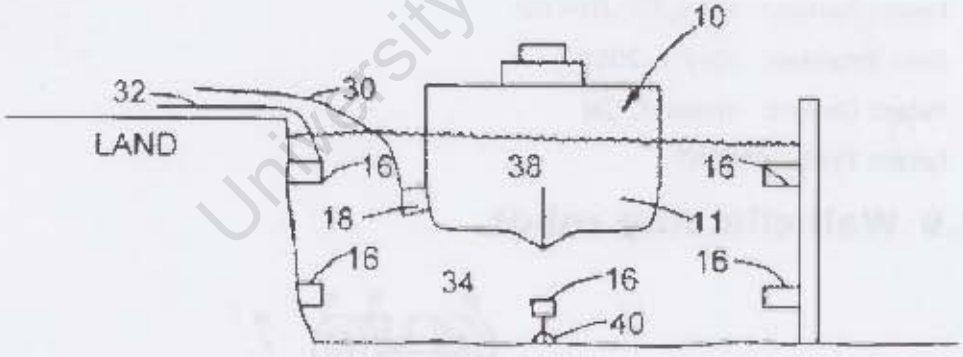

FIGURE 8-9: ROBOT LOCATION

Figure 8-9 above presents a cross-sectional view of the vessel in dock, with the robotic system attached. All the points labelled 16 are ultrasonic beacons, which enables exact control and positioning of the robot on the structure.

Patent Location: UNITED STATES PATENT

Patent Number: 6,317,387 B1

Date Patented: Nov 13, 2001

Patent Owners: D'Amaddio, Eugene R.; Harris, Stewart E. ; Bergeron, Emile E. ; Slate, Edwin V.

Patent TYPE: PATENT

8.8 Robotic apparatus and method for treatment of conduits

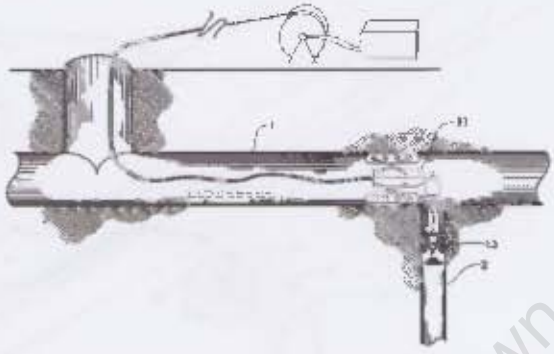

FIGURE 8-10: ROBOTIC CONDUIT INSPECTION SYSTEM

This patent covers the inspection of conduit systems with the aid of a robotically controlled platform. This particular system is capable of deploying smaller inspection units into conduits that branch off the main artery. This requires the main platform to traverse only the main artery, while branches can be inspected by the on-board mini-robot.

Patent Location: UNITED STATES PATENT

Patent Number: US 6,887,014 B2

Date Patented: May 3, 2005

Patent Owners: Holland, Cal

Patent TYPE: PATENT

8.9 Wall climbing robot

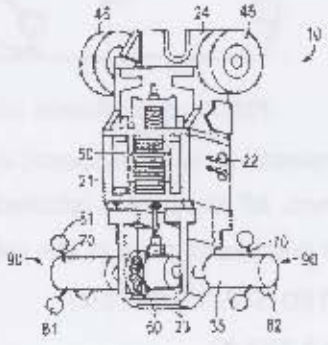

FIGURE 8-11: WALL CLIMBING ROBOT

This particular wall climbing robot (**Figure 8-11**, previous page) is capable of climbing vertical surfaces, as well as making the transition from horizontal to vertical. It accomplishes this by means of re-usable hot-melt adhesives (labelled 81) on rotors (labelled 90). Designer De Fazio makes the observation that magnetic climber robots are only useful on ferromagnetic surfaces, while robots employing suction cups falter on surfaces that are irregular or dirty.

Patent Location: UNITED STATES PATENT

Patent Number: US 6,793,026 B1

Date Patented: Sep 21, 2004

Patent Owners: De Fazio, Thomas L.

Patent TYPE: PATENT

9. CONCLUDING REMARKS

As can be seen from the number of inspection robots, pipe and duct inspection platforms are readily available in the commercial sector. A wide variety of tethered, and tether-less systems can be purchased for most needs, from 1" piping inspectors to sewer-mapping platforms. Some systems are capable of accommodating a variety of inspection methods, while some are dedicated purely to one inspection method.

However, what becomes apparent from the literature survey is the fact that the majority of the systems are not inter-disciplinary. All the robots reviewed were designed for one specific environment; be it pipe, duct or aircraft inspection. Every aspect of their design was focused on their one task, no robot could be found that would easily adapt to different environments.

From this, the concept of a multi-disciplinary robot capable of a variety of inspection techniques becomes a feasible idea. One robot that is capable of performing duct, pipe, aircraft, marine and storage inspection becomes a commercially attractive prospect. Even if the platform is not completely inter-disciplinary, if it can just perform a few of the various industry inspections, this will promote far greater consumer interest than a dedicated sole-purpose inspection platform.

REFERENCES

[1] 2006, *"History of Ultrasound"*, NDT Resource Centre. Accessed on January 12th 2007. Available at: http://www.ndt-ed.org/EducationResources/CommunityCollege/Ultrasonics/Introduction/history.htm

[2] 2006, *"NASA's Mars Exploration Program – Mars Pathfinder"*, NASA Jet Propulsion Laboratory. Accessed on January 12th 2006. Available at: http://mars.jpl.nasa.gov/missions/past/pathfinder.html

[3] 2006, *"Mini-ANDROS II"*, Northrup Grumman. Accessed on January 12th 2007. Available at: http://www.es.northropgrumman.com/remotec/miniandros2.htm

[4] Morse, D., 1998, *"Mobile Robotics Research at Sandia National Laboratories"*, Sandia National Laboratories, Albuquerque NM.

[5] Bar-Cohen, Y. Bao, O., Grandia, W., 1998, *"Rotary Ultrasonic Motors Actuated by Travelling Flexural Waves"*, Proceedings of the Smart Structures and Materials Symposium, San Diego CA, 1-5 March 1998, Paper 3329-82

[6] 2006, "ERS-7M3 AIBO", SONY® Electronics. Accessed on January 12th 2007. Available at: http://www.sony.net/Products/aibo/index.html

[7] 2007, *"Mindstorms"*, Lego Mindstorms. Accessed on January 12th 2007. Available at: http://mindstorms.lego.com/

[8] Clark, J. et al, 2002, *"Fast and Robust: Hexapedal Robots via Shape Deposition Manufacturing"*, the International Journal of Robotics Research, Vol. 21 Issue., 10/11, October – November, pp861-868.

[9] 2007, *"Asimo - The Honda Humanoid robot"*, Honda. Accessed on January 12th 2007. Available at: http://world.honda.com/ASIMO/

[10] 2007, *"RoboSense – Project Summary and background"*, IT Innovation. Accessed on January 12th 2007. Available at: http://www.it-innovation.soton.ac.uk/robosense/summary.shtm

[11] 2007, *"Mobile Robotics Research Group – Our Robots"*, Mobile Robotics Research Group, Edinburgh University. Accessed on January 12th 2007. Available at: http://www.ipab.inf.ed.ac.uk/mrg/robots.html

[12] Binnard, M.B, 1995, *"Design of a Small Pneumatic Walking Robot"*, Masters Thesis, Department of Mechanical Engineering, Massachusetts Institute of Technology.

[13] Daya, B., 1999, *"A Multilayer Perceptrons Model for the Stability of a Bipedal Robot"*, Neural Processing Letters, Vol. 9 pp221-227, Kluwer Academic Publishers, Printed in the Netherlands.

[14] Anton, M., et al., 2004, *"Towards a biomimetic EAP robot"*, Proceedings of the 2004 Towards Autonomous Robotic Systems (TAROS) Conference, Colchester, UK.

[15] Flynn, A. M., 1998, *"Performance of Ultrasonic Mini-motors using design of experiments"*, Journal of Smart Materials and Structures, Vol. 7, no. 3, pp286-294, Great Britain.

[16] 2006, *"Magnetics Technology Center – PM Applications Guide"*, Arnold Magnetic Technologies. Accessed on January 12th 2007. Available at: http://www.arnoldmagnetics.com/mtc/magnets_permanent_apps.htm

[17] 2006, *"MAGCRAFT Advanced Magnetic Materials"*, Rare Earth Magnets. Accessed on January 12th 2007. Available at: http://www.rare-earth-magnets.com/

[18] 2007, *"Chapter 1: Magnetism – Calculating the strength of a magnet"*, Science Toys. Accessed on January 12th 2007. Available at: http://sci-toys.com/scitoys/scitoys/magnets/calculating/calculating.html

[19] 2007, *"Otherland Toys"*, Otherland Toys. Accessed on January 12th 2007. Available at: http://www.otherlandtoys.co.uk/climbtronverti2_800w.jpg

[20] 2005, *"Vortex HC LLC – VMRP Wall Climbing Robot"*, Vortex Holding, LLC. Accessed on January 12th 2007. Available at: http://www.vortexhc.com/

[21] 2006, *"Basic Principles of Ultrasonic Testing"*, NDT Resource Center. Accessed on January 12th 2007. Available at: http://www.ndt-ed.org/EducationResources/CommunityCollege/Ultrasonics/Introduction/description.html

[22] 2006, *"Characteristics of Piezoelectric Transducers"* NDT Resource Center. Accessed on January 12th 2007. Available at: http://www.ndt-ed.org/EducationResources/CommunityCollege/Ultrasonics/EquipmentTrans/characteristicspt.htm

[23] 2007, *"EMAT Technology"*, Innerspec Technologies. Accessed on January 12th 2007. Available at: http://www.innerspec.com/site/emat.asp

[24] Chahbaz, A., Brassard, M., Pelletier, A., 2000 *"Mobile Inspection System for Rail Integrity Assessment"* Proceedings of the 15th World Conference of Non-Destructive Testing, 15-21 October, Rome

[25] 2006, *"Basic principles of Eddy Current Inspection"* NDT Resource Center. Accessed on January 12th 2007. Available at: http://www.ndt-ed.org/EducationResources/CommunityCollege/EddyCurrents/Introduction/IntroductiontoET.htm

[26] Good, G.W., Nakagawara, V.B., 2005, *"Vision Standards and Testing Requirements for Non-Destructive Inspection (NDI) and Testing (NDT) Personnel and Visual Inspectors"*, for Krebs, W.K., Aviation Maintenance Human Factors Program Manager, Final Report, 15 August.

[27] 2006, *"Introduction and History of Penetrant Inspection"* NDT Resource Center. Accessed on January 12th 2007. Available at: http://www.ndt-ed.org/EducationResources/CommunityCollege/PenetrantTest/Introduction/history.htm

[28] 2007, *"SMAE Photographs"* Institut Laue-Langevin. Accessed on January 12th 2007. Available at: http://www.ill.fr/pages/science/DPT/Mechanics/photos.html

[29] 2006, *"Penetrant Testing Materials"* NDT Resource Center. Accessed on January 12th 2007. Available at: http://www.ndt-ed.org/EducationResources/CommunityCollege/PenetrantTest/PTMaterials/ptmaterials.htm

[30] Bar-Cohen, Y., *"Biomimetics - using nature as an inspiring model for innovation"*, Jet Propulsion Laboratory, (JPL) California Institute of Technology, Pasadena CA

[31] Slifko, A., et al., 1999 *"Pioneer: A Robot for Structural Assessment of the Chernobyl Shelter"*, Proceedings of the 8th International Topical Meeting on Robotics and Remote Systems, American Nuclear Society, Pittsburgh, Pennsylvania.

[32] La Rosa, G., Messina, M., Muscato, G., Sinatra, R., 2002, *"A Low-cost lightweight climbing robot for the inspection of vertical surfaces"* Journal of Mechatronics, Vol. 12, pp 71-96

[33] 2006, "Center for Energy Systems Research: Inspection Robots", Tennessee Tech University. Accessed on January 12th 2007. Available at: http://www.cesr.tntech.edu/research/robot/robot.html

[34] Schempf, H., 2006, "Explorer II: *Wireless Self-powered Visual and NDE Robotic Inspection System for Live Gas Distribution Mains"*, Phase I Topical Report, Carnegie Mellon University, The Robotics Institute, Pittsburgh, PA

[35] Suzumori, K., et al., 1999 *"Micro Inspection Robot for 1 – in Pipes"*, IEEE/ASME Transactions on Mechatronics, Vol. 4, no. 3, September.

[36] 2007, *"American Standard Robotics: Ground Robots"*, American Standard Robotics. Accessed on January 12th 2007. Available at: http://www.asrobotics.com/products

[37] 2006, *"Duct Cleaning Equipment"*, DanDuct Clean. Accessed on January 12th 2007. Available at: http://www.danduct.com/

Appendix B

Design and Manufacture

SUMMARY

This Appendix forms part of the eRobot project at the University of Cape Town.

FIGURE (A) 1: EROBOT TRAVELLING ON A VERTICAL WALL

The purpose of this Appendix is to present the reader with an overview of the design process for each module of the robot. A breakdown of the novel or unique features of each aspect is highlighted, and the Appendix concludes with a review of the design process.

[Please see accompanying DVD for all 3D models. Note that all models are fully viewable in Pro/ENGINEER's ProductView Express.]

[Please see the Accompanying DVD for all 3D models]

TABLE OF CONTENTS

List of Figures

1. INTRODUCTION

FIGURE 1-1: EXPLODED VIEW OF EROBOT

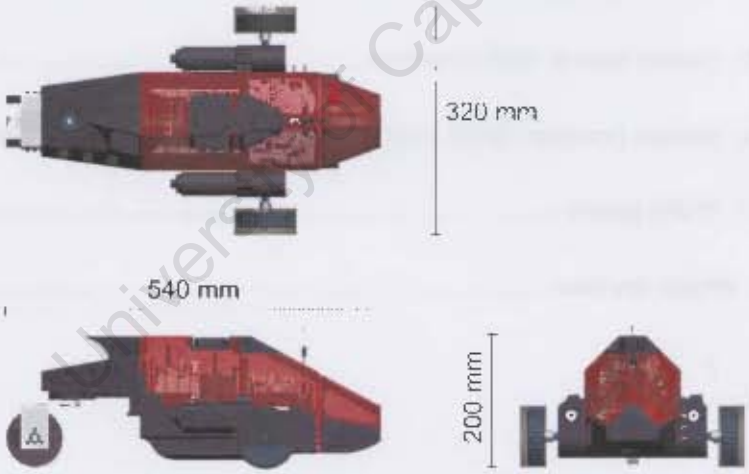

Figure 1-1 is an exploded view of the robot, showing the various modules that comprise the overall system. Design of the vehicle required a high degree of modularity if the platform was going to be capable of performing in different environments.

The design methodology used in the robot was very much "top-down". Parts and components were created in the overall assembly, and then refined at the part level. This ensured that all components mated correctly after manufacture.

The vehicle is comprised of four separate modules: the **Drive Units**, main **Frame**, the **Tail Unit** and the **Payload Bay**. A review presenting the main design features of each module is presented next.

2. Drive Units

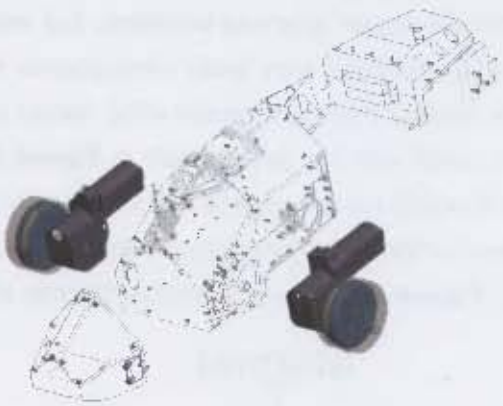

Figure 2-1: Drive Units

2.1 Wheels

Design of the wheels had to account for the fact that the robot was required to adhere firmly to a ferro-magnetic surface, whilst concurrently maintaining a low rolling resistance. It became apparent quickly that wheels would have to be custom made and as such a local company, **A**dvanced **M**aterials **T**echnology (**AMT**), was consulted.

Figure 2-2: Wheel testing: Mold manufacture (left) and trials (centre, right)

Shown in **Figure 2-2** is the machining of a mold-negative on the CNC (left), as well as the initial prototypes. The initial attempt (**Figure 2-2**, centre) was made with a type of readily-available casting silicon, with which the author had had some success previously. The silicon casts easily and sets within 8 hours. As can be seen from the photograph, the wheel had failed completely. Although the traction on the

testing area was excellent, the silicon had a tendency to rip easily. As the finish of the wheel was excellent (meaning the silicon had cured properly), an alternative compound was tried. **Figure 2-2** (right) shows the results of the new compound, a type of poly-urethane. Again grip was excellent, but resilience was an issue. However, the surface was still very tacky (implying an incomplete cure) and so was re-attempted. In addition, the galvanised-steel ribbed plates that were manufactured to assist with the grip (visible in **Figure 2-2** at the top of each of the centre and right frames) served only to initiate tears on the inside of the wheel. The wheel design was revised to accommodate rounded PVC-jackets to ensure tears were minimised. **Figure 2-3** shows an exploded view of the final design:

FIGURE 2-3: FINAL DESIGN

Figure 2-4 shows the components before (left) and after assembly (right). The ribs that are visible in the image were designed in to give the wheel more traction during operation; however the effect of this was minimal and could have been left out.

FIGURE 2-4: WHEEL COMPONENTS (LEFT) AND ASSEMBLED (RIGHT)

As the previous curing attempt of the poly-urethane compound had been unsuccessful, a revised method was implemented.

FIGURE 2-5: CASTING OPERATION

The presence of air bubbles in the casting matrix of the wheel meant a low pressure environment would have to be implemented to remove them.

Shown in **Figure 2-5** is the author's implementation of a dedicated casting environment. A plastic Tupperware® container with a Festo® quick-fit connector formed the casting chamber, with conventional silicon paste used as the sealant. Adjacent to the chamber is a conventional vacuum pump with a silicon-tubing hose and nozzle. The wooden boards visible on the left frame of the image are required to maintain the structural integrity of the chamber whilst under low pressure.

Figure 2-5 (right) shows the elements used in the casting procedure. On the left in the image is the vacuum chamber, with the casting reactants and release-spray in the centre, and a digital scale to ensure accuracy on the right.

FIGURE 2-6: NEW WHEEL (LEFT) AND ORIGINAL (RIGHT)

Figure 2-6 shows a comparison of the final wheel and the original. The final wheels worked very well and lasted the length of the project without requiring replacement.

2.2 Gearboxes

Critical to the success of the project were the design and development of the drive wheels. Standard windshield-wiper motors from a Toyota Corolla were used as the prime movers. However, the standard aluminium castings that housed the units were not suitable for the project, and so the housings were redesigned.

FIGURE 2-7: LEFT DRIVE UNIT

Figure 2-7 shows the main components (shaded) of the left gearbox. As can be seen from the figure, the gearbox consisted of two **H**igh **D**ensity **P**oly-**E**thylene (**HDPE**) components forming the main housing. The drive shaft runs on two deep-groove ball bearings to ensure alignment with the driving worm gear on the rotor.

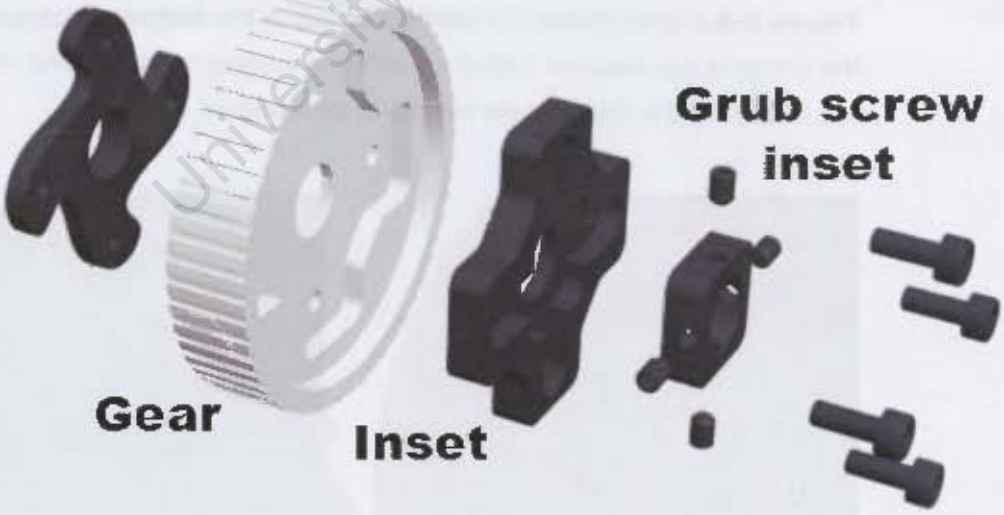

FIGURE 2-8: GEAR SUB-ASSEMBLY

Transferring torque to the drive shaft from the main gear required a solid mechanical connection. An inset was machined into the main gear which allowed for the design of a mating PVC inset. This provided a mounting point for four grub screws that would secure the main drive shaft to the gear.

FIGURE 2-9: GEAR MACHINING (LEFT) AND COMPONENTS (RIGHT)

This arrangement ensured that the shaft did not slip on the main gear, which was an issue in previous prototypes. Shown in **Figure 2-9** is the gear having the main inset machined (right) and the various components of the sub-assembly (right). Implementation of this gear sub-assembly insured excellent torque-transfer, while at the same time being relatively easy to disassemble.

FIGURE 2-10: GEARBOX COMPONENT

Figure 2-10 above shows one component of the gearbox assembly. Every effort was made to reduce the weight of these gearboxes, as can be seen by the weight saving features visible above. Although the gearboxes themselves were light, each gearbox (inclusive of motor casings and wheels) weighed over a kilogram, an issue which will have to be addressed in future versions.

As the drives were only simple DC motors, speed control had to be integrated into the design. As ready-made encoders could not be located easily, the decision was made to implement a custom solution.

The encoder design needed to ensure that it was isolated from the main gearbox and the rotor/brushes to ensure it did not become contaminated with grease and/or carbon deposits.

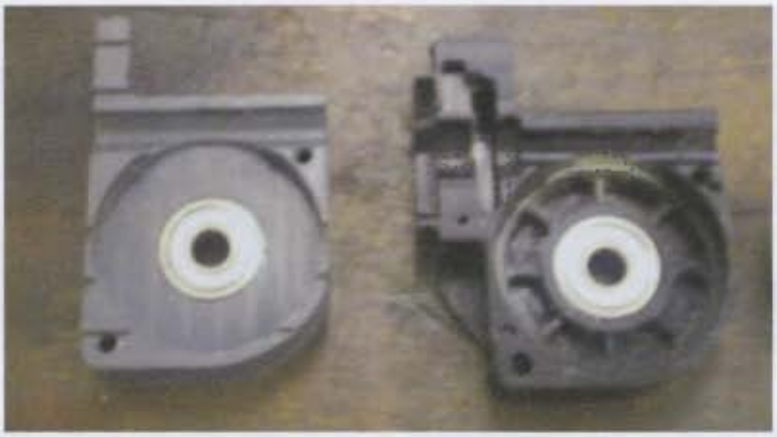

FIGURE 2-11: GEARBOX COMPARISONS

Figure 2-11 shows a side-by-side comparison of one of the early gearbox efforts and the final version. Visible in the new version are the recesses for the custom-built encoder wheels, as well as the weight-reducing features arrayed around the main bearing housing.

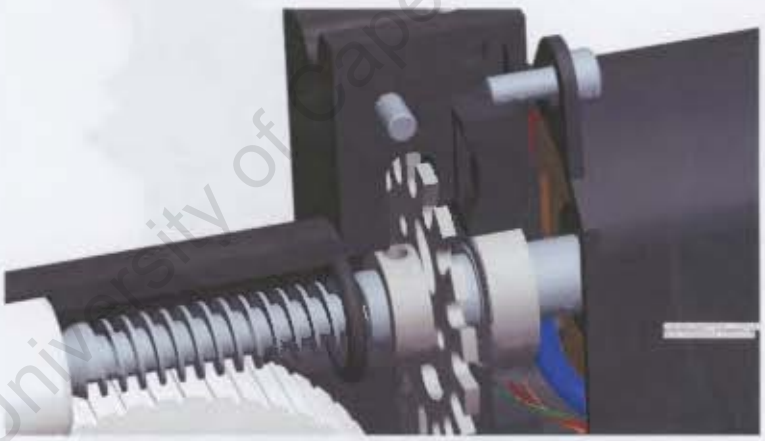

FIGURE 2-12: ENCODERS

For the encoder rotors, aluminium discs were designed and fabricated, with the encoder slots being machined on the CNC. Each encoder was fastened to the rotor shaft by means of a grub screw. Several attempts were made to manufacture the gearboxes before a complete set was successfully fabricated.

The encoder is isolated from the main gearbox by means of a standard o-ring located on the rotor shaft. When assembled, both HDPE components mesh completely around the encoder itself, isolating it from the rotor and brushes.

The encoder itself has 20 slots, which at the rotor's running speed of approximately 1200 rpm gives 800 "transitions" per second.

FIGURE 2-13: ASSEMBLY: REAR VIEW

Shown in **Figure 2-13** is the rear view of the left-side gearbox, with the drive wheel and motor casing outlined. The motors used relied on a simple bushing at the rear of the motor casing to locate the rotor. This generated a substantial amount of heat when operated continuously, and is an issue that requires further consideration.

FIGURE 2-14: THE TRIALS OF DEVELOPMENT

As mentioned before, the gearboxes took some trial and error before a full workable set was made. **Figure 2-14** shows the "gearbox graveyard".

3. FRAME

The Frame formed the core module of the system, and was required to interface with all the other modules. The frame was responsible for housing the **C**omputing **M**odule (**CM**), **E**lectronics **M**odule (**EM**) and **P**ower **S**upply **U**nit (**PSU**), in addition to being rigid enough to provide structural strength for the entire vehicle.

3.1 Design

FIGURE 3-1: FRAME

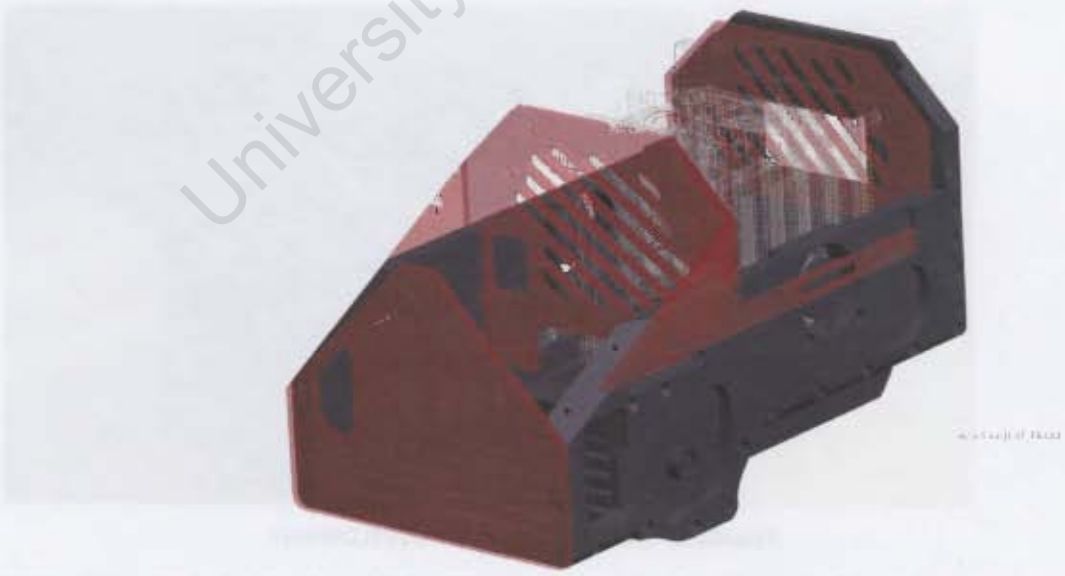

FIGURE 3-2: FRAME SECTIONS

As can be seen in **Figure 3-2**, the frame is a composition of HDPE panels and Perspex© sections and bulkheads. Shown in faint wireframe in the image is the outline of the PC/104 "stack" forming the core of the CM.

FIGURE 3-3: CANOPIES

The canopy sections of the vehicle were essential for isolating the robots' interior electronics from the environment. The top canopy section (**Figure 3-3**, left) was also responsible for housing the uBlox Antaris GPS antenna. This was housed outside the robot to allow for maximum signal acquisition.

FIGURE 3-4: FRAME: EXPLODED

The exploded view in **Figure 3-4** shows the various components that constitute the frame. Also visible in the image are the fans and fan-recesses that were required to keep the PC/104 motherboard cool. The location of the fans allowed for the simultaneous cooling of the PC/104 and the exterior cases of the Drive Units.

FIGURE 3-5: CM AND FRAME

Shown in **Figure 3-5** on the previous page are the CM and the assembled components of the frame. As the supports for the PC/104 stack in the Computing Module were not load-bearing members, weight-reducing grooves were machined in as much as possible. This operation proved difficult as thin Perspex® features cracked relatively easily during machining.

3.2 Manufacture

As much as was possible, components were machined from solid HDPE to reduce the need for fasteners and complex assembly. Shown below as an example is the procedure for machining the bottom cover (the component responsible for shielding the internals of the robot from the underlying surface) starting with **Figure 3-6**.

FIGURE 3-6: BOTTOM-COVER MACHINING (I)

A stock piece of plywood was machined out to accommodate a solid block of HDPE as shown in **Figure 3-6** (left) above. The slots that would allow the unit to slide into the frame were machined in next, as shown in **Figure 3-6** (right).

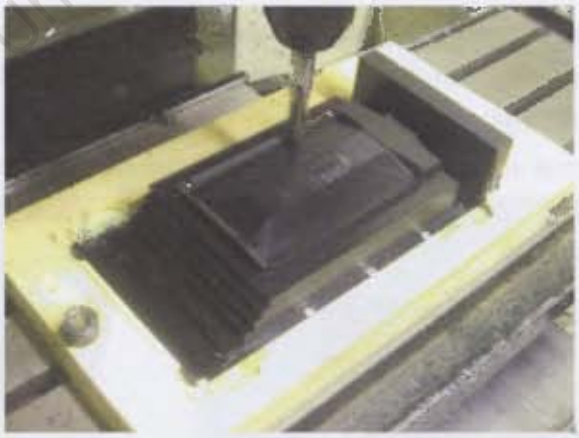

FIGURE 3-7: BOTTOM-COVER MACHINING (II)

Once the piece was secured, it was roughed and then the exterior was finished with a ball nose cutter as shown in **Figure 3-7** above.

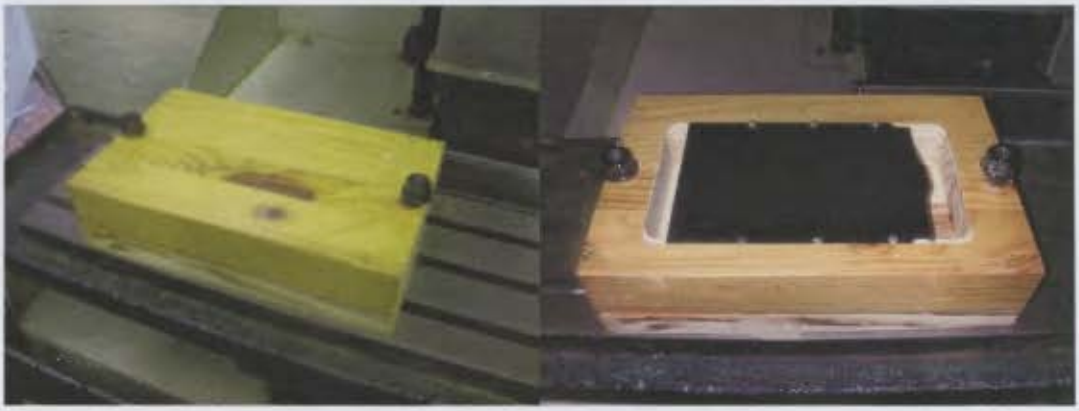

FIGURE 3-8: BOTTOM-COVER MACHINING (III)

As holding the component in a vice to machine the interior would have been impractical (with the designed wall thickness, the component would have begun to deform once machining began) a solid block of wood (shown in **Figure 3-8**, left above) was hollowed out on the CNC to accommodate the semi-finished component (**Figure 3-8**, right).

FIGURE 3-9: BOTTOM-COVER MACHINING (IV)

This arrangement allowed machining out of the interior of the component without any problems. Shown in **Figure 3-9** is the component being machined (left) and once finished (right). **Figure 3-10** shows the left-side panel (left) and front section (centre) being machined, with the final frame components on the right.

FIGURE 3-10: VARIOUS MACHINING OPERATIONS

4. TAIL UNIT

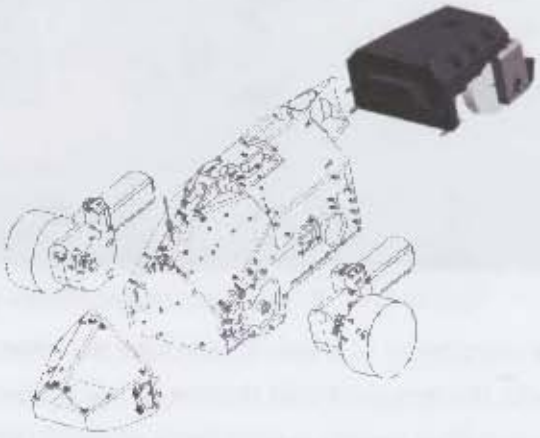

FIGURE 4-1: TAIL UNIT

4.1 Wheel

As the design of the robot required a tri-cycle arrangement, the **T**ail **U**nit (**TU**) was responsible for housing the rear jockey wheel. Design and development of the front drive wheels had resulted in units that were resistant to wear, had a low rolling resistance and provided good adhesion to an underlying metallic surface.

However the design requirements for the rear wheel were different. In the case of this trailing jockey wheel, the design must allow the interior magnet to adhere to an underlying metallic surface whilst allowing it to slip easily on the surface (as well as being resistant to wear).

FIGURE 4-2: JOCKEY WHEEL ASSEMBLY

Shown in **Figure 4-2** is the original design. A solid aluminium section accommodates two extended brass bushings with nylon stabilisers. Two silver-steel half shafts ran on the bushes and were located on two steel hubs attached to the magnet. The advantage of this design was that no modification of the magnet itself

was required. Large electrical heat-shrink tubing was shrunk over the assembly, both to add additional integrity to the hub/magnet/hub sub-assembly and to provide a low friction surface between the wheel and the underlying surface.

Unfortunately, the half-shafts did not run smoothly inside the bores of the bushes (which was attributed to rusting, which became visible after only a day or two) and therefore a re-design was necessary.

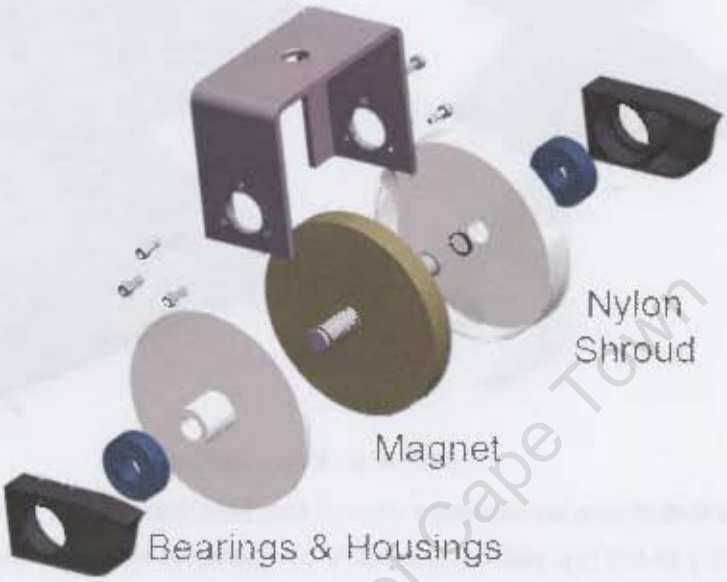

FIGURE 4-3: HITCH: EXPLODED

Figure 4-3 shows an exploded view of the final design. As the solid aluminium section worked well, it was incorporated into the final design. However, it was necessary to machine a bore into the magnet, which was accomplished by Mr. Glen Newins of the UCT Mechanical Engineering workshop.

A solid aluminium shaft was fabricated (to prevent both rusting and the channelling of magnetic flux into the bearings, reducing their life) which was pressed into the magnet. Nylon shrouds encompassed the magnet and provided an excellent low-friction interface between the wheel and the underlying surface.

The bearing housings were designed as to make use of the previous locating holes for the brass bushings.

4.2 Design

Design of the **T**ail **U**nit (**TU**) required it to be structurally sound as it would be supporting more than 1/3rd of the weight of the robot. It also needed to

accommodate the hitch assembly and allow it to perform a 360° rotation, so as to allow the robot to travel backwards.

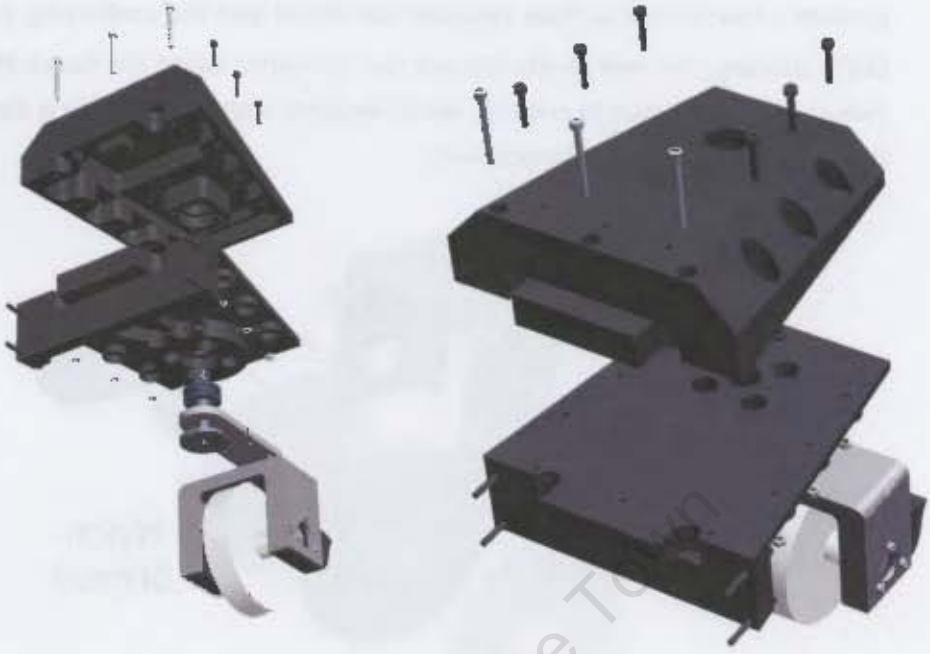

FIGURE 4-4: REAR: EXPLODED

Figure 4-4 shows an exploded view of the final design. The complex internal geometry of the top and bottom HDPE components was implemented to reduce the overall weight of the unit.

FIGURE 4-5: FIRST DESIGN ATTEMPT

Shown in **Figure 4-5** above is the top section of the first design. Although the design was aesthetically pleasing and had excellent surface finishes, it had locating defects and was excessively heavy. Further work was done on the 3D models to ensure that the weight of the design was reduced.

Very elementary **F**inite **E**lement **A**nalysis (**FEA**) was conducted on the assembly to determine whether it was still structurally sound after all the weight-reducing features had been added.

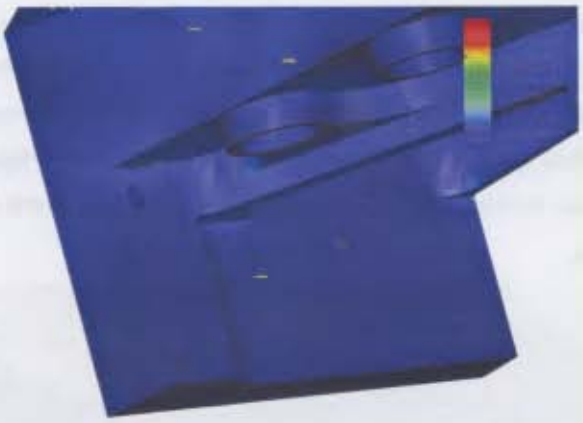

FIGURE 4-6: REAR FEA

Figure 4-6 above shows a screenshot of the FEA done on the rear assembly. A uniformly distributed load of 10 kilograms was placed on the internal bearing recess of the lower section. This was 125% of the design weight of the entire robot, leaving a large safety factor. The resultant maximum von-Mises stress was 1.9MPa, and with the yield strength of HDPE being approx 25MPa, there was a substantial safety factor for the assembly. In the above figure, the red gradient corresponds to 7.0 MPa, whilst blue is unstressed.

FIGURE 4-7: REAR COMPONENTS

Figure 4-7 above shows the interior detail of the final sections.

4.3 Manufacture

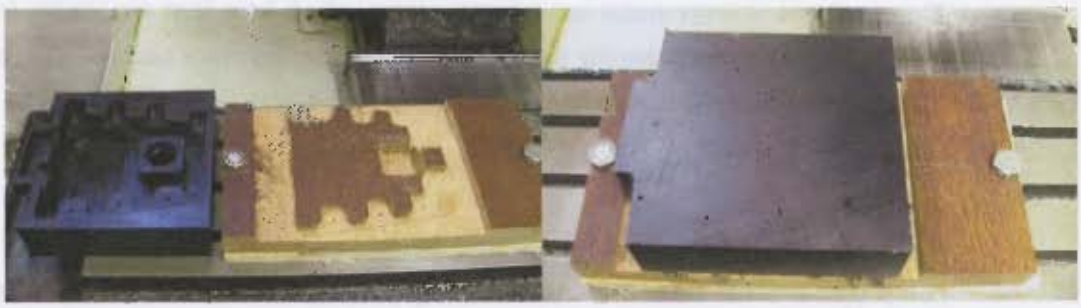

FIGURE 4-8: MACHINING REAR (I)

Sometimes due to the complex geometry of a part, it became almost impossible to fix it into a vice or with standard clamps. As such, a common method developed was to machine the negative of a part into a block of wood. This allowed the part to be accurately and rigidly located in place. Shown in **Figure 4-8** (previous page) is the rear top-section before and after mounting. **Figure 4-9** shows the part during machining.

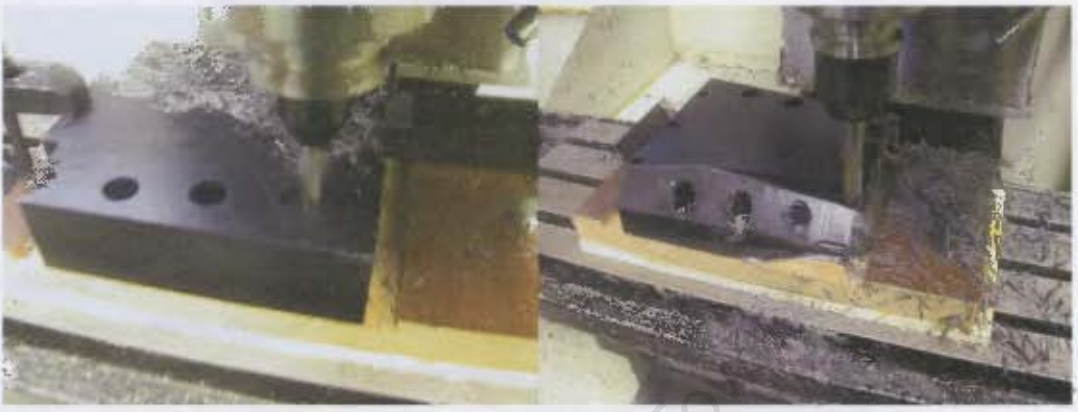

FIGURE 4-9: MACHINING REAR (II)

Assembly of the Tail Unit was relatively simple once the lengthy machining process was complete. Shown in **Figure 4-10** below is the lower section being assembled into the robot:

FIGURE 4-10: REAR ASSEMBLY (I)

The quadrant of large holes around the central shaft hole that are visible in the left frame of **Figure 4-10** are for tightening of the bearing plate bolts of the top bearing assembly. This allows for tightening of the bolts without having to disassemble the entire TU.

Figure 4-11 overleaf shows the shaft, bearing and other components that completed the Tail Unit. The use of sliding (H7/h7) fits on the shaft allowed for easy assembly/disassembly.

FIGURE 4-11: REAR ASSEMBLY (II)

5. PAYLOAD BAY

5.1 Design

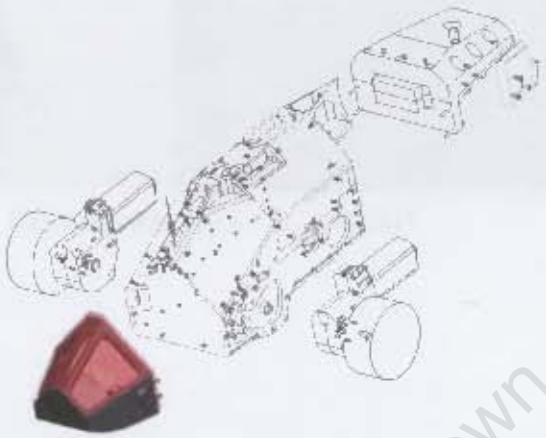

FIGURE 5-1: PAYLOAD BAY

As the name suggests, the Payload Bay module was responsible for carrying the robots Non-Destructive Evaluation payload. For testing purposes a FireWire camera was used to take images of the underlying surface. Although the FireWire camera was inferior to an industry standard inspection camera, it sufficed for a testing platform.

FIGURE 5-2: FRONT (LEFT) AND EXPLODED (RIGHT)

Figure 5-2 shows the Payload Bay and its exploded view. Arrival of the Mechanical Engineering Department's new CNC milling machine allowed the author to machine the Payload Bay from a solid stock of HDPE.

This greatly simplified assembly issues, although the piece required 24 sequences in 12 separate machining operations.

FIGURE 5-3: FRONT SHOWING FIREWIRE CAMERA

Shown in **Figure 5-3** is the rear view of the assembled Payload Bay. In the centre of the figure is the FireWire camera. As the FireWire connectors and cabling had very large bend radii, they were included in the 3D model to ensure that the camera assembly would fit into the designated space inside the bay.

Also visible in **Figure 5-3** are the weight-saving insets. These were added after the first round of machining as it was found that the solid section was too heavy to be effectively used by the vehicle.

5.2 Manufacture

FIGURE 5-4: PAYLOAD BAY AS DESIGNED (LEFT) AND DURING MANUFACTURE (RIGHT)

Figure 5-4 (previous page) shows the solid unit as designed in Pro/ENGINEER (left) and during the manufacturing process (right). At this stage in the manufacture, the faceted faces of the unit are being smoothed with a ball-nose cutter. The cutter is stepping across at 0.3mm, meaning that the entire operation took in excess of 6 machining hours to complete.

FIGURE 5-5: ROUGHING (LEFT) AND INNER MILLING (RIGHT)

The use of the roughing and finishing procedures in Pro/MANUFACTURE (an add-on prismatic-machining module to Pro/ENGINEER) greatly simplified the machining procedures. **Figure 5-5** shows the component during the roughing stage (left) and during the inner-milling phase (right).

FIGURE 5-6: COMPARISON OF INITAL STOCK AGAINST THE FINAL ASSEMBLY

Figure 5-6 shows a comparison of the original stock size against the final component.

6. ELECTRONICS

Design of the **E**lectronics **M**odule (**EM**) began with a mock-up to ensure that the intended boards and components would fit into the robot's designated electronics bay.

6.1 Mechanical Design & Manufacture

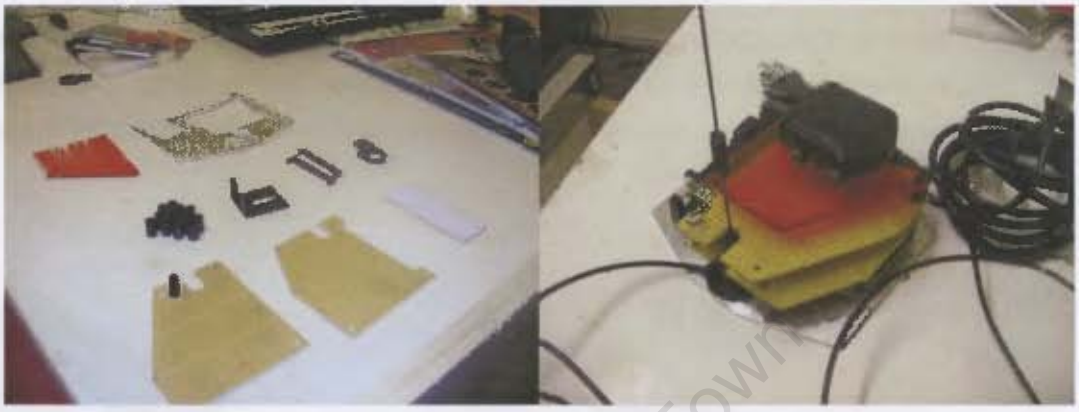

FIGURE 6-1: EM MOCK-UP

Figure 6-1 shows the first mock-up of the EM. As can be seen in the components view (left), two electronics boards were initially designed for. This was revised later on in the design process to three. Also, the uBlox Antaris GPS antenna was mounted in the EM. This was also changed as multi-path errors and obstruction by the overhead canopy was a concern.

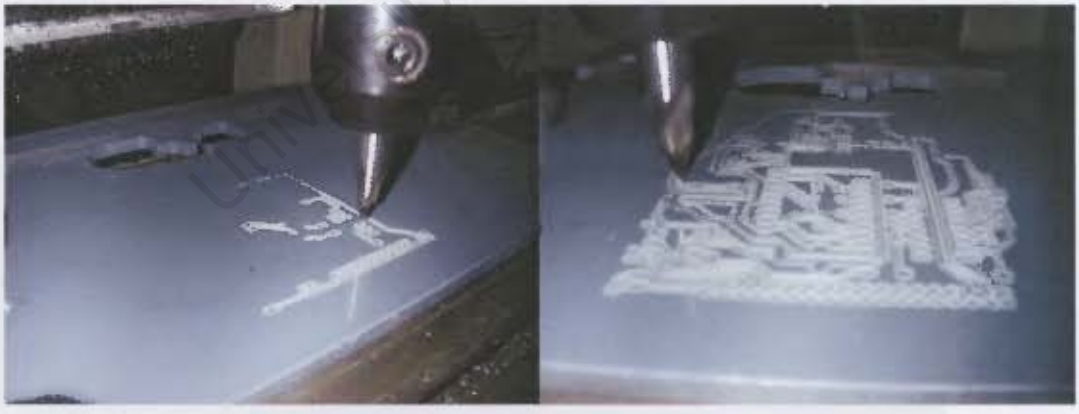

FIGURE 6-2: G-CODE EVALUATION

Once design of the electronics was complete (see **6.2 Electrical Design**) it was necessary to manufacture the boards. As time was pressing and the out-sourcing of a board to a dedicated **P**rinted **C**ircuit **B**oard (**PCB**) manufacturer would have been costly and time consuming, it was decided to attempt in-house board manufacture. Eagle CAD, the electrical design package, has a very large on-line support community. One of the tools that was developed and published on the Eagle

website was a G code generator. This package was downloaded and a custom Linux shell script written to convert the generic G-code to a G-code format that the Hercus CNC mill was compatible with.

Figure 6-2 shows a test of the G-code on a piece of PVC. The "tool" in this case was a broken end-mill that had been sharpened to a point. As can be seen from the photograph, the tracks are clearly discernable, and so it was decided to proceed to the next phase of board development.

Several PCB cutters were obtained from CadShop, a Pretoria based PCB specialist. As the tools supplied were long series, an adaptor was designed to accommodate them into the mill's standard tool adaptors and to provide support for the tool neck as shown in **Figure 6-3**:

FIGURE 6-3: TOOL ADAPTOR

A piece of scrap single-sided board was obtained from Mr. Samuel Ginsberg of UCT Electrical Engineering, and a trial board was milled, shown in **Figure 6-4**:

FIGURE 6-4: TRIAL BOARD

There were mixed results for the first board. For the initial cutting stages, the cut was excellent. Unfortunately the whole process was very slow. This was because a

conventional PCB milling machine has a spindle speed of about 20,000 revolutions per minute (**rpm**) whereas the maximum spindle speed of the Hercus is 4,000 rpm. Therefore the recommended cutting speed was reduced by a factor of 5, which translated into 1 inch per minute, or approximately 25 mm per minute. The 0.5 mm cutter used initially cut well; however it broke mid-cycle, visible in the top-left of **Figure 6-4** (previous page, right). This was replaced with a 0.7mm cutter, which initially cut too deep and slow (**Figure 6-4**, right, right hand side) leaving a substantial burr.

Once the initial speeds and feeds had been determined (through more trial and error) a steel plate was ground and CNC-drilled to be used as a PCB mount **Figure 6-5**, left). This allowed for the PCB to be fastened by a twenty-four 3mm hex-bolts, ensuring that the board was completely flat (**Figure 6-5**, centre-left).

FIGURE 6-5: FIRST BOARD

The first production board was then milled (**Figure 6-5**, centre right) and routed out (**Figure 6-5**, right).

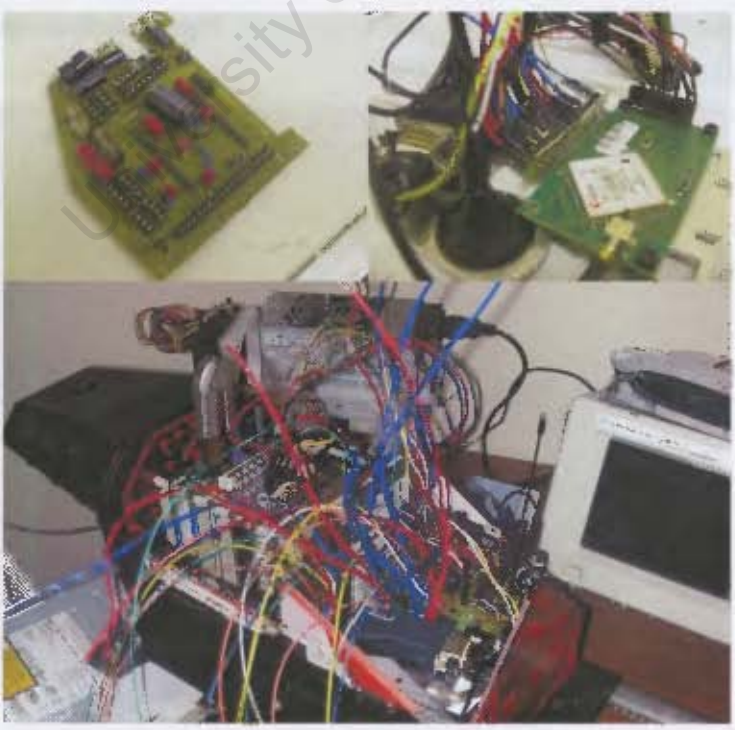

FIGURE 6-6: BOARD POPULATION AND INSTALLATION

Once the board was populated with components (**Figure 6-6**, previous page, top-left) it was mounted on the EM base (on which the H-bridge driver chips were mounted, **Figure 6-6**, top-right) and mounted in the robot's electronics bay (**Figure 6-6**, centre). As can be seen from the image, there was an excess of wiring, and this ultimately led to the design being unworkable. The board was redesigned as shown in **Figure 6-7**:

FIGURE 6-7: BOARD RE-DESIGN

This board did not have the GPS interface as the first design did, and was solely responsible for H-bridge control, leading to a much cleaner board. In addition the H-bridge chips were mounted on the board's solder side, eliminating the need for interconnect wires (as in the first prototype) whilst still allowing for a solid thermal connection with the underlying aluminium. **Figure 6-8** compares the final board (left) with the initial one (right).

FIGURE 6-8: BOARD COMPARISON

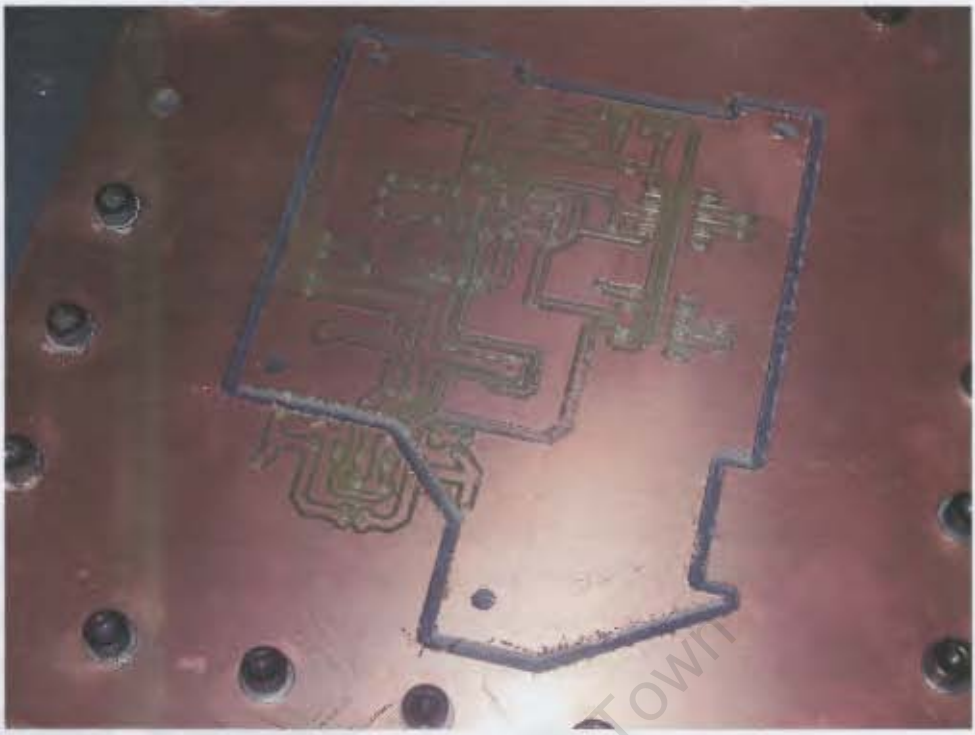

FIGURE 6-9: WHAT NOT TO DO

6.2 Electrical Design

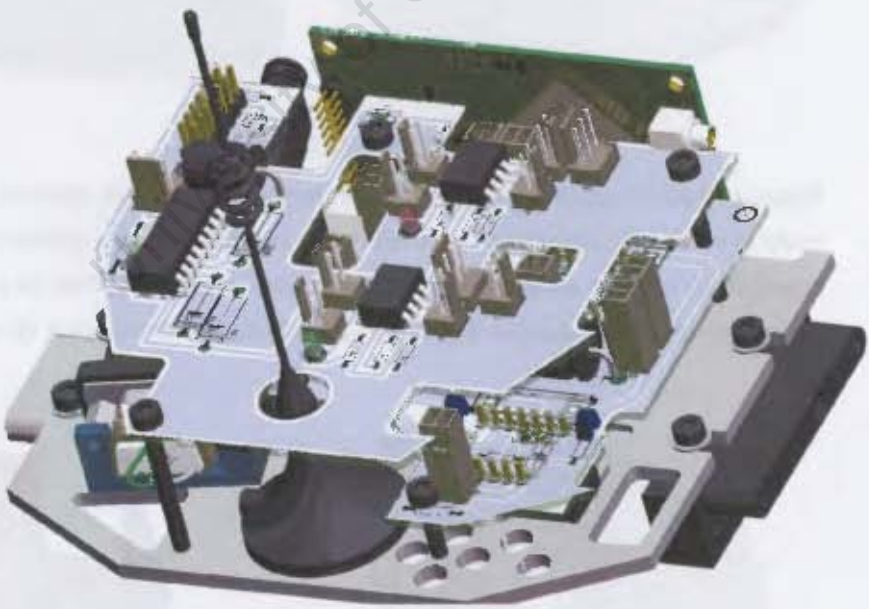

FIGURE 6-10: FINAL ELECTRONICS MODULE

Shown in **Figure 6-10** is the final Electronics Module. The module was capable of controlling the two drive motors and interfacing with the uBlox GPS board. **Figure 6-11** overleaf shows a schematic of the lower board:

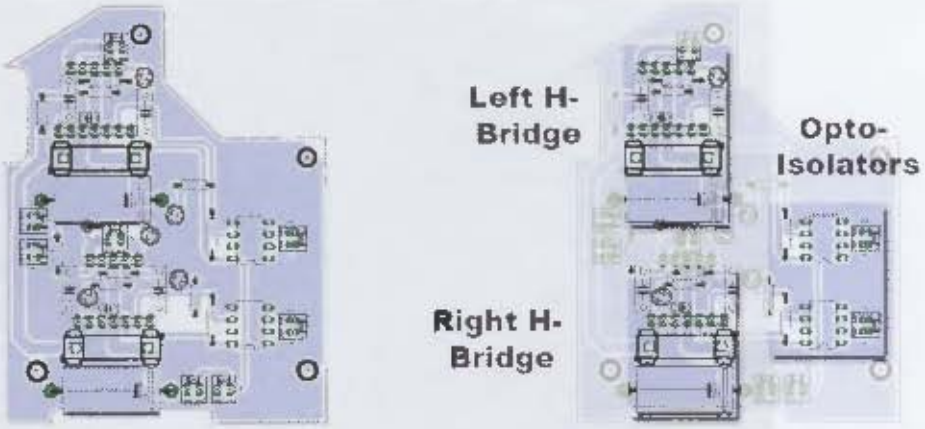

FIGURE 6-11: LOWER BOARD SCHEMATIC

After the initial prototype of the board proved impossible to successfully implement, the bottom board was redesigned to be solely responsible for the H-bridge control. The board incorporated fuses to prevent current overload and opto-isolators to physically separate the incoming control signal from the rest of the board.

FIGURE 6-12: LOWER BOARD

Figure 6-12 shows the Pro/ENGINEER model of the final bottom board. As the mating of the H-bridges to the underlying aluminium was crucial to ensure conduction of heat away from the board, they were mounted on the underside (solder side) of the board. **Figure 6-13** shows a thermal plot of the H-bridges:

FIGURE 6-13: LOWER BOARD: HEAT CONSIDERATIONS

This very basic model placed two heat sources at the rear of the H-bridge tabs. As in the H-bridge documentation it states that the outputs are no longer driven at 158°C, this was determined to be the temperature where the maximum thermal stress would occur. The surrounding temperature was assumed to be 25°C, and this was assumed to be at the interface of the aluminium board and the exterior of the vehicle.

Once the lower board design was completed, the middle board was designed around it. The function of the middle board was to interface with the uBlox Antaris GPS unit and the temperature and speed sensors of the drive units. The cut-out sections are for lower-board Molex® connectors to pass through.

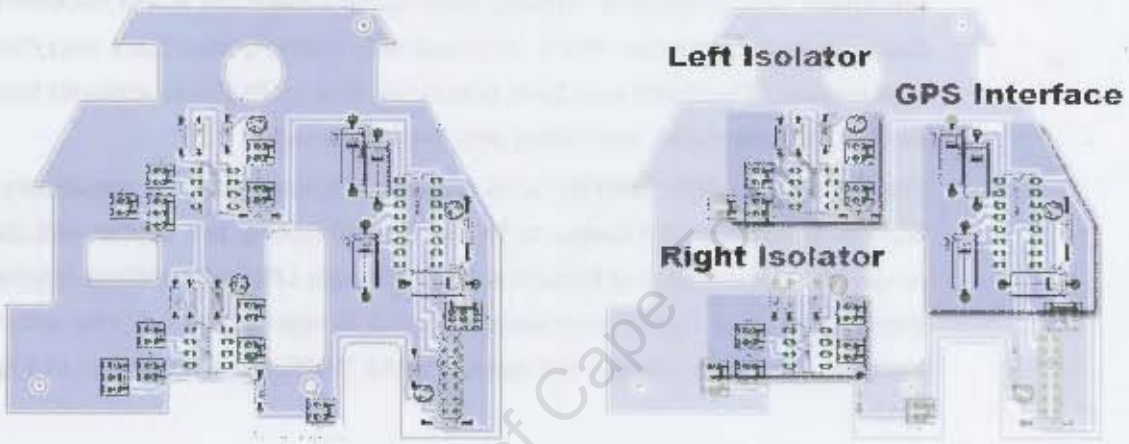

FIGURE 6-14: CENTRE BOARD

Figure 6-14 shows a schematic of the lower board. Interfacing the uBlox to the Computing Module required the use of both a USB-to-serial and a RS-232-to-TTL level shifter. In this case a USB-to-TTL converter would have been more appropriate; however a RS-232 to serial converter was readily available. Shown in **Figure 6-15** below is the interface between the USB-to-serial and the RS-232-to-TTL (MAX-232 **I**ntegrated **C**ircuit):

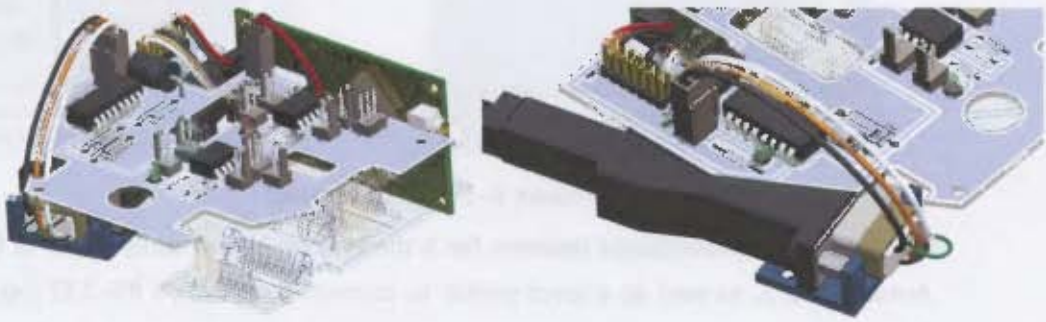

FIGURE 6-15: CENTRE BOARD: GPS INTERFACE

Design of the boards took place in an iterative fashion. The outline of the board was generated in Pro/ENGINEER to ensure mechanical compatibility with the module.

This outline was then exported as a *.dxf* file, and then imported into Eagle CAD as a board outline. **Figure 6-16** shows the design process:

FIGURE 6-16: DESIGN PROCESS: SOLID MODEL->*.DXF*->EAGLE CAD->*.TIF*->SOLID MODEL

Once the outline was imported into Eagle, all the track routing and component placement was completed, making sure not to violate the board boundary. This placement was exported into a *.tif* image file, and imported back into Pro/ENGINEER as a texture. The board was then populated and, once it was ensured that there were no interferences, the board was manufactured.

The **D**ifferential **GPS** (**DGPS**) node required a board designed specifically for the PC/104 stack. Per kind favour of Mr. Samuel Ginsberg, the author was taught how to use the Department of Electrical Engineering's LPKF PCB milling machine. This allowed for much tighter tolerances (±5mils as opposed to ±27mils with the Hercus method), and thus allowed the design of the DGPS board as shown in **Figure 6-17** below:

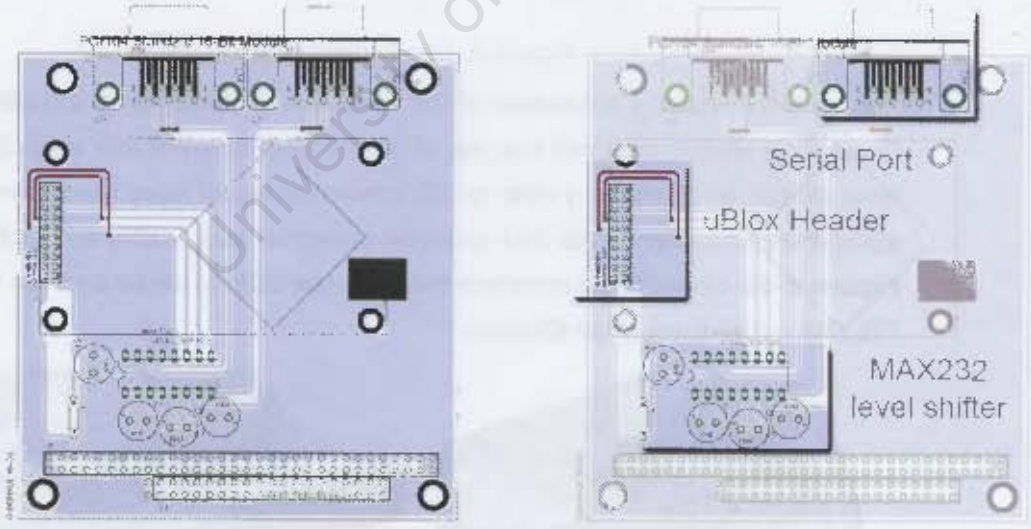

FIGURE 6-17: DGPS BOARD

This board accommodated headers for a the two on-board serial ports of the uBlox Antaris board, as well as a level shifter to convert the PC/104 RS-232 logic to TTL logic.

7. CONCLUDING REMARKS

As design is by nature an iterative process, there are a number of improvements that could be made to the system in the next stage of the vehicle's development. Each module is analysed below and recommendations are made for design improvements:

7.1 Drive Units

Although care was taken to reduce the weight of the drive units, each one still weighed over a kilogram, including the wheels. This weight reduces the payload that the vehicle can carry. As such, the re-design of the wheels with a reduced amount of poly urethane would be beneficial.

FIGURE 7-1: WHEEL REVISION

Figure 7-1 shows a possible implementation. Hollow HDPE inserts are responsible for housing the magnets, with the grip being provided by a relatively thin poly urethane insert, significantly reducing the amount of dead weight.

7.2 Frame

The frame interfaced well with the other modules; however a re-design incorporating an aluminium skeleton and thinner HDPE panels would reduce the weight of the robot whilst not compromising on structural integrity or strength.

7.3 Tail Unit

Overall the Tail Unit fulfilled its purpose, however the internal weight-reduction features provided a large amount of space that was not effectively utilised. Battery-monitoring electronics or other intelligent modules could be incorporated into the rear unit without compromising on weight.

7.4 Payload Bay

Implementation of proper NDE testing equipment or a high-definition camera would make the Payload Bay more effective.

7.5 Electronics

Although the H-bridges worked adequately, a better solution would be the implementation of power MOSFET's and a MOSFET driver chip for each drive unit. Incorporation of a battery-monitoring circuit would allow for more accurate monitoring of the robot's condition.

As the heat generated from the PC/104 was of primary concern, the cooling fans were wired to be permanently on. This is not required when the robot is idling (i.e. CPU usage is low). Therefore implementation of fan-control circuitry would allow for extended battery life.

Appendix C

Computer System Setup & Code

SUMMARY

This Appendix forms part of the eRobot project at the University of Cape Town.

FIGURE (A) 1: EROBOT TRAVELLING ON A VERTICAL WALL

This Appendix details the design of the computing network and code that was implemented for the eRobot system. A detailed physical breakdown is given of all the systems used in the project, followed by flowcharts and descriptions of the individual code segments that constituted the binaries on both host and client-side of the network. The final section draws conclusions from the design and performance of the code, as well as making recommendations for future design work.

[All code is available on the accompanying DVD]

TABLE OF CONTENTS

LIST OF TABLES

1. INTRODUCTION

This Appendix provides the reader with a detailed breakdown of the computing systems used in the eRobot project. The system was a mixture of Linux and Windows® operating systems, all operating on a wireless network. The system made use of a large amount of computing hardware from the PC/104 embedded form factor to standard IBM-clone PC's.

Previous experience with the wireless robot communications had shown that high-level languages introduced excessive latency into the system, and therefore all coding was done in C++ to maximise the system responsiveness. All source code is given on the accompanying DVD, and compilation suggestions are given for all code segments.

Shown in **Figure 1-1** below are shots of the PC/104 "stack" at the beginning and end of the project.

FIGURE 1-1 : PC/104 EVOLUTION

Figure 1-2 shows testing of the PWM code (left) and of the GPS system (right).

FIGURE 1-2: SYSTEM TESTING: PWM (LEFT) AND GPS (RIGHT)

2. System Diagram

2.1 System Overview

Figure 2-1: Local Area Network topology

Figure 2-1 shows the architecture of the **L**ocal **A**rea **N**etwork or **LAN** that was implemented for the project. Vital to the success of the project was the availability of an internet connection for every node on the network.

With the internet's propensity for viruses and other malicious code, connecting an unprotected machine or network to the internet is very unwise. Therefore a **gateway** machine was used to act as a filter for the internal network from the outside world.

Data redundancy is always necessary, and as such a dedicated **backup server** was added to ensure data integrity in the case of a system failure.

Wireless connectivity (or WiFi) is provided by the Linksys® **W**ireless **A**ccess **P**oint (**WAP**). Clients on the network consisted of a Compaq® **laptop** for the operator, as well as the **DGPS node** and the **robot client** itself. Brief descriptions of the various elements are given overleaf:

2.2 Descriptions

GATEWAY

The gateway server (running Ubuntu Dapper Drake) was responsible for filtering out malicious attacks from the internet, whilst permitting the clients to access any data streams they may require. These streams included the RTCM-sc104 DGPS data stream on port 2101, the **H**yper-**T**ext **T**ransfer **P**rotocol (**HTTP**)on port 80, and standard **f**ile **t**ransfer **p**rotocol (**ftp**) and **s**ecure **sh**ell (**ssh**) (ports 20-21 and 22). It is never a good idea in terms of security to give ports public access, particularly ftp which is susceptible to a variety of attacks.

Conventional firewall tactics on Linux machines make use of **iptables** (an administration tool for IPv4 packet filtering and **N**etwork **A**ddress **T**ranslation, **NAT** [c1]); however a novice user can do more harm than good on a machine. Another alternative is the use of the **Firestarter** [c2] firewall daemon.

FIGURE 2-2: SCREENSHOT: FIRESTARTER

Firestarter is a simple firewall with a very user-friendly **G**raphical-**U**ser **I**nterface (**GUI**) that enables the user to block ports, filter traffic and restrict LAN activity.

The daemon also allowed port forwarding, so that any request on port 80 (the standard HTTP port for internet traffic) would be forwarded to the robot, which hosted the web-page for the system.

As any node on the element would have to pass domain-name resolutions (for example, mapping of the domain name such as www.google.co.za to 209.85.129.147) onto the gateway, it was decided to implement a **D**omain-**N**ame

Server (**DNS**) on the gateway, speeding up the query-response of the system. This was accomplished with the **BIND** [c3] package.

Backup Server

Ubuntu Edgy Eft was installed on the backup server. This server had one 20 **G**iga-**B**yte (**GB**) and three 80 GB hard-drives specifically for data storage. The server was configured as a **N**etwork **F**ile **S**erver (**NFS**) on the network. As such any node could be configured to have access to the data.

The main (gateway) server mounted the three hard drives locally as network-drives. Therefore when any data was written to those "local" drives it was in fact being transferred to the hard-drives on the backup server.

Cron is a Linux daemon that allows the regular scheduling of any user-specified jobs and is ideal for a backup. Entries were made in the gateway's **crontab** file to write compressed (or tarred) archives of all data on the disk every day. Once a day this compressed archive would be written to the 20GB hard drive.

Router

Figure 2-3: Linksys Wireless-G Access Point

The author had access to a Linksys Wireless-G Access Point, and this was used to provide wireless access for the network. The access point was **g**-standard, meaning that a maximum of 54 **M**ega-**b**its (**Mb**) per second at 2.4GHz was possible. Taking into account the cluttered effect of a dockyard environment, it may be prudent in future versions to make use of the Wireless **a**-standard, which operates in the 5 GHz band and has less potential for RF interference [c4].

As the unit is just an access point, it does not have routing capabilities. This was not required though, as the gateway server would provide access to the internet.

Laptop

Ubuntu Breezy Badger was installed on the user laptop. Breezy (as it is more commonly known) is a version of **Linux** that is very easy to install, and the in-built package manager known as **apt** resolves dependencies automatically, making installation of new packages a simple task.

As with most other flavours of **Linux**, use of the system without an internet connection is a very tedious affair. UCT has a local mirror of a broad array of Linux software, called the **Linux Enthusiasts Group** or **LEG**. The LEG website was instrumental in the development of all the **Linux** machines [c5].

The laptop in question was a Compaq Presario 1.8GHz AMD Athlon-XP machine, with 512 **Mega-Bytes** of **RAM**. This machine previously had Windows® XP Professional **Service Pack 2** (SP2) installed, and ran very slowly. With the installation of Breezy, machine performance was noticeably better (although installation of a less power-hungry **Operating System** (**OS**) such as Windows® 2000 would also have improved performance).

Robot client: Software

RedHat Linux was chosen as the operating system for the robot. This choice was made fairly early on in the development cycle, for a number of reasons.

Firstly, it was observed that the loading and unloading of drivers in Windows® 2000 was sometimes erratic. This may have been due to the way the device drivers were loaded (i.e. only when calls were made to the device driver). Also, nodes on the previous wireless network had a nasty habit of displacing other nodes at random times (although in retrospect this may have been due to the **ad-hoc** architecture of the network) and Linux offered more powerful network-configuration tools.

Secondly, from the documentation on the two RTD Digital I/O boards, RedHat Linux 9.0 (Shrike) was the most recent open-source platform for which development had been done. As most of the chipsets that were being used were common to standard PC's, compatibility for the rest of the PC/104 components was not an issue.

Although open-source RedHat has been discontinued (and has been re-named Fedora) RedHat 9.0 was still supported as a legacy build at UCT's **Linux Enthusiast's Group** (**LEG**) website.

ROBOT CLIENT: HARDWARE

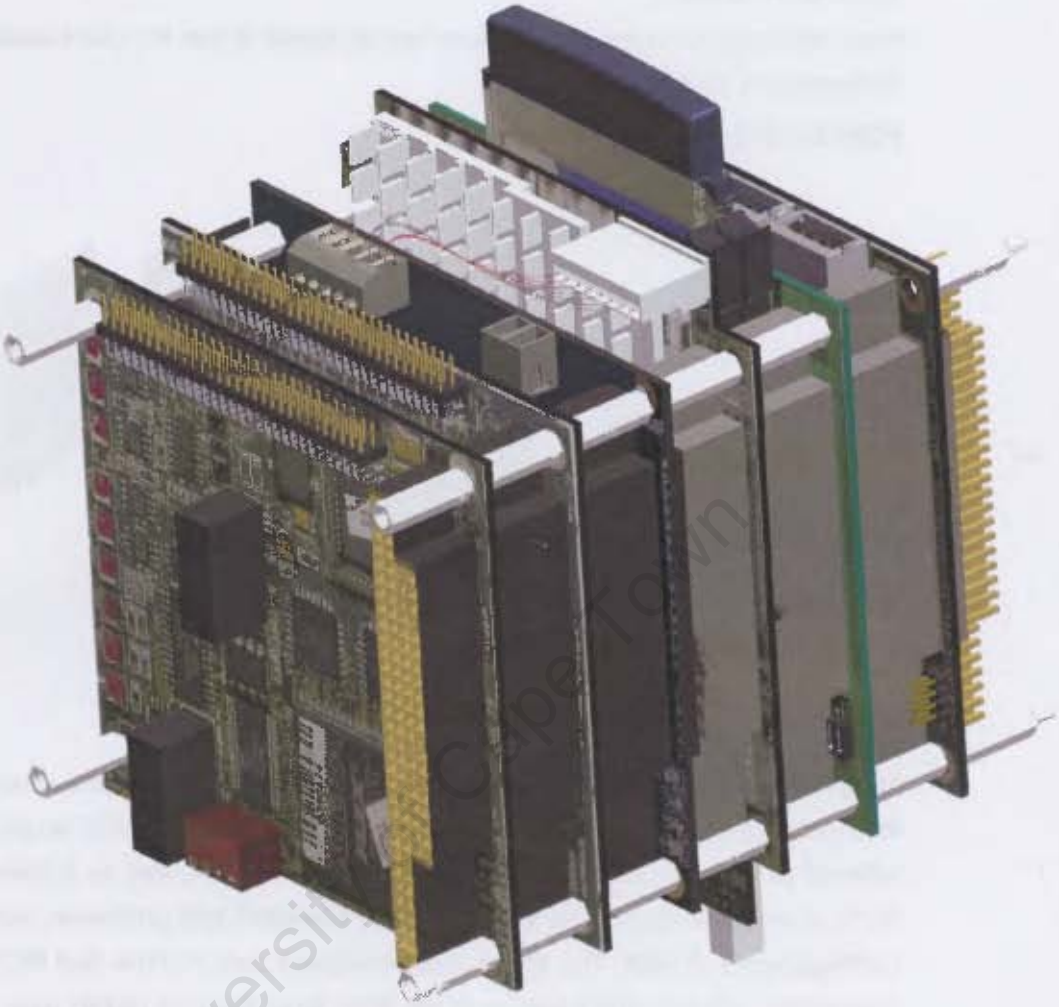

FIGURE 2-4: THE PC/104 "STACK" (RENDERED)

Central control and communication for the robot platform was achieved with use of an embedded PC/104 stack. The PC/104 format is a particular computing standard that promotes stacking – that is, various modules can be stacked progressively onto each other adding capabilities to the base motherboard, and is very common in **A**utomated **T**eller **M**achine's (**ATM**'s) and other high-intensive embedded applications. Shown in **Figure 2-4** above is a Pro/ENGINEER rendering of the PC/104 stack. The stack itself is a mixture of **RTD Embedded Technologies** Digital I/O boards, and **Advantech** conventional PC/104 and PC/104-*Plus* components.

The PC/104 architecture is very modular and used for a variety of embedded tasks where robustness and size is important. Amongst other things, PC/104's can be found in vending machines, medical instruments and industrial control systems. The

system used in this case is also PC/104-*Plus* compatible, meaning both ISA and PCI buses are available.

More information on the architecture can be found at the PC/104 Embedded Consortium's website [c6].

PCM-3370 & POWER SUPPLY

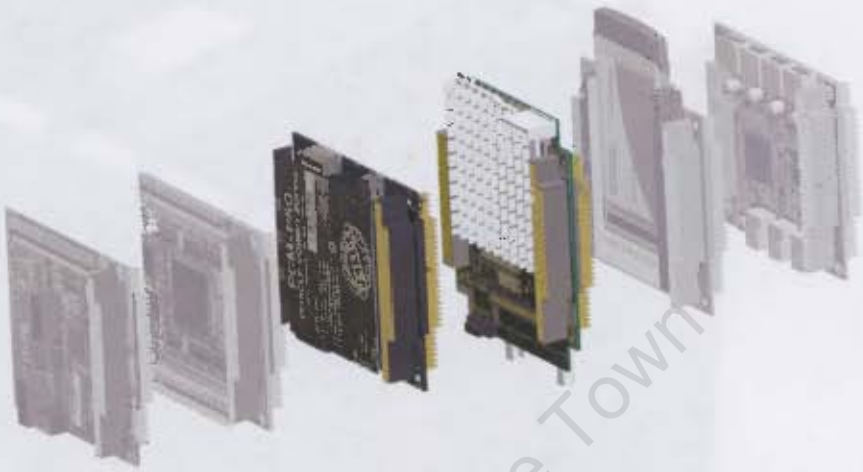

FIGURE 2-5: ADVANTECH PCM3370

Each PC/104 unit is commonly referred to as a "stack". Each stack must have a motherboard and **C**entral **P**rocessing **U**nit (**CPU**), which together is commonly referred to as a **S**ingle-**B**oard **C**omputer (**SBC**). This SBC was an Advantech PCM-3370, running an **U**ltra-**L**ow **V**oltage (**ULV**) Celeron© 650 processor, with 512Megabytes of RAM. The board accommodated both PC/104 and PC/104-*Plus* connectors, allowing the addition of the **R**eal **T**ime **D**evices (**RTD**) data acquisition boards and the USB and PCMCIA expansion boards. In its factory-configuration, the PCM 3370 had 3 free interrupts available for peripheral devices, however the **B**asic **I**nput-**O**utput **S**ystem (**BIOS**) allowed for peripherals (such as the on-board USB, serial ports, Ethernet port and so on) to be disabled, freeing up resources.

The PCM-3370 was a power-hungry unit, requiring two 11.1**V**olt Lithium-Ion batteries configured in parallel in order to provide sufficient power to the unit. In the cases where the battery voltages started to drop (and were not capable of providing 3 Amps peak current) the unit would exhibit erratic boot behaviour.

A 50W PCM-P50 power supply regulated the power from the robot's battery pack and provided +12V, +5V, ground, -5V and -12V supplies. Unfortunately, the power supply did not have a through-header for the PC/104-*Plus* bus, which required the stack to be assembled in a certain order.

DM6420

FIGURE 2-6: RTD DM6420

Real **T**ime **D**evices (**RTD**) are manufacturers of a large variety of "computer modules and systems for **I**ndustrial and **A**erospace Applications" [c7]. In particular they develop a large number of **I**nput/**O**utput (**IO**) devices in the PC/104 form factor. One of these boards that the Department possessed was a DM6420 Data Acquisition board, with 8 differential (16 single-ended) analogue input channels, a 12 bit **A**nalogue-to-**D**igital **C**onverter (**ADC**) and a host of timers and counters, all useful for sensor monitoring and sampling.

DM6816

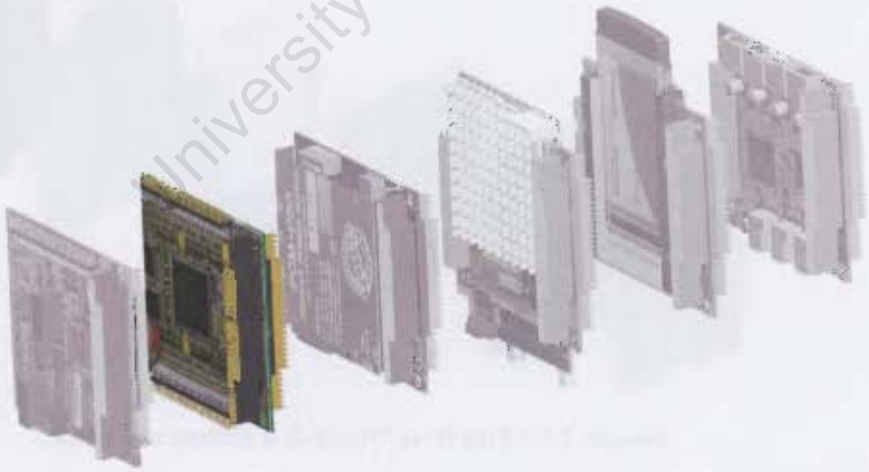

FIGURE 2-7: RTD DM6816

Also developed by RTD is the DM6816, which is a **P**ulse **W**idth **M**odulator (**PWM**) and Digital I/O board. The DM6816 has 8 dedicated 8-bit PWM channels and 8 digital I/O ports, making it very useful for controlling motors.

DM6420

FIGURE 2-6: RTD DM6420

Real **T**ime **D**evices (**RTD**) are manufacturers of a large variety of "computer modules and systems for Industrial and Aerospace Applications" [c7]. In particular they develop a large number of **I**nput/**O**utput (**IO**) devices in the PC/104 form factor. One of these boards that the Department possessed was a DM6420 Data Acquisition board, with 8 differential (16 single-ended) analogue input channels, a 12 bit **A**nalogue-to-**D**igital **C**onverter (**ADC**) and a host of timers and counters, all useful for sensor monitoring and sampling.

DM6816

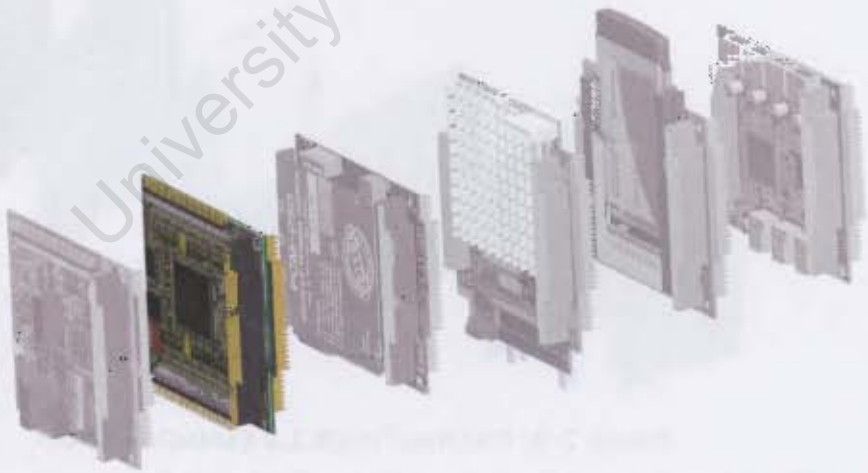

FIGURE 2-7: RTD DM6816

Also developed by RTD is the DM6816, which is a **P**ulse **W**idth **M**odulator (**PWM**) and Digital I/O board. The DM6816 has 8 dedicated 8-bit PWM channels and 8 digital I/O ports, making it very useful for controlling motors.

PCMCIA Expansion Board

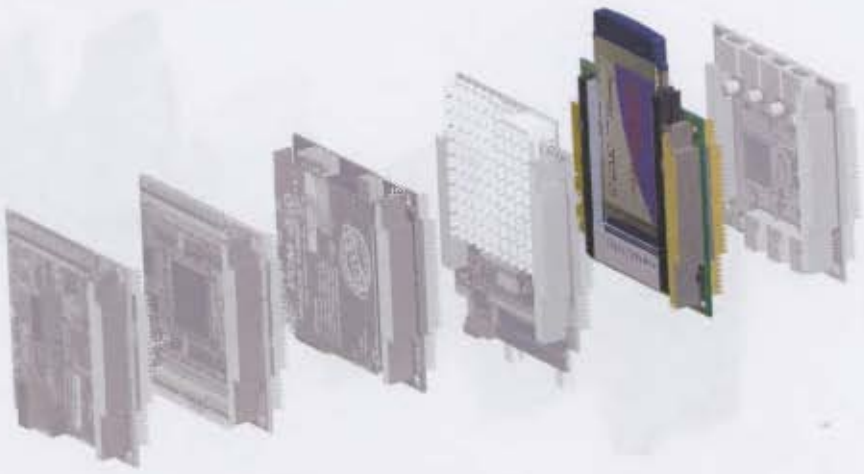

Figure 2-8: Advantech PCMCIA Expansion Board

Wireless networking capacity was provided by the PCMCIA expansion board, which had two slots for Type I/II/III or CardBus cards. In the case of eRobot, an 802.11g WiFi card was used. In conjunction with the booster aerial, the card had a rated working range of 1km. This was very optimistic, however as the network became unstable (excessive numbers of dropped packets) over 250 metres.

IEE1394 FireWire©/USB 2.0 Expansion Board

Figure 2-9: FireWire©/USB 2.0 Expansion Board

As the PCM-3370 motherboard only had two USB 1.1 connections, an add-on expander board was used to provide 3 FireWire© ports and two USB 2.0 ports. However, the **usb-uhci** and **usb-ohci** Linux drivers would not allow peripheral access to **both** the on-board and the expansion board ports. Therefore the low-speed native USB 1.1 ports were sacrificed for the add-on USB-2.0 ports.

DGPS NODE: SOFTWARE

The DGPS node consisted of another PC/104 node with Wireless Networking capability. The only PCMCIA adaptor available was a dual slot PM-1038 adaptor board. Unfortunately, this board was not PC/104-*Plus* compatible, meaning that only the **I**ntegrated **S**ystem **A**rchitecture (**ISA**) bus was available. Linux has notorious ISA support, and therefore Windows© 2000 was installed on the machine. Use of the Windows© OS allowed access to a greater number of binaries (executable files) developed for GPS applications than would otherwise have been possible with a Linux-only architecture. In addition the incorporation of a Windows machine exhibits the compatibility of the system for a variety of operating systems.

DGPS NODE: HARDWARE

WIRELESS NETWORKING

Figure 2-10 highlights the wireless adaptor board. A Surecom© b-standard 11 Mega-Bit wireless card was used to connect to the wireless network.

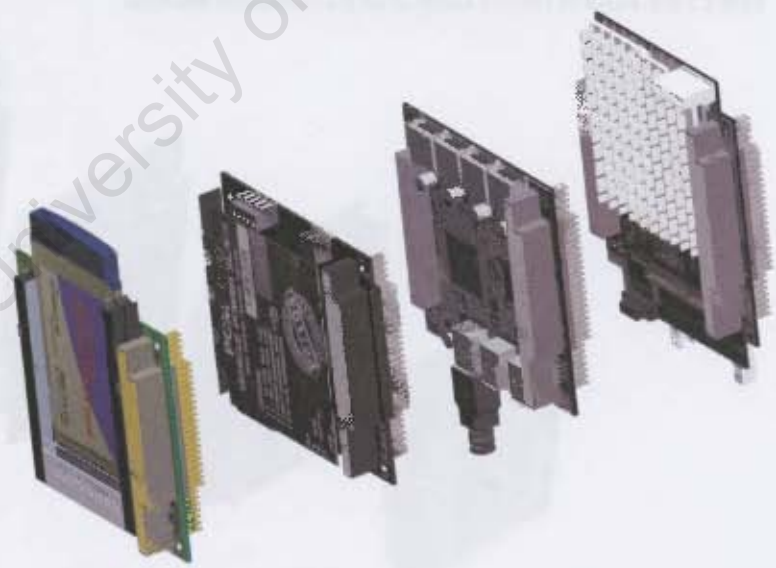

FIGURE 2-10: DGPS: WIRELESS ADAPTOR

Although this allows a transfer speed of only 1.375 **M**ega-**B**ytes, this was more than sufficient for the DGPS node. RTCM-data is typically in the order of 50 bytes-per-second [c8], which constitutes less than a percent of the network traffic. Even with other additional networking overhead, the bandwidth would be far from saturated.

Power Supply and Single Board Computer (SBC)

Figure 2-11: DGPS: Power supply and SBC

These were identical to the Power Supply and SBC used in the Robot client stack. In the case of the DGPS stack, the wireless-networking adaptor had to be adjacent to the power supply, as neither unit had a PC/104-*Plus* header.

IEE1394 FireWire©/USB 2.0 Expansion Board

Figure 2-12: DGPS: IEEE394/USB2.0 Expansion Board

Although the DGPS node did not require the use of high-speed Firewire or USB 2.0 connections, this board was included to allow for future expandability of the unit.

3. HOST-SIDE CODE

The host-side code was required to analyse the human input from a joystick, and translate that into a robot "message" that would be transmitted to the vehicle. The advantage of this system is that the addition and/or modification of behaviour on the robot itself will not require modification of the host-side code. This will allow the addition of more robots into the network without having to re-develop the system.

3.1 Flowchart

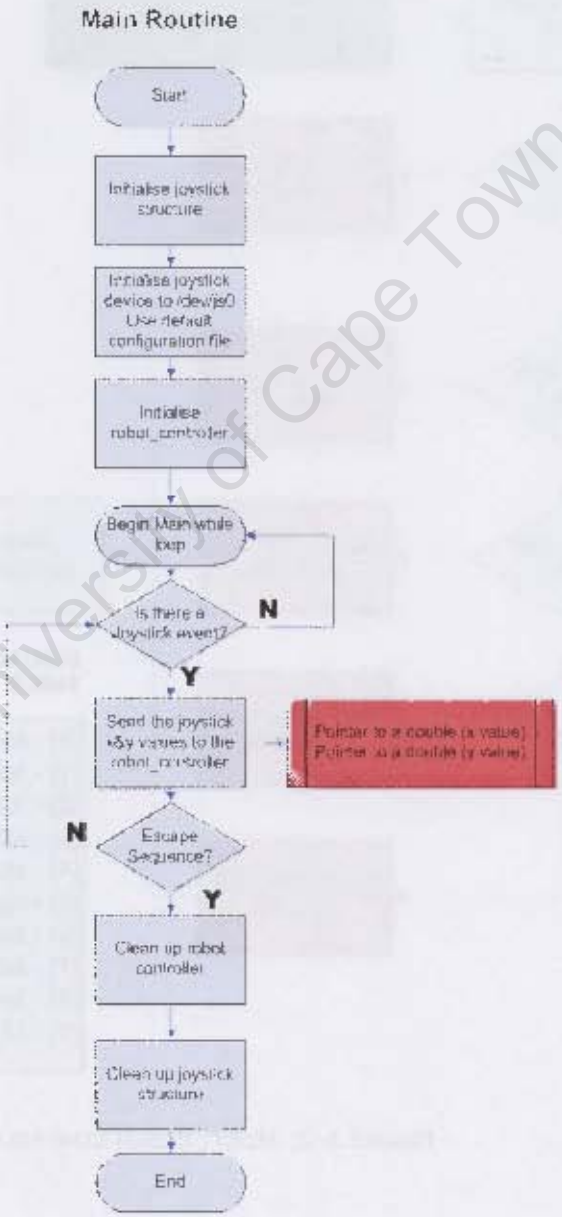

FIGURE 3-1: HOST: MAIN ROUTINE

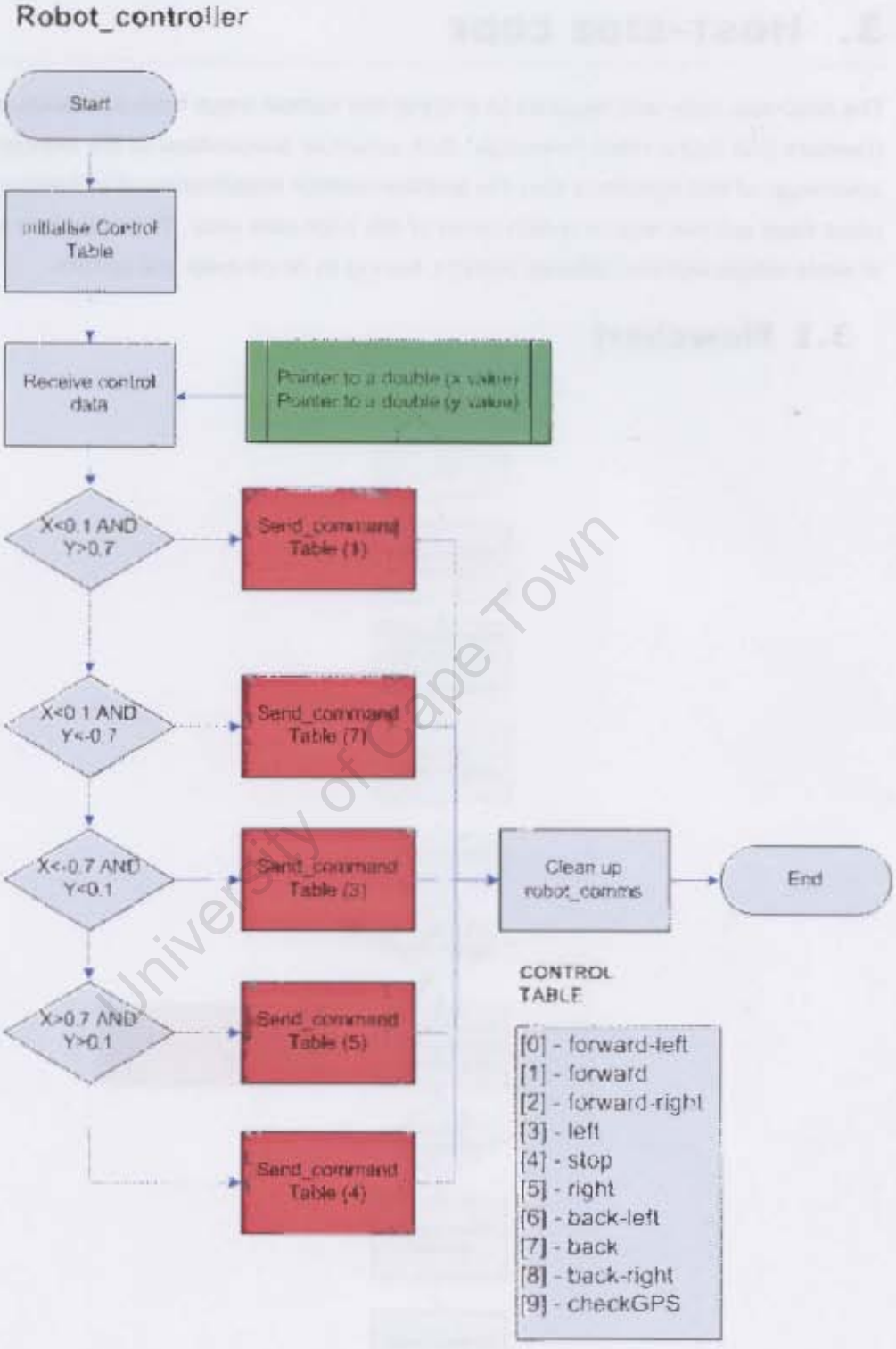

FIGURE 3-2: HOST: ROBOT CONTROLLER

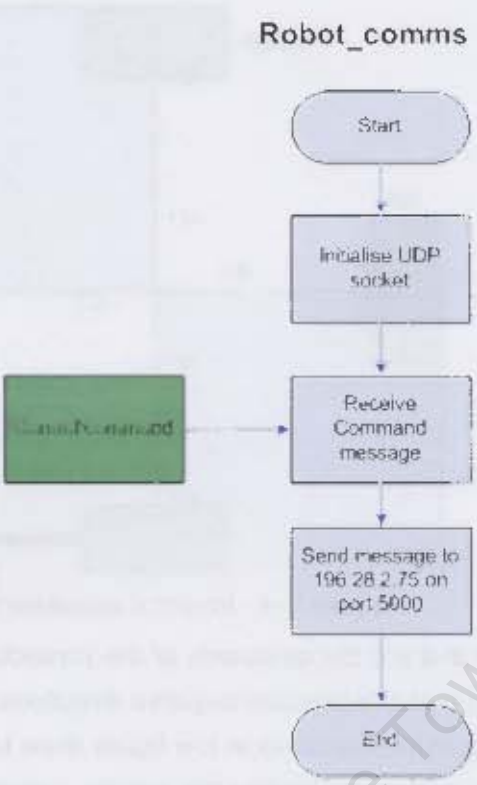

FIGURE 3-3: HOST: ROBOT COMMS

3.2 Description

As can be seen in the flow-diagram of **Figure 3-1**, the main routine consists of an infinite ***while*** loop. If a joystick event occurs, then the value of the **x** and **y** axes are passed to the *robot_controller* code (via **pointers**). Note all output data is shown in red and input data in green.

The code also checks for a designated escape sequence, defined as buttons 6, 7 and 8 on the joystick. If all three are pressed simultaneously, then the code breaks out of the while loop and exits gracefully. It is also possible (but not advised) to exit the code by pressing Ctrl+c (Linux) to kill the process.

Once the *robot_controller* function has been passed the pointers to the x and y data values, it passes them through a chained **if....else if** ladder. This section of the code is very rudimentary; however it manages to perform within the specified design requirements. If the x and y values correspond to a pre-determined condition, a control command will be issued.

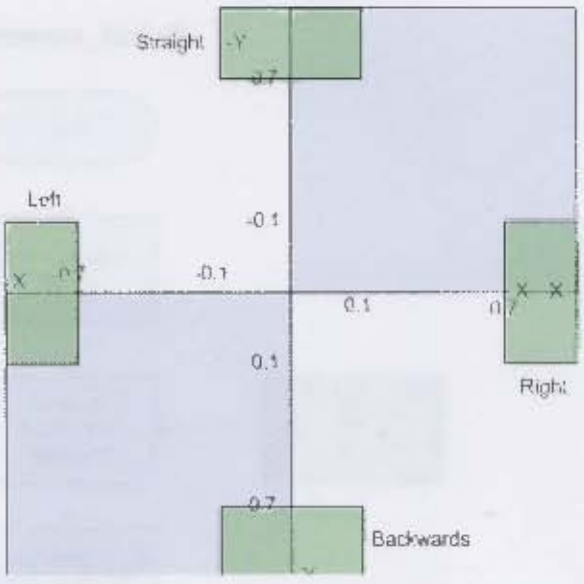

FIGURE 3-4: JOYSTICK QUADRANTS

Shown in **Figure 3-4** are the quadrants of the joystick. One unusual aspect of the joystick to note is that the positive/negative directions of the Y-axis have been reversed. The highlighted sections in the figure show the different control command regions that were utilised for testing the vehicle, namely; forward, backwards, left and right. All other positions are designated "stop". This was to ensure that the robot did not start moving if it somehow received an errant packet from the network.

The *robot_controller* would then pass the required command to the *robot_comms* code. The sole function of this code (shown in **Figure 3-3,** previous page) is to send the command message across the network to the eRobot client node (with a network IP address of 196.28.2.75) on port 5000.

3.3 Limitations

This code is very rudimentary and served only to test the robot. However design of the code attempted to follow **O**bject **O**rientated (**OO**) principles so that improved functionality could be quickly implemented.

For instance if a better design is implemented for the *robot_controller* code such as a hashed lookup table instead of an **if...else if** ladder, then the *robot_controller* object module could simply be replaced and the code re-compiled.

3.4 Required code/libraries

Requires:

Description	Linking notes
Joystick wrapper library for interfacing with the library	-ljsw (**library**)
Simple C++ sockets for transmitting UDP packets	-lSockets -lpthread -lssh (**libraries**)
robot_controller	Compile to object module robot_controller.o
robot_comms	Compile to object module robot_comms.o
robot_hid	Compile to object module robot_hid.o

TABLE 1: REQUIRED CODE/LIBRARIES: HOST

When compiling the binary executable, the following procedure could be used:

3.5 Compilation steps

g++ -c robot_controller.cpp

g++ -c robot_comms.cpp

g++ -c robot_hid.cpp

g++ robot_controller.o robot_comms.o robot_hid.o -o **binary_executable** -ljsw -lSockets -lpthread -lssh

[All code is available on the accompanying DVD]

4. CLIENT-SIDE CODE

The client-code was responsible for analysing a control message sent from a user/operator, and implementing the corresponding low-level control functionality. Code for the client was kept as generic as was feasible, allowing for code modification without having to rewrite the project.

4.1 Flowchart

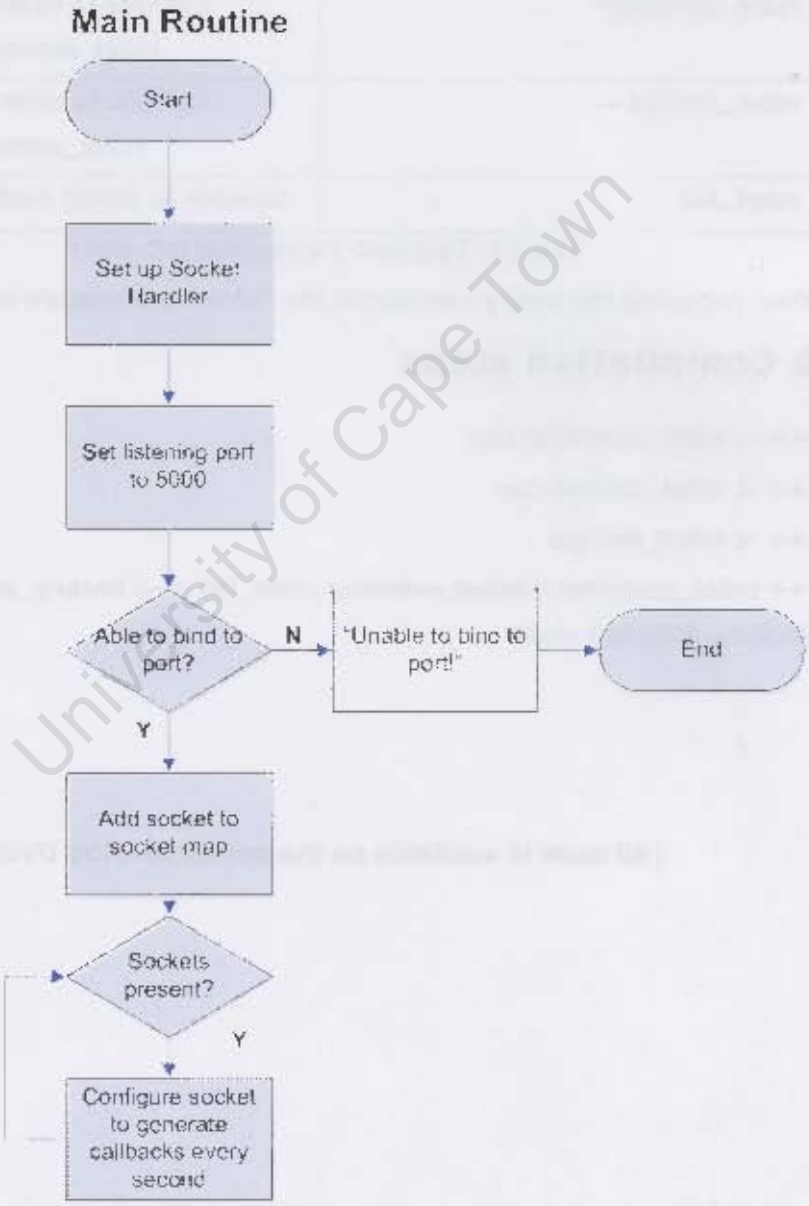

FIGURE 4-1: CLIENT: MAIN ROUTINE

robotSocketClient

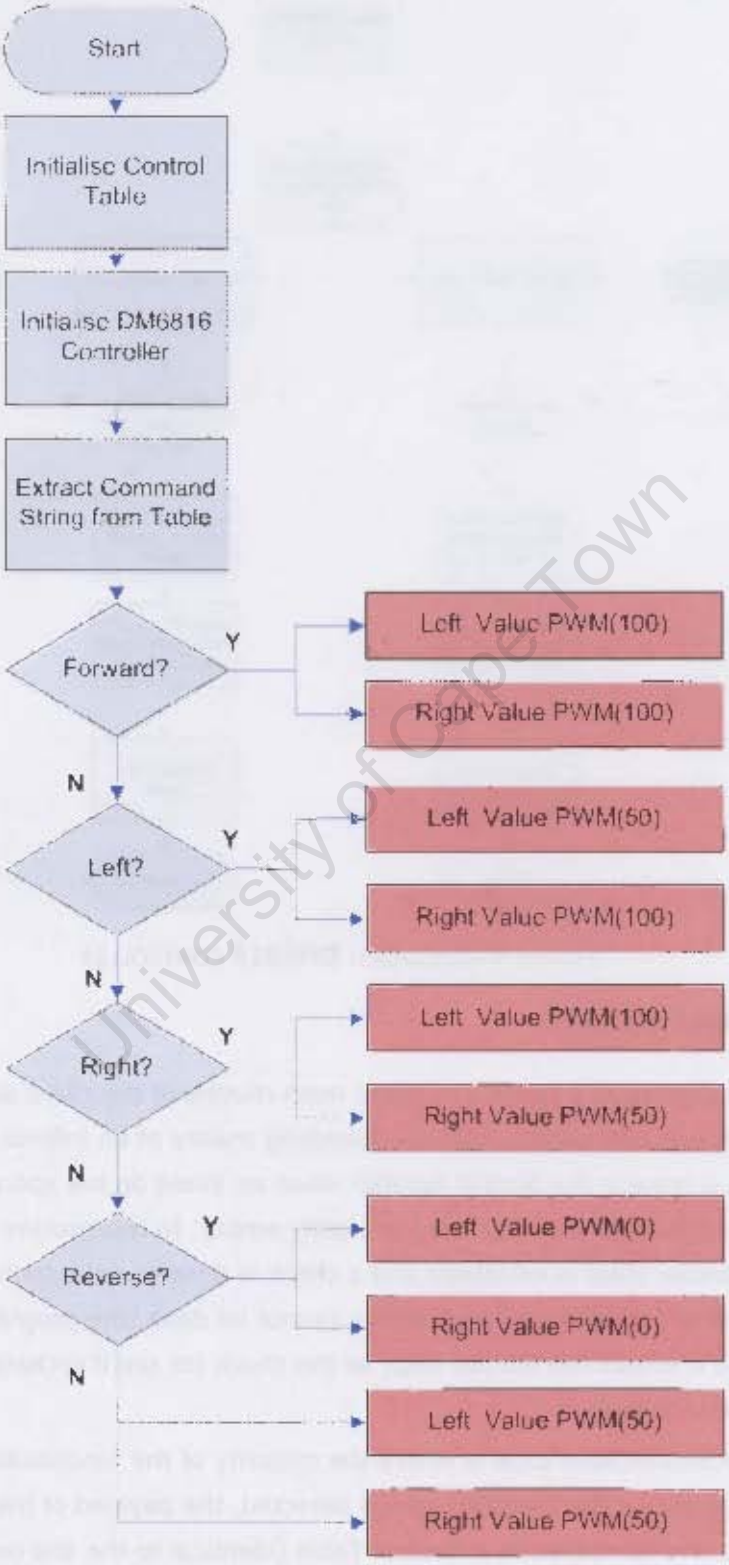

FIGURE 4-2: CLIENT: SOCKET HANDLER

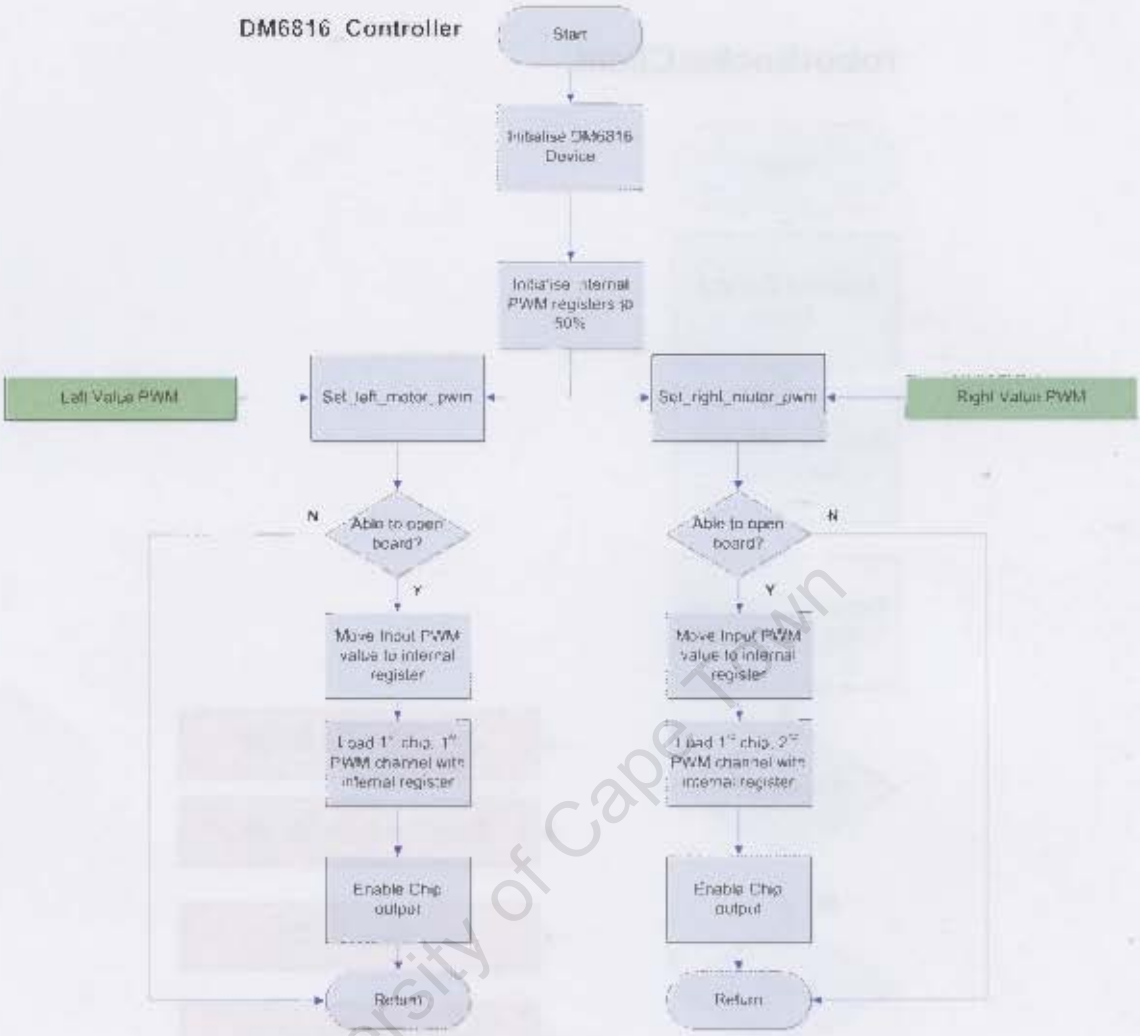

FIGURE 4-3: CLIENT: DM6816 CONTROLLER

4.2 Description

Shown in **Figure 4-1** (page 22) is the main routine of the client-side code. As can be seen it is a very simple routine, consisting mainly of an infinite loop. All the data handling is done in the Socket handler when an event on the specified port is detected; therefore the main loop is mostly empty. In this routine the SocketHandler class is initialised and a check is done to see whether the program can attach or "bind" to the port. If this cannot be done, the program terminates. Otherwise it enters the infinite loop, as the check (to see if sockets are present) always returns **true**.

The robotSocketClient code is where the majority of the functionality is performed. Once an event on the specified port is detected, the payload of the packet is extracted and compared to a Control Table (identical to the one on the Host-side code). When a match is found (through a ladder of **if...else if** statements) the

appropriate set **P**ulse **W**idth **M**odulation (**PWM**) commands are sent to the DM6816 motor controller.

In the flow diagram (**Figure 4-2**) the PWM value is given as a percentage. In the case of the robot, 100% is defined as the motor fully on going forwards. 50% is stationary and 0% is fully on going backwards. Once the desired motion has been established (i.e. turning **left** will require the **left motor** to be **stationary** (0%) and the **right motor** to be **full on forwards** (100%)) the DM6816_controller functions Set_left_motor_pwm and Set_right_motor_pwm are called with the corresponding values.

The DM6816 controller's functions test to see if the driver for the board is loaded correctly, and if not, exits. If the driver is loaded, the 1st PWM chip on the board is activated, and the 1st and 2nd channels of the chip are loaded with the left and right PWM value.

4.3 Limitations

Although the system is far from optimised, the entire process from user input to the PWM value being sent to the motors is within tens of milliseconds, well within the design requirements. Refinements to the code could include running the program as a process or a daemon to prevent it dominating control of the console. Also, the use of more refined look-up methods (hash-tables have been mentioned previously) would avoid the use of laddered **if...else if** statements.

4.4 Required code/libraries

Description	Linking notes
Simple C++ sockets for transmitting UDP packets	-lSockets -lpthread -lssh (**libraries**)
DM6816 Library	ldm6816 -lpthread
robot_client	Compile to object module robot_client.o
robot_socket_client	Compile to object module robot_socket_client.o
DM6816_controller	Compile to object module DM6816_controller.o

TABLE 2: REQUIRED CODE/LIBRARIES: CLIENT

4.5 Compilation steps

When compiling the binary executable, the following procecure could be used:

g++ -c robot_client.cpp

g++ -c robot_socket_client.cpp

g++ -c DM6816_controller.cpp

g++ robot_client.o robot_socket_client.o DM6816_controller.o -o **binary_executable** -lSockets -lpthread -lssh -ldm6816 -lpthread

[All code is available on the accompanying DVD]

5. CONCLUDING REMARKS

Although the implemented code worked sufficiently well to satisfy the design criteria, there are several improvements that can be made to the system. Though every attempt was made to modularise the code completely, some of the routines are too inter-dependant. Refinement of the individual modules will allow for more rapid future code development.

Although no errant packets or commands were encountered throughout the course of the project, more error checking and intelligence will have to be built into the system when more nodes are added and there is a resultant increase in network traffic.

Implementation of a GUI on the server side would give the user a more intuitive feel for the control of the robot. In addition, video-feed and other data could be incorporated into the interface.

REFERENCES

[c1] "**iptables**" - Ubuntu Manual Pages – Accessed on January 16 2007.

[c2] 2007, *"Firestarter – A graphical interfaced Open Source firewall for Linux"*. Accessed on January 16 2007. Available at: http://www.fs-security.com/

[c3] 2007, *"Berkeley Internet Name Daemon"*, ISC BIND. Accessed on January 16 2007. Available at: http://www.isc.org/sw/bind/

[c4] 2007, *"Wireless Networking Standards"*, Web-o-pedia. Accessed on January 16 2007. Available at: http://www.webopedia.com/quick_ref/WLANStandards.asp

[c5] 2007, *"Linux Enthusasts Group"*, LEG UCT. Accessed on January 16 2007. Available at: http://www.leg.uct.ac.za

[c6] 2006, *"PC/104 Embedded Consortium"*, PC104.org. Accessed on January 16 2007. Available at: http://www.pc104.org/

[c7] 2007, *"RTD Embedded Technologies, Inc."* RTD.com. Accessed on January 16 2007. Available at: http://www.rtd.com/

[c8] Weber, G., *"EUREF and Real Time Products"*, Bundesamt für Kartographie und Geodäsie (BKG), Frankfurt, Germany.

ACRONYMS

DGPS – Differential GPS

FTP – File Transfer Protocol

GPS – Global Positioning System

GUI - Graphical User Interface

HTTP – Hyper-Text Transfer Protocol

ISA – Integrated Systems Architecture

OS – Operating System

PCI – Peripheral Connect Interface

PWM – Pulse Width Modulation

RAM – Random Access Memory

RTCM – Radio Technical Commission for Maritime Services

SBC – Single Board Computer

SSH – Secure Shell

EROBOT: DVD